Synthesis and application of ion imprinted polymers for selective extraction of metal ions from different matrices

By

Masindi Muphulusi Lizzy (11630093)

A dissertation submitted in fulfilment of the requirements of the degree of Masters of Science

In the

Department of Chemistry

Faculty of Science Engineering and Agriculture, Department of Chemistry

University of Venda

Thohoyandou, Limpopo

South Africa

Supervisor: Dr Mudzielwana R

Co-supervisor: Dr Tavengwa N

February 2024

Declaration

I, **Masindi Muphulusi Lizzy** (student number 1130093), hereby declare that this dissertation titled "Synthesis and use of ion imprinted polymers for selective extraction of metal ions from different matrices" for the degree of Master of Science in Chemistry at the University of Venda, this work, which I have submitted, has never been submitted before for credit toward any degree at this or any other university. Both the design and the implementation are wholly unique, and all referenced sources have been correctly cited.

18/02/2024

Candidate signature……. Date ……..

Acknowledgements

First and foremost, I am utterly grateful to God Almighty for providing me with the wisdom, courage, grace, and persistence necessary to undertake this study and finish it as best I could. Without his favors, I could not have accomplished this.

Thank you so much for being there for me, Drs. Nikita Tavengwa and Rabelani Mudzielwana. You were more than just my supervisors.

I express my gratitude to Professor Nditshedzeni Eric Maluta for his unwavering support during my academic journey.

It was a real pleasure to work in the same lab as my colleagues in the analytical chemistry research group; thank you.

In particular, I would want to thank my mother Mavis Masindi for all of her help with my graduation work.

Dedication

This work is devoted to my family, especially my mother (Mavis), Uanea, and Riphuluse, who supported me throughout my Master's program and showed me love and encouragement beyond words.

Abstract

Exposure to toxic metal ions such as Zn^{2+} and Pb^{2+} can lead to several diseases including cancer on human being. This study aims to synthesize $Zn^{2+}$and Pb^{2+} ion imprinted polymers (IIPs) for removal of Zn^{2+} and Pb^{2+} from various sample matrixes. Polymerization was achieved by mixing the methacrylic acid (MAA) as a functional monomer, ethylene glycol di-methacrylate (EGDMA) as a cross-linker, azobis (isobutyronitrile) (AIBN) as initiator and methanol as a progen. The temperature was increased to 80 ^{o}C while stirring for 7 h. The identical procedure was used to make non- imprinted polymer (NIP), but no template was used. Imprinted polymers were extracted with 2 M HCl for the removal of templates.

The point of zero, or pHPZC, was determined and infrared spectroscopy was used to characterize the final products. The results of the Fourier-transform infrared (FTIR) analysis demonstrated the removal of ion templates by broad O-H peak at a wavelength of 3500 cm^{-1} and pH_{PZC} results revealed that, at acidic solution, the imprinted polymers carried positive charges, and at basic solution pH, the imprinted polymers carried negative charges the pH_{PZC} was found 6.98 and pH level was 7.0.

The maximum percentage of Zn^{2+} removal using the Zn-IIP was found to be 80% when the solution pH of 7.0, adsorbent dose was 5 mg, contact time at 15 min at shaking speed of 100 rpm and initial metal ion concentration of 25 mg/L were used. The adsorption kinetic data corresponded to pseudo-second order reaction kinetics with R_2 = 0.99, indicating that the process occurred by chemisorption. The Langmuir isotherm showed an excellent fit with an adsorption capacity of up to 9.03 mg g-1 and R_2 = 0.99, implying that adsorption was on a monolayer surface. This study shows that zinc ion imprinted polymer has higher efficiency towards Zn^{2+} in the solution. The finding indicates that zinc ion imprinted polymer has high adsorption efficiency of 94.00 (mg/g) in removing zinc ion from the honey sample.

The removal of Pb (II) from wastewater using Pb (II) IIP was found to be 90%. Further the re-usability study was evaluated 7 times and the adsorption efficiency was high at 90%, for this study the waste material can be beneficial for reused. The functional groups of both the imprinted polymer and the non-imprinted polymer were characterized by FTIR, and the point of zero charge was determined using the optimum conditions of 50 mg adsorbent dose, initial solution pH 9, and 15 min contact time. The adsorptive nature of the IIP and NIP was evaluated by means of Langmuir and Freundlich isotherms. The Langmuir adsorption isotherm modelled

the data better, as shown by the Langmuir and Freundlich correlation coefficients of 0.999 and 0.975, respectively.

An inventive answer has evolved in the form of ion-imprinted polymer, which was produced using the molecular imprinting approach as a basis. Higher selectivity coefficients have been demonstrated by IIPs compared to non-imprinted polymers.

Table of Contents

List of Figures

List of Tables

List of Abbreviations

AAS	Atomic absorption spectrometry
ABCN	Azobis cyclohexanecarbonitrile)
ATRP	Atom transfer radial polymerization
BET	Brunauer-Emmett-Teller
BPO	Benzoylperoxide
DSPE	Dispersive phase extraction
DVB	Divinylbenzene
EGDMA	Ethylene glycol dimethacrylate
FTIR	Fourier-transform infrared spectroscopy
HPLC	High-performance liquid chromatography
ICP-OES	Inductively coupled plasma atomic emission spectroscopy
ICP-MS	Inductively coupled plasma atomic mass spectrometry
IIP	Ion imprinted polymer
IOCs	Inorganic contaminants
LOD	Limit of detection
LOQ	Limit of quantification
MAA	Methacrylic acid
MIP	Molecularly imprinted polymer
MISPE	Molecularly imprinted solid-phase extraction
MSPD	Matrix solid phase extraction
NMP	Nitroxide-mediated polymerization
POPs	Persistent organic pollutants

RAFT	Reversible addition-fragmentation chain transfer
SEM	Scanning Electron Microscopy
SPE	Solid phase extraction
SPME	Solid phase micro-extraction
TGA	Thermogravimetric analysis
4-VP	4-vinylpyridin

Chapter 1: Introduction

1.1 Background

Global environmental and public health concerns about contamination of all ecosystems by toxic metals have increased in recent years (Okereafor et al., 2020). This is mainly because these toxic metals such as Zn^{2+}, Pb^{2+} and Cd^{2+} are enduring in the surroundings and they might amass and bio-magnify in the environment and contaminate the food web (Ali et al., 2019; Guo et al., 2020; Tamjidi et al., 2020). Moreover, human exposure to toxic metals poses various health risk. For example, cadmium reduces kidney function, lead give rise to memory failures while consuming large amounts of zinc over a long period causes anaemia, nervous system disorders, damage the pancreas and low level of good cholesterol (Alengebawy et al., 2021; Awuchi et al., 2020: Hussain et al., 2012).

The man-made activities have contributed immensely into the availability of these toxic metals into the surroundings (Chen et al., 2021; Dai et al 2019; Duru et al., 2019). For example, Tariq (2021) reported the concentrations of 0.613, 0.316, 0.162, 0.065, 0.041 and 0.028 mg L^{-1} for Ni, Cd, Pb, Cr, Cu, and Zn, correspondingly in the wastewater from industry Zvinowanda et al. (2009) detected Pb, Se, Sr, U and V in groundwater samples which was contaminated by mine wastewater, a study was conducted in South Africa with concentrations ranging from 0.05 – 1.11 mg/L, 0.07 – 0.16 mg/L, 0.15 - 3.40 mg/L, 0.23 – 0.38 and 0.08 – 2.14 mg/L, respectively.

As a natural product, honey's composition varies depending on the location, pollen, honey drew, and nectar source. Natural honey may contain distinct minerals, trace elements and toxic metals at various concentrations (Gałczyńska et al. 2021; Carreck et al., 2020). The research was done in Ethiopia by Adugna et al. (2020) found the toxic metals Cd, Cr, Cu, Mn, Pb and Zn in honey samples with concentrations of 0.017 μg g^{-1}, 0.15 μg g^{-1}, 1.15 μg g^{-1}, 7.29 μg g^{-1}, 2.53 μg $g^{-1}$and 16.03 μg g^{-1}, respectively. This amounts are below the permissible limits.

Toxic metals are often found to be above maximum allowable limits in environmental and food samples. It is therefore important to extract these toxic metals as they are harmful to the environment. Toxic metals can now be removed employing a range of methods, encompassing both biological and chemical ones. These methods have several limitations. For example: membrane technique is expensive (Low et al., 2017), chemical precipitation: produce large volumes of sludge, moreover slow metal precipitation and poor settling requires-treatment (Kumar et al., 2019). Aeration techniques is required high capital cost for aeration equipment

(Marsidi et al., 2018). Table 1.1 demonstrates a few techniques that have been employed to eliminate hazardous metals from various environmental media.

Table 1. 1 Removal methods for heavy metals.

Removal methods	Advantages	Disadvantages	Ref
Chemical coagulation	Sludge settling Dewatering	Excessive cost Large consumption of chemicals	Bahrodin et al. (2021)
Ion exchange	Metal selective High treatment capacity	Elevated Maintenance cost	Jang et al. (2022)
Chemical precipitation	Low cost Easy to perform	Disposal problem Sludge is produced in prohibitive cost	Crini & Lichtfouse (2019)
Membrane filtration	Membrane is found in distinct size ultrafiltration, nanofiltration and osmosis	Low flow rate Prohibitive cost	Rezakazemi et al. (2018)

Adsorption is a highly effective method used to remove certain target compounds, such as drugs and other organic compounds, and toxic elements and other ions from various matrices (Khan et al., 2020; Rasheed et al., 2020). The process by which a substance (adsorbate, or sorbate) builds up on a solid surface (adsorbent, or sorbent) is called sorption, more precisely adsorption. The adsorbate binds to the adsorbent whether it is liquid or gaseous. The unsaturated forces of the solid surface to establish bonds with the adsorbate are what propel adsorption. The adsorption process has intrigued many researchers due to its minimal cost and excellent efficiency, and design flexibility (Dey et al., 2021; Pérez-Botella et al., 2022; Velusamy et al., 2021). Adsorption can take two forms: chemical adsorption and physical adsorption. Numerous bonding processes, including hydrogen bonds, van der Waals forces, electrostatic forces, and hydrophobic interactions, are what lead to the physical adsorption process. Adsorbent and adsorbate undergo a chemical reaction that interacts to generate an

electrical connection. (Scheufele et al., 2016). Figure 1.1 shows the general physical and chemical adsorption

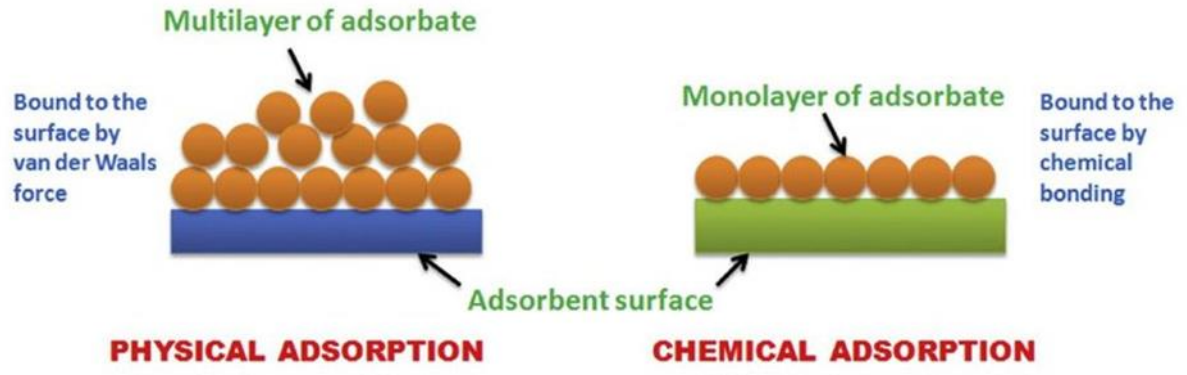

Figure 1.1: General adsorption process

Adsorbents can be natural or manufactured and employed in the adsorption process. Zeolites and clays are examples of natural adsorbents; MIPs and IIPs are examples of synthetic adsorbents. (Alipoori et al., 2021: Zhang et al., 2021).

Ion-imprinted polymers (IIPs) are nano-porous polymeric materials that, in the presence of closely related inorganic ions, can selectively rebind, detect, or transport the target analyte upon leaching the imprint ion. Ion imprinting polymer (IIP) sorbents often improve the selectivity and quality of analytical methods. The first IIPs developed showed their value to separate and identify target ions (Płotka-Wasylka et al., 2016: Zhou et al., 2018). IIPs are sorbent substances with unique benefits such as stability and selectivity, and are straightforward to prepare and use; consequently, many applications have been developed in analytical methodology. During selection of extraction, pre-concentration and analytical methods, an optimal sorbent should also be chosen to get the highest selectivity for the target ion (Jakavula et al., 2020: Janczura et al., 2018: Shakerian et al., 2016).

Heavy metals nowadays are priority pollutants. To safeguard humans and the environment, these hazardous metals should be eliminated from various matrixes, including wastewater. Ion imprinted polymers were selected as adsorbents for this study because high selectivity, reusability and absorptivity can be achieved by choosing a suitable functional monomer and cross-linker (Lai et al., 2019). The functional monomer and cross-linker used have a significant impact on the steadiness of the polymer intricate generated during the polymerization process as well as the effectiveness of IIPs' interaction with target ions (Zhou et al., 2018). While

methacrylic acid can interact with a template ion by hydrogen bonding, ethylene glycol dimethacrylate is highly reactive and produces polymers with high hardness and stability (Fauziah et al., 2018).

1.2 Problem statement

Inorganic pollutants like zinc, lead, and cadmium have negative health effects causing various health conditions such as cancer, brain damage, kidney disease and lung cancer. The exposure routes which include ingestion, dermal contact and deposition (Alengebawy et al., 2021). These heavy metals matrix include sewage, sludge, weathering, industries and forest fires (Ali et al., 2019). Due to various heath conditions, there are methods developed to remove toxic metals in the honey/water which include osmosis, filtration and ion exchange (Chai et al., 2021). Adsorbents that have been used are mineral, organic and inorganic materials which include activated clay mineral, zeolite, farming waste and activated carbon, the challenges regarding this adsorbent include no regeneration, expensive, time consuming and even the sorbent used are not selectivity (Crini et al., 2019). In this research, IIPs (Targeting zinc, cadmium and lead) were synthesized to remove toxic metals in presence of competing ions because of their selectivity, low-cost preparation, easy storage, reusability and long life since other polymers had drawbacks which include sensitivity and binding site can be destroy during grinding.

1.3. Aim and objectives

1.3.1. Aim

The main aim of this study is to synthesize ion imprinted polymers for application in the extraction of Pb^{2+} and Zn^{2+} from different matrices.

1.3.2. Objectives

- To synthesize ion imprinted Pb^{2+} and Zn^{2+} polymers and further determine their physicochemical characteristics.
- To evaluate the efficiency of the synthesized polymers towards the extraction of Pb^{2+} and Zn^{2+}.
- To model adsorption data using kinetics and adsorption isotherms models.
- To assess reusability of the prepared ion imprinted polymers.

1.4 Research questions

- Can ion imprinted polymers for Zn and Pb be effective in removal of Zn^{2+} and Pb^{2+} ions?
- What is the efficiency of the synthesized ion imprinted polymers in removal of Zn^{2+} and Pb^{2+} ions in different matrices?
- Can the ion imprinted polymers be re-used?

1.5 Significance of the study

Metals are suited to sustainable development goals. They are not biodegradable and have unlimited lifespan including potential recyclability. Heavy metals are eliminated from water and consumer products like honey can prevent damage to the ecosystem and even life-threating complications such as cardiovascular and neurological conditions**.**

1.6 Thesis structure

Chapter 1: Introduction and background information.

Chapter 2: Literature review.

Chapter 3: Synthesis, characterization and use of a Zn (II)-IIP to extract and determine Zn (II) in honey.

Chapter 4: Synthesis of a Pb (II) -IIP to selectively extract Pb (II) from wastewater.

Chapter 5: Conclusions and Recommendation

References

Adugna E, Hymete A, Birhanu G and Ashenef A, 2020. Determination of some heavy metals in honey from different regions of Ethiopia. *Cogent Food & Agriculture*, *6*(1), 1764182.

Alengebawy A, Abdelkhalek ST, Qureshi SR and Wang MQ, 2021. Heavy metals and pesticides toxicity in agricultural soil and plants: Ecological risks and human health implications. *Toxics*, *9(3)*, 42.

Ali H, Khan E and Ilahi I, 2019. Environmental chemistry and ecotoxicology of hazardous heavy metals: environmental persistence, toxicity, and bioaccumulation. *Journal of Chemistry*, *2019*.

Alipoori S, Rouhi H, Linn E, Stumpfl H, Mokarizadeh H, Esfahani MR, Koh A, Weinman ST and Wujcik EK, 2021. Polymer-based devices and remediation strategies for emerging contaminants in water. *ACS Applied Polymer Materials*, *3*(2), 549-577.

Awuchi CG, Igwe VS and Amagwula IO, 2020. Nutritional diseases and nutrient toxicities: A systematic review of the diets and nutrition for prevention and treatment. *International Journal of Advanced Academic Research*, *6*(1), 1-46.

Bahrodin MB, Zaidi NS, Hussein N, Sillanpää M, Prasetyo DD and Syafiuddin A, 2021. Recent advances on coagulation-based treatment of wastewater: Transition from chemical to natural coagulant. *Current Pollution Reports*, *7*(3), 79-391.

Carreck NL, Dietemann V, Neumann P and Ellis JD, 2020. The coloss beebook: Global standards in honeybee research. *Journal of Apicultural Research*, *59*(3), 1-4.

Chai WS, Cheun JY, Kumar PS, Mubashir M, Majeed Z, Banat F, Ho SH and Show PL, 2021. A review on conventional and novel materials towards heavy metal adsorption in wastewater treatment application. *Journal of Cleaner Production*, *296*, 126589.

Chen XW, Wong JTF, Wang JJ and Wong MH, 2021. Vetiver grass-microbe interactions for soil remediation. *Critical Reviews in Environmental Science and Technology*, *51*(9), 897-938.

Crini G and Lichtfouse E, 2019. Advantages and disadvantages of techniques used for wastewater treatment. *Environmental Chemistry Letters*, *17*(1), 145-155.

Crini G, Lichtfouse, E, Wilson LD and Crini MN, 2019. Conventional and non-conventional adsorbents for wastewater treatment. *Environmental Chemistry Letters*, *17*(1), pp.195-213.

Dai Y, Zhang N, Xing C, Cui Q and Sun Q, 2019. The adsorption, regeneration and engineering applications of biochar for removal organic pollutants: a review. *Chemosphere*, *223*, 12-27.

Dey S, Haripavan N, Basha SR and Babu GV, 2021. Removal of ammonia and nitrates from contaminated water by using solid waste bio-adsorbents. *Current Research in Chemical Biology*, *1*, 100005.

Duru CE, Enedoh MC and Duru IA, 2019. Physicochemical assessment of borehole water in a reclaimed section of Nekede mechanic village, Imo State, Nigeria. *Chemistry Africa*, *2*(4), 689-698.

Fauziah S, Soekamto NH, Taba P and Amran MB, 2018, March. Selectivity of β-Sitosterol Imprinted Polymers as Adsorbent. In *Journal of Physics: Conference Series* 979 (1), 012059

Fu J, Chen L, Li J and Zhang Z, 2015. Current status and challenges of ion imprinting. *Journal of Materials Chemistry A*, *3*(26), 13598-13627.

Gałczyńska M, Gamrat R, Bosiacki M, Sotek Z, Stasińska M and Ochmian I, 2021. Micro and macroele-ments in honey and atmospheric Pollution (NW and Central Poland). Resources 2021, 10, 86.

Guo JJ, Huang XP, Xiang L, Wang YZ, Li YW, Li H, Cai QY, Mo CH and Wong MH, 2020. Source, migration and toxicology of microplastics in soil. *Environment International*, *137*, 105263.

Huang Y and Wang R, 2018. An efficient lithium ion imprinted adsorbent using multi-wall carbon nanotubes as support to recover lithium from water. *Journal of Cleaner Production*, *205*, 01-209.

Hussain RT, Ebraheem MK and Moker HM, 2012. Assessment of heavy metals (Cd, Pb and Zn) contents in livers of chicken available in the local markets of Basrah city, IRAQ. *Metabolism*, *12*, 13.

Ito R, Kawaguchi M, Sakui N, Okanouchi N, Saito K, Seto Y and Nakazawa H, 2009. Stir bar sorptive extraction within situ derivatization and thermal desorption–gas chromatography–mass spectrometry for trace analysis of methylmercury and mercury (II) in water sample. *Talanta*, *77*(4), 1295-1298.

Jakavula S, Biata NR, Dimpe KM, Pakade VE and Nomngongo, PN, 2020. A critical review on the synthesis and application of ion-imprinted polymers for selective preconcentration, speciation, removal and determination of trace and essential metals from different matrices. *Critical Reviews in Analytical Chemistry*, 1-13.

Janczura M, Luliński P and Sobiech M, 2021. Imprinting technology for effective sorbent fabrication: Current state-of-art and prospects. *Materials*, *14*(8), 1850.

Jang J, Kim M, Shin J, Yang D, Kim, M and Kim B, 2022. Experimental Study on Ion Transport in Microfluidic Electrodialysis Using Partially Masked Ion Exchange Membranes. *Micromachines*, *13*(3), 356.

Kumar LR, Yellapu SK, Tyagi RD and Zhang X, 2019. A review on variation in crude glycerol composition, bio-valorization of crude and purified glycerol as carbon source for lipid production. *Bioresource Technology*, *293*, 122155.

Lai W, Zhang K, Shao P, Yang L, Ding L, Pavlostathis SG, Shi H, Zou L, Liang D and Luo X, 2019. Optimization of adsorption configuration by DFT calculation for design of adsorbent: A case study of palladium ion-imprinted polymers. *Journal of Hazardous Materials*, *379*, 120791.

Liu R, Chi L, Wang X, Sui Y, Wang Y and Arandiyan H, 2018. Review of metal (hydr) oxide and other adsorptive materials for phosphate removal from water. *Journal of Environmental Chemical Engineering*, *6*(4), 5269-5286.

Marsidi N, Hasan HA and Abdullah SRS, 2018. A review of biological aerated filters for iron and manganese ions removal in water treatment. *Journal of Water Process Engineering*, *23*, 1-12.

Okereafor U, Makhatha M, Mekuto L, Uche-Okereafor N, Sebola T and Mavumengwana V, 2020. Toxic metal implications on agricultural soils, plants, animals, aquatic life and human health. *International journal of environmental research and public Health*, *17*(7), 2204.

Pérez-Botella E, Valencia S and Rey F, 2022. Zeolites in Adsorption Processes: State of the Art and Future Prospects. *Chemical Reviews*, *122(24)*, 17647-17695.

Płotka-Wasylka, J., Szczepańska N, de La Guardia M and Namieśnik J, 2016. Modern trends in solid phase extraction: new sorbent media. *TrAC Trends in Analytical Chemistry*, *77*, 23-43.

Raouf MS, Abdel; Raheim ARM, Abdul (2016). Removal of heavy metals from industrial wastewater by biomass-based materials: A Review. *Journal of Pollution Effects & Control*, 5(1), –180.

Rasheed T, Shafi, S, Bilal M, Hussain T, She F and Rizwan K, 2020. Surfactants-based remediation as an effective approach for removal of environmental pollutants—A review. *Journal of Molecular Liquids*, *318*, 113960.

Rezakazemi M, Khajeh A and Mesbah M, 2018. Membrane filtration of wastewater from gas and oil production. *Environmental Chemistry Letters*, *16*(2), 367-388.

Scheufele FB, Módenes AN, Borba CE, Ribeiro C, Espinoza-Quiñones, FR, Bergamasco R and Pereira NC, 2016. Monolayer–multilayer adsorption phenomenological model: kinetics, equilibrium and thermodynamics. *Chemical Engineering Journal*, *284*, 1328-1341.

Shakerian F, Kim KH, Kwon E, Szulejko JE, Kumar P Dadfarnia S and Shabani AMH, 2016. Advanced polymeric materials: Synthesis and analytical application of ion imprinted polymers as selective sorbents for solid phase extraction of metal ions. *TrAC Trends in Analytical Chemistry*,83, 55-69.

Tamjidi S, Moghadas BK, Esmaeili H, Khoo FS, Gholami G and Ghasemi M, 2021. Improving the surface properties of adsorbents by surfactants and their role in the removal of toxic metals from wastewater: A review study. *Process Safety and Environmental Protection*, *148*, 775-795.

Tariq FS, 2021. Heavy metals concentration in vegetables irrigated with municipal wastewater and their human daily intake in Erbil city. *Environmental Nanotechnology, Monitoring & Management*, *16*, p.100475.

Velusamy S, Roy A, Sundaram S and Kumar Mallick T, 2021. A review on heavy metal ions and containing dyes removal through graphene oxide-based adsorption strategies for textile wastewater treatment. *The Chemical Record*, *21*(7), 1570-1610.

Zhang G, Ali MM, Feng X, Zhou J and Hu L, 2021. Mesoporous molecularly imprinted materials: From preparation to biorecognition and analysis. *TrAC Trends in Analytical Chemistry*, *144*, 116426.

Zhou Z, Kong D, Zhu H, Wang N, Wang Z, Wang Q, Liu W, Li Q, Zhang W and Ren Z, 2018. Preparation and adsorption characteristics of an ion-imprinted polymer for fast removal of Ni (II) ions from aqueous solution. *Journal of Hazardous Materials*, *341*, 355-364.

Zvinowanda CM, Okonkwo JO, Sekhula MM, Agyei NM and Sadiku R, 2009. Application of maize tassel for the removal of Pb, Se, Sr, U and V from borehole water contaminated with mine wastewater in the presence of alkaline metals. *Journal of Hazardous Materials*, *164*(2-3), 884-891.

Chapter 2: Literature review

2.1. Preamble /introduction

Human exposure to toxic metal has long lasting health effects including cancer amongst other diseases due to their persistence in human body and are composed of long life that last for decades (Ayangbenro and Babalola, 2017; Rahman et al., 2019). The prime topic of this chapter is reviewing the occurrence of heavy metals in honey and wastewater, health effects, detection and removal methods and molecular imprinting in details.

2.1.1. Occurrence of trace elements in wastewater and honey

These heavy metals may be found in wastewater because of human or natural activity (Dhaliwal et al., 2020: Sun et al., 2019). Geographical processes like volcanic eruptions, rock weathering, and leaching into rivers, lakes, and oceans are the sources of trace metals in the surrounding (Gautam et al., 2016: Liu et al., 2019: Weldeslassie et al., 2018). Agoro et al. (2020) assessed Cu, Cd, Fe and Pb levels in wastewater and sewage sludge in the Eastern Cape and reported concentrations of 1.17 mg/L, 14 mg/L, 69.789 mg/L and 0.999 mg/L, respectively.

The composition of honey depends on nectar and honeydews, it composed of carbohydrate such as glucose, sucrose, fructose and maltose as well as flavonoid, minerals, vitamins and pollen grains (Pavlova et al., 2018: Bobis et al., 2020). Primary nectar and honeydew are the sources of the mineral components of honey. Honey's mineral content is determined by the minerals that plants naturally absorb from the soil and surrounding environment. It is known that honey pollutes the environment. Because honey bees can travel over an area of about 50 km^2 and come into interaction with the ground, water, and air, the concentration of trace elements in honey corresponds to the amount of that region (Ogidi et al., 2020;Jovetić et al., 2017). Trace elements are the ash essence of honey, it contains elements such as Zn, Pb and Cd. Zinc is essential for metabolism but at above maximum allowable limit, it is toxic like lead and cadmium (Vetrimurugan et al., 2017). Because bees inhabit broad areas, they are more exposed to chemicals in the environment. contaminants on or in fodder plants, soil, water, and air are reflected in honey. The biological and geographic origin of honey influences the amount of hazardous metals present in it (Mračević et al., 2020). Measurable concentrations of trace elements like Zn (0.76 to 3.41 mg/L), Pb (0.05 to 3.81 mg/L), and Cd (15.00 to 36.40 mg/L) have been detected in honey by Barth et al. (2020).

2.1.2. Health effects

Trace elements have negative impact on human health, for example imbalanced Zn and Cd can interfere with glucose level, potentially leading to cardiovascular diseases (Jomova at el., 2022:

Leal et al., 2023). Trace elements accumulate in brain, heart, liver and kidneys, which are important organs in the human body. The health risk associated with toxic elements depend on the concentration of this elements and the length of exposure (Yousefi et al., 2021). Table 2.1 shows toxicity of metals in honey and wastewater.

Table 2. 1: Metal toxicity of human in wastewater and honey.

Metal	Toxicity effect	Permissible limit in wastewater ($mg\ L^{-1}$)	Ref	Permissible limit in honey ($mg\ L^{-1}$)	Ref
Cadmium	Lung, liver and kidney damage	0.10	Kinuthia et al., 2020	0.2	Aghamirlou et al., 2015
Lead	Lung and liver damage	5.0		0.3	
Zinc	Anaemia and nausea	2	Agoro et al., 2020	1	

2.2. Detection method

A convenient detection method is needed to monitor heavy metal concentrations. Different methods are used to detect metal in honey/wastewater sample (Bommuraj et al., 2019; Donner et al., 2019; Henriques et al., 2019; Kosek et al., 2019; Sixton et al., 2019). These analyses are most important to guarantee the honey and wastewater purity and safety. Several detection approaches, such as spectrophotometry, electrochemistry, inductively coupled plasma-optical emission spectrometry (ICP-OES) and atomic absorption spectroscopy (AAS), have been developed for heavy metal detection. Some of the techniques are extremely sensitive and precise; Table 2.2 shows various heavy metal detection levels.

Table 2. 2: Methods for detection of heavy metals.

Methods	Metal detected	Detection level (mg kg^{-1})	Sample	Reference
	Cd	0.005		
Microwave plasma-atomic emission (MIP-AES)	Pb	0.123	honey	Malhat et al., 2019
	Zn	0.244		
	Cd	0.030		
Atomic absorption spectroscopy (FAAS, GFAAS)	Zn	14.62	honey	Adugna et al., 2020
	Pb	2.53		
	Zn	5.39		
Plasma optical emission spectroscopy (ICP-OES)	Pb	1.50	honey	Leblebici and Aksoy (2008)
	Cd	0.24		
	Zn	0.1		
Sensor	Cd	0.1	wastewater	Hwang et al., 2018
	Pb	0.2		

2.3 Removal of toxic metals

Water and honey contamination is a major problem.; therefore, the effective development of suitable methods for extraction of toxic metals in honey and water is necessary.

2.3.1. Chemical precipitation

The transformation of substances dissolved in water into solid particles is known as chemical precipitation. Ionic components are extracted from water by chemical precipitation by adding counter-ions to lessen their solubility (Dayarathne et al., 2021: Priya 2021 et al., Wang et al., 2021).

Numerous variables affect the effectiveness of the chemical precipitation process, such as the kind and amount of ionic metals in the solution, the precipitating agent used, the pH of the solution, and the existence of additional precipitation-related components that could interfere with the reaction (Chen et al., 2018: Sis & Uysal 2014: Wanga et al., 2019: Sun at el. 2020). Table 2.3 shows chemical precipitation methods that were used to remove trace elements.

Table 2. 3: Chemical precipitation removal of heavy metals.

Heavy metal	Precipitant	Removal efficiency (%)	Reference
Cu and Zn	Lime	99.65 and 99.00	Chen et al., (2018)
Zn	Vermiculite	97.00	Sis & Uysal, (2014)
Fe, Cr and Vo	Magnesium hydroxy carbonate	99.90	Zhanga & Duan (2020)
Hg, Cd, Cu and Pb	Dipotassium salt of 1,3 benzenediamidoethanethiol	90.00	Pohl (2020)
Hg, Pb and Cu	Sulfide yeasts	-	Sun et al., (2020)
Cu	Bicarbonate activated hydrogen peroxide	78	Wang et al., (2019)

2.3.2. Membrane filtration

Membrane filtrations allows water to pass through a membrane materials through a membrane materials due to a pressure difference and remove impurities (Lee et al., 2022: Ling et al 2017: Yang et al., 2019). Water components with a circumference greater than the membrane pore size are deposited on the surface, according to the size of the particles thatneed to be separated (Gao et al., 2018: Gouda et al., 2023: Lie et al., 2020). The benefits of membrane filtration are that there are no phase changes involved, the feed and product streams stay liquid, the processes can operate efficiently at low temperatures, and there is little energy required. The drawbacks of membrane filtration are that the processes are susceptible to membrane fouling effects, which cause the permeate flux to decrease, and costly cleaning and regeneration schemes may be required (Aktij et al., 2020: Hube et al., 2020). The high flow rates of cross-flow feed may shear sensitive materials It might be expensive to purchase equipment. Inadequate performance during separation may arise if the membrane production process is not properly managed, from membranes with a significant pore size dispersion (Afome at al., 2019: Germikli et al., 2020). Table 2.4 shows membrane filtration removal methods of heavy metal including removal efficiency.

Table 2. 4: Membrane filtration removal method of heavy metals.

Membrane	Heavy metal	Medium	Removal efficiency	Reference
Nano fibrous metal organic framework	Pb	Wastewater	18-37 %	Efome et al., (2019)
PAN/PANI-nylon core-shell nanofibers	Pb Cd	Aqueous solution	87.57 % 86.00 %	Almasion et al., (2018)
Polymer	Pb, Cd and Cu	wastewater	90.00 %	Cao et al., (2018
Cu-ETDA	Cu	wastewater	71.40 %	Li et al., (2020)
N-methyl-D-glucamine	As and B	Water	86.00 %	Çermikli et al., (2020)
Cellulose nitrate	Cd, Co, Cu, Ni and Pb	Water and food	95.00%	Gouda et al., (2023)

2.3.3 Adsorption

A material (adsorbate, or sorbate) is gathered surface-level of a strong material (adsorbent, or sorbent) through the process of adsorption. Adsorbate may exist in a gaseous or liquid phase. Unsaturated strengths at the strong surface that can frame bonds with the adsorbate are the driving constraint for adsorption (Basu et al., 2021; Han et al., 2022; Abu Taleb et al., 2022). Usually, these advantages are reversible or electrostatic (van der Waals intelligent). Coordination of the irreversible electron exchange between the sorbent and the sorbate is a more pragmatic intuitive concept. The nature of this interaction determines how easy or difficult it is to expels (desorb) the adsorbate in order to recover the adsorbent and retrieve the adsorbate. The degree of surface contact and relative accessibility of a single component in a bolster blend determine the unique character of the adsorbent (Lonappan et al., 2018). The allocation between the liquid and strong stages serves as the isolating instrument, and the strong is the mass-separating operator. To invert the process and recover the sorbent, an energy-separating operator is used, usually a weight or temperature change. Adsorbents are categorized into three categories: natural, agricultural, and synthetic (Chakroborty et al., 2022; Ghorbani et al., 2020; Osagie et al., 2021; Syafiuddin et al., 2020; Xue et al., 2022). Because of their high effectiveness, metal recovery, generative nature, and economy, these adsorbents are found to be encouraging in the removal of toxic metals (Jatoi et al., 2021). Molecular imprinted polymers and ion imprinted polymers, which fall within the molecular imprinting category, are examples of synthetic adsorbents (Balouch et al., 2019: Liang et al., 2020). The capacities a selection of the adsorptive materials used to extract heavy metals are shown in Table 2.5.

Table 2.5: Adsorbents used to remove heavy metals.

Metal ion	Adsorbent	Adsorption capacity (mg/g)	*Reference*
Cu and Pb	Porous lignin	276.00 and 332.00	Wang et al., (2020)
As	Iron CS microspheres	120.70	Lebo et al., (2020)
As	Magnetic CS coated GO	45.00	Sherlala et al., (2019)
Cd	CS- pectin gel beads	117.60	Shao et al., (2021)
Cd	CS- based hydrogels	234.80	Viela et al., (2019)
Pb and Cd	Coconut waste	263.00 and 285.00	
Hg	Black oak bark	400.00	Alalwan et al., (2020)
Cr	Wheat brans	310	
Fe and Zn	Rambutan peels	17.40 and 14.00	Low et al., (2023)
Pb	Ion imprinted polymer	40.02	Huang et al., (2019)

2.4. Molecular imprinting

Molecular imprinting was first discovered by Polyakov (1931). He polymerized silica carbonate in the presence of a specific porogen (e.g., xylene or toluene) and the resulting silica demonstrated preferential binding capacity for the solvent in the solution. Frank Dickey (1955) polymerized silica gels when dyes are present and observed that silica prepared in the presence of one of several dyes showed higher selectivity than with other dyes (Lofgreen & Ozin, 2014).

After two decades of the MIPs discovery, there was a decrease in the study of molecular imprinting of silica because of the introduction of the organic molecular imprinting. Cross-linker was introduced in 1972 to improve the adsorption capacity by Takagish and Kotz. In the 1970s and 1980s, Wulff's group published many papers of organic MIPs capable of selective adsorption of enantiomers of glyceric acid. Mosh and Arshady (1981) reported organic ion imprinted polymer that was prepared using non-covalent approach.

By using a process called molecular imprinting, polymers with unique recognition sites that are made to resemble a target ion or molecule in terms of size, shape, or functional group can be produced (Amatatongchai et al., 2019: Dar et al., 2020: Zouaoui et al., 2020). The functional monomer and the template must form a complex in order for this process to proceed, which is then followed by polymerization and cross-linking. Various methods can be used to remove the template after synthesis, such as extraction by high-pressure hot water, organic solvents, or microwave irradiation (Sun et al., 2017, Wang et al., 2018: Zhang et al., 2021: Liang et al., 2020: Zhu et al., 2021). As a result, the resulting MIPs bind to the template and similar molecules in a mixture only because their binding sites are compatible with the template (Herrera-Chacón et al., 2021).

Ion imprinting techniques are derived from the MIP technique, using an ion instead of a molecule. Nishide et al. (1976) reported the metal ion imprinting by complexing with Hg^{2+}, Ni^{2+}, Zn^{2+}, Co^{2+}, Cu^{2+} and Cd^{2+} with poly(4-vinylpridine) and 1,4-dibromobutene as monomer and cross-linker respectively. Figure 2.1 schematically shows the principles of the polymerization process.

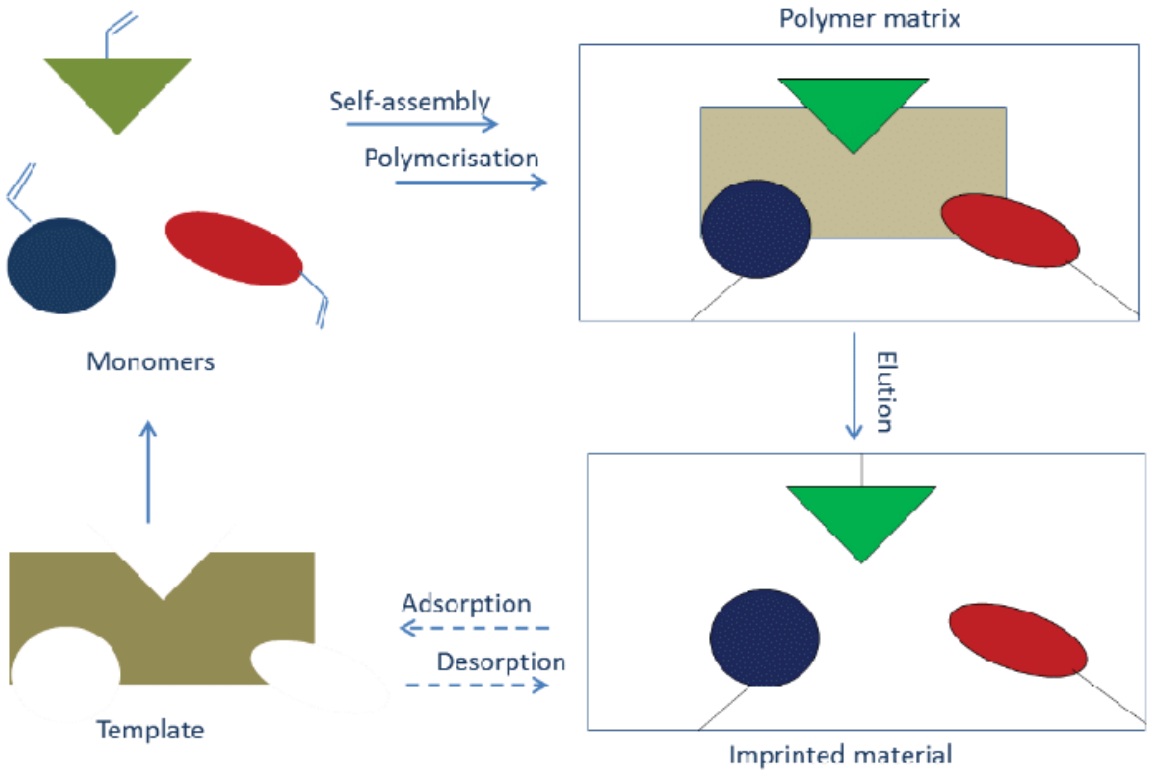

Figure 2.1: General principle of imprinting polymers.

2.5. Components of IIPs

2.5.1. Template

The template molecule is crucial in ion imprinting processes, as its ion structure dictates the selection of a useful monomer for synthesis. The chemical bonds between the template and functional monomer are essential for successful ion recognition (Suriyanarayanan et al., 2017). Under the circumstances of polymerization and synthesis, it is critical that the template be stable and chemically inert (Sun et al., 2017).

2.5.2. Functional monomer

Functional monomers are responsible for creating recognition sites on the imprinted polymer by their interaction with the template molecule (Mier et al., 2021). Selection of an appropriate functional monomer determines the structure of the binding site, and the quantity of monomer used affects the number of recognition sites. However, an excessive amount of functional monomer can cause non-specific adsorption site formation on the ion imprinted polymer (Chen et al., 2020: Polyakova et al., 2016). The bond between the monomer and ion can be either covalent or non-covalent, and it plays a crucial role in achieving a highly selective recognition site (Zhang et al., 2021). Figure 2.2. Shows examples of functional monomers.

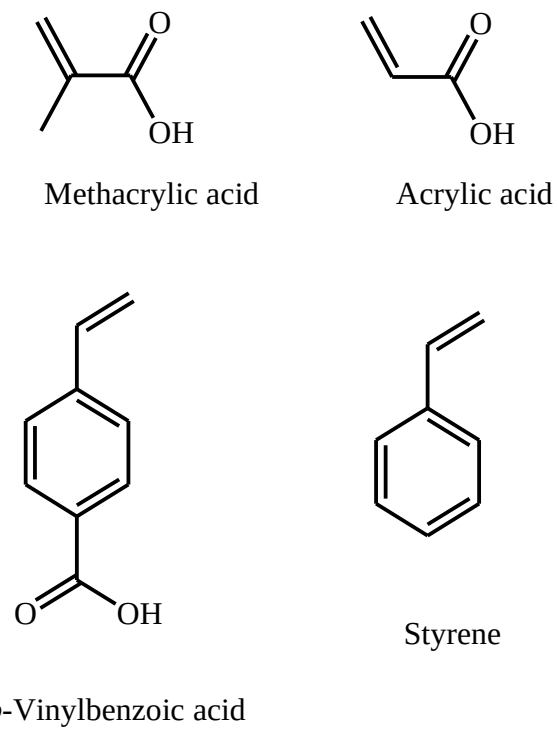

Figure 2.2: Structure of common function monomers.

2.5.3. Cross-linker

The primary functions of a cross-linker are to (i) regulate the polymer matrix morphology, (ii) enhance the stability of the binding sites formed by imprinting, and (iii) provide mechanical strength to the polymer matrix (Ersoy et al., 2016: Mahani et al., 2021). During polymerization, a higher ratio of cross-linkers is generally favoured to achieve good porosity (Masoumi et al., 2021). Figure 2.3 illustrates commonly utilized cross-linkers.

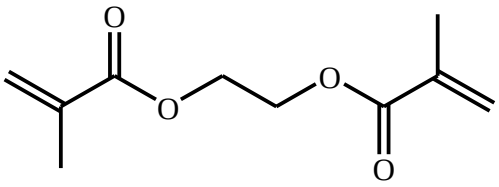

Ethylene gylcol dimethacrylate

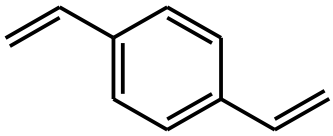

Divinylbenzene

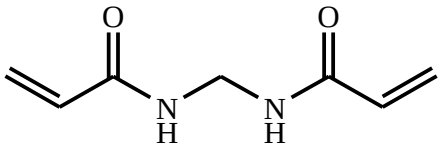

N,*N*'-Methylenebisacrylamide

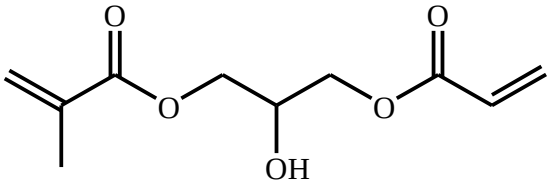

3-(Acryloyloxy)-2-hydroxylpropyl methacrylate

Figure 2.3: Examples of IIP cross-linkers.

2.5.4. Solvent (porogen)

Porogens are solvents employed in the polymerization process, wherein they must can dissolve the template, cross-linker, functional monomer, and initiator. The polarity of the porogen contributes to the replacement of the template with the functional monomer (Liu et al., 2019: Madikizela et al., 2016).

2.5.5. Initiator

The initiator promote reaction during polymerization. The initiator generates radicals during its decomposition to initiate reaction (McKenzie et al., 2019). Figure 2.4 shows examples of initiators.

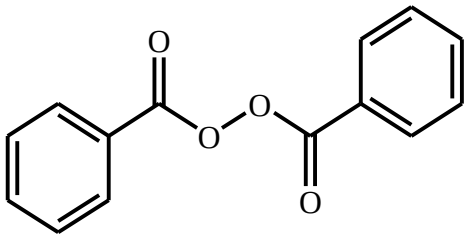

Benzoylperoxide

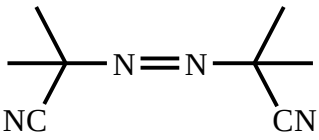

Azobis(isobutyronitrile)

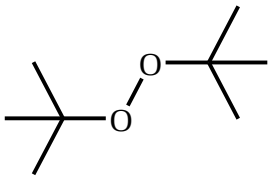

Di-*tert*-butylperoxide

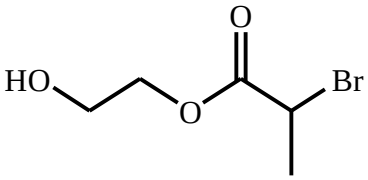

2-Hydroxyethyl 2-bromopropionate

Figure 2.4: Commonly used initiators.

2.6. Imprinting approaches

Imprinted polymers can be synthesized using three distinct approaches: covalent, non-covalent, and semi-covalent.

2.6.1. Covalent approach

In the covalent approach, a chemical connection develops between a functional monomer and the template molecule by sharing electrons before the polymerization process. This is depicted in Figure 2.5 (Xie et al., 2021). Elution, or the separation process, is achieved through a chemical reaction where the obtained imprinted polymers (IIPs) selectively rebind to the template molecule via covalent interactions. The monomer/template complex remains stable, and various conditions can be employed in this approach (Hasanah et al., 2021).

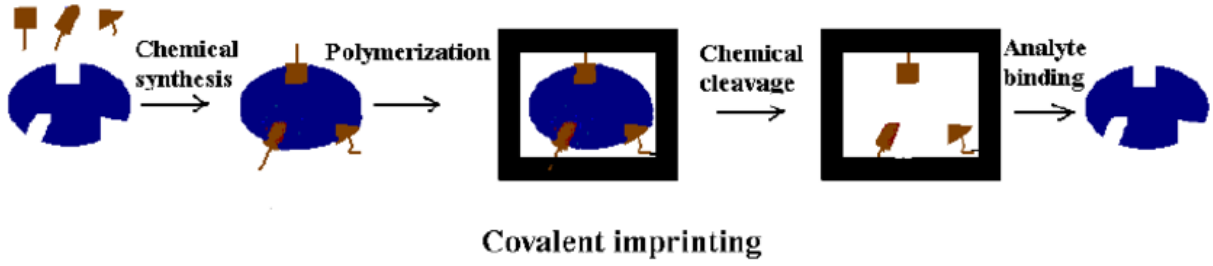

Figure 2.5: Covalent ion imprinting (Yan et al., 2006).

2.6.2. Non-covalent approach.

The non-covalent approach entails the establishment of weak interactions like van der Waals forces or hydrogen bonds, and between the template and an appropriate monomer before polymerization. This is achieved by mixing the template and monomer together (Kumar et al., 2021: Shen et al., 2021). Elution of the template is accomplished by solvent washing. This approach is widely employed due to its advantages, including easy preparation and efficient removal of the template from the polymer (Zhang et al., 2021). Figure 2.6 illustrates a general depiction of non-covalent imprinting.

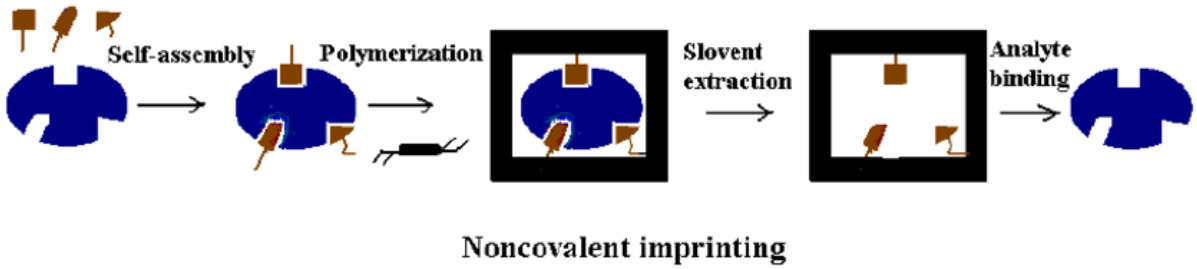

Figure 2.6: Non-covalent ion imprinting (Yan et al., 2006).

2.6.3. The semi-covalent approach

This method incorporates components from the non-covalent and covalent techniques. It involves the capacity of the template to rebind with the polymer, akin to non-covalent imprinting, and the production of a stable and stoichiometric complex, akin to covalent imprinting (Iacob et al., 2018).

2.7. Polymerization mechanisms

2.7.1. Free radical polymerization

Under particular reaction conditions, one method for performing free radical polymerization is when a solution or in bulk. Three steps are involved in the mechanism of free radical polymerization: initiation, propagation, and termination.

2.7.1.1. Initiation

Chain initiation in free radical polymerization occurs in two stages. First, an initiator is dissociated, resulting in formation of free radicals, as depicted in Figure 2.7. The second stage involves the addition of a monomer to these free radicals. Benzoyl peroxide and 2,2'-azo-bis-(isobutyrylnitrile) (AIBN) are commonly used as radical initiators (Liang et al., 2019: Pirman et al., 2021). Both compounds usually dissociate into two one-electron radicals. These radicals react with an alkene monomer by forming a new bond with one of the electrons of the alkene monomer, while the remaining electron becomes a new free radical (Hussein et al., 2020: Mavroudakis et al., 2021).

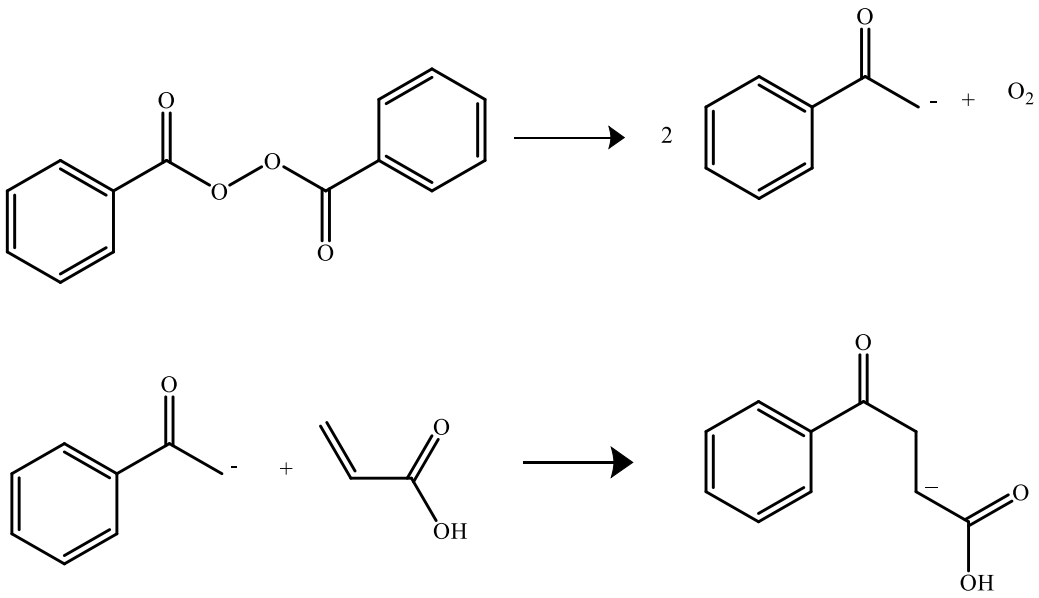

Figure 2.7: Schematic representation of initiator decomposition.

2.7.1.2. Propagation

Propagation in free radical polymerization refers to the continuous polymer chain lengthening by the continuous reaction of monomers with the active (radical) centres. This addition of each monomer occurs rapidly, typically within a millisecond. Within a minute, thousands of monomer additions can occur (Mueller et al., 2014).

2.7.1.3. Termination

Termination in free radical polymerization refers to the deactivation of the radical active centres. At this point, two mechanisms could happen: combination and disproportionation. Combination is the process of joining two expanding strands to create a single polymer chain. Conversely, disproportionation is the process of moving a hydrogen atom from one polymer chain to another, which creates distinct end groups. Zhang et al. (2014) and Konkolewicz et al. (2013).

2.7.2. Controlled radical polymerization) using reversible addition-fragmentation chain transfer agent

One of the most popular and adaptable synthesis techniques is called RAFT (Reversible Addition-Fragmentation Chain Transfer) polymerization (Hu et al., 2020). According to Gyorgy et al. (2021) and Yildiko et al. (2021), it has a number of benefits, such as (i) compatibility with a broad range of monomers, (ii) operation at mild conditions, (iii) feasibility of polymerization by various methods, and (iv) fine control over the material structure. The qualities of IIPs are improved by this technique.

2.8. Formats of IIPs

Imprinted polymers (IIPs) can be fabricated in various formats using different techniques, depending on their intended applications. The choice of format and fabrication technique directly impact the adsorption capacity and the accessibility of binding cavities within the IIPs.

2.8.1. Bulk polymerizations

Bulk polymerization, sometimes referred to as mass polymerization, uses a reaction mixture without a porogen (solvent) that consists of a monomer and a soluble initiator. In this combination, polymerization occurs. After that, grinding and sieving procedures are usually used to the resultant polymer (Suzuki et al., 2012; Wang et al., 2019).

2.8.2. Emulsion polymerization

A polymer in the form of monodispersed particles, usually with a size range of tens to hundreds of nanometers, is produced via emulsion polymerization. An oil-in-water emulsion is typically used in this procedure, where the monomer droplets, which function as the oil phase, are distributed throughout a continuous water phase. During polymerization, stable emulsion droplets are formed.

2.8.3. Suspension polymerization

Suspension polymerization is a process that creates polymers by vigorously stirring a polymeric reagent into a solvent. This procedure causes monomer droplets to separate, which then creates a homogeneous suspension and ultimately produces polymer beads (Trojanowska et al., 2017).

2.8.4. Precipitation polymerization

When monomers and cross-linkers in a homogeneous system experience radical initiation, polymerization takes place. Chain propagation then takes place, creating a polymer network that precipitates in an unsuitable solvent. A narrow size distribution of polymer particles is formed as a result of the precipitation process, without the use of any stabilizer or surfactant (Sajini and Mathew, 2021; Nishizawa et al., 2020). Figure 2.8 provides an overview of the general polymerization process involved.

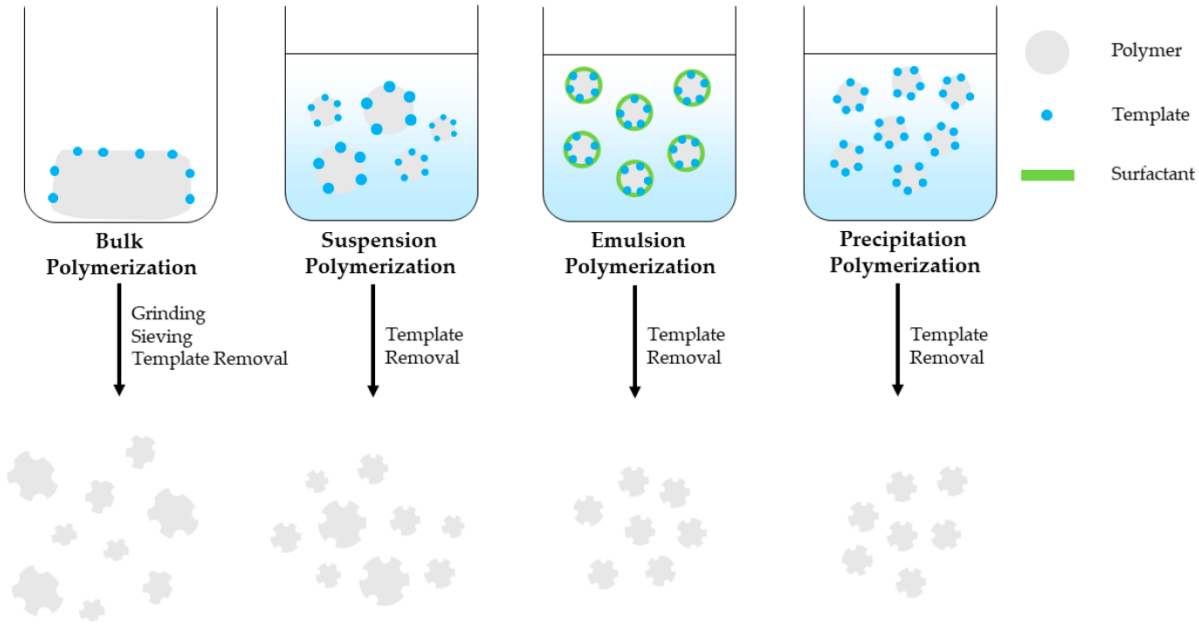

Figure 2. 8: Polymerization process

2.9. Application of IPPs

Among the applications of IIP are catalysis and synthesis reactions, selective extraction, the removal and separation of contaminants from biological and environmental samples, chemical analysis, and the detection of metal ions in a variety of materials.

2.9.1 Sensors

Electrochemical and optical sensors are among the newer applications for IIP polymers. IIP polymers are being used as recognition elements in a new generation of electrochemical sensors that produce signals (Sala et al., 2022: Wang et al., 2021). Polymer particles are inserted into a PVC film or a mixture of carbon powder to construct the electrochemical sensor as a modified ion-selective electrode. Optical sensors have also been made using IIP polymers. Cu(II) ions and Al(III) have been detected using optical sensors based on IIP polymers. Modified glass carbon electrode (GCE) Pt(IV) ions in the catalyst and plant samples were detected using an ammeter using the Pt-IIP film made via in situ polymerization.

2.9.2. Membrane

Thanks to developments in polymer science, membrane technology—which includes wastewater treatment, food processing, and environmental applications—is showing great promise. Ion-imprinted membranes, or IIMs, have drawn particular interest as a result (Yu et al., 2022: Zeng et al., 2019: Chen et al., 2022). Their easy operation, low energy and time consumption, and convenient preparation are their defining features. Several initiatives have been made to enhance the mechanical stability, flexibility, and hydrophilic and hydrophilic permeability of membranes. Certain metal ions, for example, are too tiny to be efficiently recovered or separated using IIM porous methods; instead, membrane adsorption and polymer-reinforced ultrafiltration have been developed. There have been several approaches put forth for creating polymeric films imprinted with metal ions (Ma et al., 2017: Xia et al., 2018: Zahid 2018). Modulation Zn(II)-IIM is done by applying the water-in-oil (W/O) emulsion polymerization surface printing process. Crown ether is used as a functional monomer and lithium as a model ion in the surface method imprint polymerization of Ag nanoparticles to create a nanocomposite membrane imprinted with ion (IINcMs). IIM can also be prepared in a single step without the need for extra crosslinking mixing using an effective and straightforward approach (Zhang et al., 2020; Eddaif et al., 2019). By directly combining poly (vinylidene fluoride) (PVDF) with metal-polymer complexes including matrix ions and amphoteric copolymers, selective Pt(IV)IIM films were created. Despite developments in membrane preparation techniques, there is only one. They are known to have a few real-world uses. Layer-by-layer self-assembly technology (LbL) is used to create Cu(II) surface Ion-imprinted composite films (Liu et al., 2019: Zhang et al., 2019).

Pre-concentration, analyte conversion, or the removal of any interferences are typically required steps in analytical methods. These steps ensure that the analyte is in a form that is

appropriate for the detection method. Solid phase extraction (SPE) is one of the many separation techniques used for this purpose, and analysts are particularly interested in it because of its simplicity, adaptability, ease of automation, and small size (Arabi et al., 2020: Faraji et al., 2019). Excellent quality options in the realm of selective absorption are offered by advanced IIP material. When competing ions are present, printing alters the printed material's ion recognition behavior, which is reflected in the polymer's selectivity. In addition, IIP polymers are helpful in speculative analysis due to their strong affinity for metallic forms. Robust adsorption IIP's capacity to remove harmful metals from biological fluids and purify various hazardous substances contaminated surface water and wastewater is advantageous (Guo et al., 2017: Zheng et al 2020).

IIP is applicable to both dynamic and static processes. Analytes can be effectively separated from a variety of materials using the static approach, which involves leaving the absorbent in making contact with the sample for a set period of time (Larki et al., 2021: Xie et al 2020). A magnetic magnet can be used to solve the absorbent and solution separation issue. IIP layers and an external magnet are used to cover the nanoparticles (Hemmati et al., 2018: Mendeles et al., 2020). The dynamic method's benefits include its simplicity of use, low reagent requirements, quick separation times, and wide range of adsorbent applications (He et al., 2017: Tang et al., 2020). Moreover, the sample integration and miniaturized pre-treatment made possible by the IIP online flow system enable the detection of analytes utilizing sensitive spectroscopic techniques (Yu et al., 2020: Faraji et al., 2019).

Primarily uses of IIP deal with the separation of metal ions that are extremely harmful to living things, such as Tl(III), CH3Hg(I), Pb(II), Cd(II), and Hg(II), before identifying them using various methods. Traces of Cd(II) have been extracted from food, water, and serum samples using polymers imprinted with the metal (Hu et al., 2021: Wang et al., 2019). Because heavy metal ions have a low affinity for ion exchange resin, heavy metal removal from wastewater treatment is challenging (Fu et al., 2022: Li et al., 2017). The most efficient method for removing Cd(II) and Hg(II) ions from wastewater has been determined to be a random copolymer of methacrylate and metha-crylamide (Wang et al., 2020: Zhao et al., 2018).

2.10. Summary

It is important to synthesize material for treating honey and wastewater, since natural adsorbent are not selective like coconut but to synthesize a new material which is specified for certain trace elements it would be better and the removal efficiency will increase. Commercial honey

also contains trace elements but most of them are below maximum allowable limits. Most of the adsorbent that are present have low removal percentage of trace element due to low specificity and selectivity, most of this adsorbent can be used once and are not economic efficiency since some of the reagents are expensive.

Due to their high specificity and selectivity, stability under extreme conditions, extended shelf life, and economic efficiency they can be reused over seven times with removal efficiencies above 80% ion imprinted polymers provide several appealing features.

References

Abu Taleb M, Halawani R, Neamtallah A, Kumar R and Barakat M, 2022. Hybrid bioadsorbents for heavy metal decontamination from wastewater: A review. *International Journal of Materials Technology and Innovation, 2(1),* 5-19.

Adugna E, Hymete A, Birhanu G and Ashenef A, 2020. Determination of some heavy metals in honey from different regions of Ethiopia. *Cogent Food & Agriculture*, *6*(1), 1764182.

Aghamirlou HM, Khadem M, Rahmani A, Sadeghian M, Mahvi AH, Akbarzadeh A and Nazmara S, 2015. Heavy metals determination in honey samples using inductively coupled plasma-optical emission spectrometry. *Journal of Environmental Health Science and Engineering*, *13*(1), 1-8.

Agoro MA, Adeniji AO, Adefisoye MA and Okoh OO, 2020. Heavy metals in wastewater and sewage sludge from selected municipal treatment plants in Eastern Cape Province, South Africa. *Water*, *12*(10), 2746.

Aktij SA, Zirehpour A, Mollahosseini A, Taherzadeh MJ, Tiraferri A and Rahimpour A, 2020. Feasibility of membrane processes for the recovery and purification of bio-based volatile fatty acids: A comprehensive review. *Journal of Industrial and Engineering Chemistry*, 81, 24-40.

Alalwan HA, Kadhom MA and Alminshid AH, 2020. Removal of heavy metals from wastewater using agricultural byproducts. *Journal of Water Supply: Research and Technology-Aqua, 69(2),* 99-112.

Almasian A, Giahi M, Fard GC, Dehdast SA and Maleknia LJCEJ, 2018. Removal of heavy metal ions by modified PAN/PANI-nylon core-shell nanofibers membrane: filtration performance, antifouling and regeneration behavior. *Chemical Engineering Journal*, *351*, 1166-1178.

Altarelli M, Ben-Hamouda N, Schneider A and Berger MM, 2019. Copper deficiency: causes, manifestations, and treatment. *Nutrition in Clinical Practice*, 34(4), 504-513.

Amatatongchai M, Sroysee W, Sodkrathok P, Kesangam N, Chairam S and Jarujamrus P, 2019. Novel three-dimensional molecularly imprinted polymer-coated carbon nanotubes (3D-CNTs@ MIP) for selective detection of profenofos in food. *Analytica Chimica Acta, 1076*, 64-72.

Arabi M, Ostovan A, Bagheri AR, Guo X, Wang L, Li J, Wang X, Li B and Chen L, 2020. Strategies of molecular imprinting-based solid-phase extraction prior to chromatographic analysis. *TrAC Trends in Analytical Chemistry*, 128, 115923.

Ayangbenro AS and Babalola OO, 2017. A new strategy for heavy metal polluted environments: a review of microbial biosorbents. *International journal of environmental research and public health*, *14*(1), 94.

Bartha S, Taut I, Goji G, Vlad IA and Dinulică F, 2020. Heavy metal content in polyfloralhoney and potential health risk. A case study of Copșa Mică, Romania. *International Journal of Environmental Research and Public Health*, *17*(5), 1507.

Basu S, Dutta A, Mukherjee SK and Hossain ST, 2021. Exploration of green technology for arsenic removal from groundwater by oxidation and adsorption using arsenic-oxidizing bacteria and metal nanoparticles. In *New Trends in Removal of Heavy Metals from Industrial Wastewater* 177-211.

Biswas TK, Yusoff MM, Sarjadi MS, Arshad SE, Musta B and Rahman ML, 2021. Ion-imprinted polymer for selective separation of cobalt, cadmium and lead ions from aqueous media. *Separation Science and Technology*, 56(4), 671-680.

Bobis O, Moise AR, Ballesteros I, Reyes ES, Durán SS, Sánchez-Sánchez J, Cruz-Quintana S, Giampieri F, Battino M and Alvarez-Suarez JM, 2020. Eucalyptus honey: Quality parameters, chemical composition and health-promoting properties. *Food chemistry*, *325*, 126870.

Bommuraj V, Chen Y, Klein H, Sperling R, Barel S and Shimshoni JA, 2019. Pesticide and trace element residues in honey and beeswax combs from Israel in association with human risk assessment and honey adulteration. *Food chemistry*, *299*, 125123.

Cao DQ, Song X, Fang XM, Yang WY, Hao XD, Iritani E and Katagiri N, 2018. Membrane filtration-based recovery of extracellular polymer substances from excess sludge and analysis of their heavy metal ion adsorption properties. *Chemical Engineering Journal*, *354*, 866-874.

Çermikli E, Şen F, Altıok E, Wolska J, Cyganowski P, Kabay N, Bryjak M, Arda M and Yüksel M, 2020. Performances of novel chelating ion exchange resins for boron and arsenic removal from saline geothermal water using adsorption-membrane filtration hybrid process. *Desalination*, *491*,114504.

Chakraborty R, Asthana A, Singh AK, Jain B and Susan ABH, 2022. Adsorption of heavy metal ions by various low-cost adsorbents: a review. *International Journal of Environmental Analytical Chemistry*, *102(2)*,342-379.

Chen L, Dai J, Hu B, Wang J, Wu Y, Dai J, Meng M, Li C and Yan Y, 2020. Recent progresses on the adsorption and separation of ions by imprinting routes. *Separation & Purification Reviews*, *49*(4), 265-293.

Chen L, Dai J, Hu B, Wang J, Wu Y, Dai J, Meng M, Li C and Yan Y, 2020. Recent progresses on the adsorption and separation of ions by imprinting routes. *Separation & Purification Reviews*, 49(4), 265-293.

Chen Q, Yao Y, Li X, Lu J, Zhou J and Huang Z, 2018. Comparison of heavy metal removals from aqueous solutions by chemical precipitation and characteristics of precipitates. *Journal of water process engineering*, *26*, 289-300.

Chen X, Li F, Du H, Liu X, Liu S and Zhang J, 2020. Fuzzy health risk assessment and integrated management of toxic elements exposure through soil-vegetables-farmer pathway near urban industrial complexes. *Science of the Total Environment*, 142817.

Dalezios NR, Angelakis AN and Eslamian S, 2018. Water scarcity management: part 1: methodological framework. *International Journal of Global Environmental Issues*, *17*(1), 1-40.

Dar KK, Shao S, Tan T and Lv Y, 2020. Molecularly imprinted polymers for the selective recognition of microorganisms. *Biotechnology Advances*, *45*, 107640.

Dayarathne, HNP, Angove MJ, Aryal, R, Abuel-Naga H and Mainali B, 2021. Removal of natural organic matter from source water: Review on coagulants, dual coagulation, alternative coagulants, and mechanisms. *Journal of Water Process Engineering*, 40, 101820.

Dhaliwal SS, Singh J, Taneja PK and Mandal A, 2020. Remediation techniques for removal of heavy metals from the soil contaminated through various sources: a review. *Environmental Science and Pollution Research*, *27*(2), 1319-1333.

Dickey FH, 1955. Specific adsorption, *Journal of Physical Chemistry*, ***59***, 695–707.

Donner MW, Arshad M, Ullah A and Siddique T, 2019. Unravelled keratin-derived biopolymers as novel biosorbents for the simultaneous removal of multiple trace metals from industrial wastewater. *Science of The Total Environment, 647,* 1539-1546.

Eddaif L, Shaban A and Telegdi J, 2019. Sensitive detection of heavy metals ions based on the calixarene derivatives-modified piezoelectric resonators: A review. *International Journal of Environmental Analytical Chemistry*, *99*(9), .824-853.

Efome JE, Rana D, Matsuura T and Lan CQ, 2019. Effects of operating parameters and coexisting ions on the efficiency of heavy metal ions removal by nano-fibrous metal-

organic framework membrane filtration process. *Science of The Total Environment*, *674*, pp.355-362.

Ersoy ŞK, Tütem E, Başkan KS, Apak R and Nergiz C, 2016. Preparation, characterization and usage of molecularly imprinted polymer for the isolation of quercetin from hydrolyzed nettle extract. *Journal of Chromatography B*, *1017*, 89-100.

Faraji M, Yamini Y and Gholami M, 2019. Recent advances and trends in applications of solid-phase extraction techniques in food and environmental analysis. *Chromatographia,* 82(8), 1207-1249.

Fu ZJ, Jiang SK, Chao XY, Zhang CX, Shi Q, Wang ZY, Liu ML and Sun SP, 2022. Removing miscellaneous heavy metals by all-in-one ion exchange-nanofiltration membrane. *Water Research,* 222, 118888.

García L, Parra L, Jimenez JM, Lloret J and Lorenz P, 2020. IoT-based smart irrigation systems: An overview on the current trends on sensors and IoT systems for irrigation in precision agriculture. *Sensors*, *20*(4), 1042.

Gautam PK, Gautam RK, Banerjee S, Chattopadhyaya MC and Pandey JD, 2016. Heavy metals in the environment: fate, transport, toxicity and remediation technologies. *Nova Sci Publishers*, *60*, 101-130.

Ghorbani F, Kamari S, Zamani S, Akbari S and Salehi M, 2020. Optimization and modeling of aqueous Cr (VI) adsorption onto activated carbon prepared from sugar beet bagasse agricultural waste by application of response surface methodology. *Surfaces and Interfaces, 18,*100444.

Gouda AA, El Sheikh R, Youssef AO, Gouda N, Gamil W and Khadrajy HA, 2023. Preconcentration and separation of Cd (II), Co (II), Cu (II), Ni (II), and Pb (II) in environmental samples on cellulose nitrate membrane filter prior to their flame atomic absorption spectroscopy determinations. *International Journal of Environmental Analytical Chemistry, 103(2),* 364-377.

Guo N, Su SJ, Liao B, Ding SL and Sun WY, 2017. Preparation and properties of a novel macro porous Ni^{2+}-imprinted chitosan foam adsorbents for adsorption of nickel ions from aqueous solution. *Carbohydrate polymers*, 165, 376-383.

Gyorgy C, Verity C, Neal TJ, Rymaruk MJ, Cornel EJ, Smith T, Growney DJ and Armes SP, 2021. RAFT Dispersion Polymerization of Methyl Methacrylate in Mineral Oil: High Glass Transition Temperature of the Core-Forming Block Constrains the Evolution of Copolymer Morphology. *Macromolecules*, *54*(20), 9496-9509.

Han L, Wang Y, Zhao W, Zhang H, Guo F, Wang T and Wang W, 2022. Cost-effective and eco-friendly superabsorbent derived from natural calcium-rich clay for ultra-efficient phosphate removal in diverse waters. *Separation and Purification Technology*, *297*, 121516.

Hasanah AN, Safitri N, Zulfa A, Neli N and Rahayu D, 2021. Factors Affecting Preparation of Molecularly Imprinted Polymer and Methods on Finding Template-Monomer Interaction as the Key to Selective Properties of the Materials. *Molecules*, *26*(18), 5612.

He M, Huang L, Zhao B, Chen B and Hu B, 2017. Advanced functional materials in solid phase extraction for ICP-MS determination of trace elements and their species-A review. *Analytica Chimica Acta*, 973, 1-24.

Hemmati M, Rajabi M and Asghari A, 2018. Magnetic nanoparticle based solid-phase extraction of heavy metal ions: a review on recent advances. *Microchimica Acta*, 185, 1-32.

Henriques B, Teixeira A, Figueira P, Reis AT, Almeida J, Vale C and Pereira E, 2019. Simultaneous removal of trace elements from contaminated waters by living Ulva lactuca. *Science of the Total Environment*, *652*, 880-888.

Herrera-Chacón A, Cetó X and Del Valle M, 2021. Molecularly imprinted polymers-towards electrochemical sensors and electronic tongues. *Analytical and Bioanalytical Chemistry*, *413*(24), 6117-6140.

Hu J, Sedki M, Shen Y, Mulchandani A and Gao G, 2021. Chemiresistor sensor based on ion-imprinted polymer (IIP)-functionalized rGO for Cd (II) ions in water. *Sensors and Actuators B: Chemical*, 346, 130474.

Hu Y, Guo X, Chen C and Wang J, 2019. Algal sorbent derived from Sargassum horneri for adsorption of cesium and strontium ions: equilibrium, kinetics, and mass transfer. *Applied Microbiology and Biotechnology*, *103*(6), 2833-2843.

Hube S, Eskafi M, Hrafnkelsdóttir KF, Bjarnadóttir B, Bjarnadóttir MÁ, Axelsdóttir S and Wu B, 2020. Direct membrane filtration for wastewater treatment and resource recovery: A review. *Science of the total environment*, 710, 136375.

Hussein SS, Ibrahim SS, Toma MA, Alsalhy QF and Drioli E, 2020. Novel chemical modification of polyvinyl chloride membrane by free radical graft copolymerization for direct contact membrane distillation (DCMD) application. *Journal of Membrane Science*, *611*, 118266.

Hwang JH, Pathak P, Wang X, Rodriguez KL, Cho HJ and Lee WH, 2019. A novel bismuth-chitosan nanocomposite sensor for simultaneous detection of Pb (II), Cd (II) and Zn (II) in wastewater. *Micromachines*, *10*(8), 511.

Iacob BC, Bodoki AE, Oprean L and Bodoki E, 2018. Metal–Ligand Interactions in Molecular Imprinting. *Ligand*, *23*, 1875-1895.

Jatoi AS, Hashmi Z, Adriyani R, Yuniarto A, Mazari SA, Akhter F and Mubarak NM, 2021. Current trends and future challenges of pesticide removal techniques–a comprehensive review. *Journal of Environmental Chemical Engineering*, *9*(4), 105571.

Jomova K, Makova M, Alomar SY, Alwasel SH, Nepovimova E, Kuca K, Rhodes CJ and Valko M, 2022. Essential metals in health and disease. *Chemico-biological interactions*, .110173.

Jovetić M, Trifković J, Stanković D, Manojlović D and Milojković-Opsenica D, 2017. Mineral content as a tool for the assessment of honey authenticity. *Journal of AOAC International*, 100(4), 862-870.

Kinuthia GK, Ngure V, Beti D, Lugalia R, Wangila A and Kamau L, 2020. Levels of heavy metals in wastewater and soil samples from open drainage channels in Nairobi, Kenya: Community health implication. *Scientific reports*, *10*(1), 1-13.

Konkolewicz D, Wang Y, Zhong M, Krys P, Isse AA, Gennaro, A. and Matyjaszewski, K., 2013. Reversible-deactivation radical polymerization in the presence of metallic copper. A critical assessment of the SARA ATRP and SET-LRP mechanisms. *Macromolecules*, *46*(22), 8749-8772.

Kosek K, Luczkiewicz A, Fudala-Książek S, Jankowska K, Szopińska M, Svahn O, Tränckner J, Kaiser A, Langas V and Björklund E, 2020. Implementation of advanced micropollutants removal technologies in wastewater treatment plants (WWTPs)-Examples and challenges based on selected EU countries. *Environmental science & policy*, *112*, 213-226.

Kumar P, Banerjee S, Radha A, Firdoos T, Sahoo SC and Pandey SK, 2021. Role of non-covalent interactions in the supramolecular architectures of mercury (II) diphenyldithiophosphates: An experimental and theoretical investigation. *New Journal of Chemistry*, *45*(4), 2249-2263.

Larki, A, Saghanezhad SJ and Ghomi M, 2021. Recent advances of functionalized SBA-15 in the separation/preconcentration of various analytes: A review. *Microchemical Journal*, 169, 106601.

Leal MFC, Catarino RI, Pimenta,AM and Souto MRS, 2023. The influence of the biometals Cu, Fe, and Zn and the toxic metals Cd and Pb on human health and disease. *Trace Elements and Electrolytes*, 40(1), 1.

Leblebici ZELIHA and Aksoy A, 2008. Determination of heavy metals in honey samples from Central Anatolia using plasma optical emission spectrofotometry (ICP-OES). *Polish Journal of Environmental Studies*, 17 (4), 549-555.

Lee T, Speth,TF.and Nadagouda MN, 2022. High-pressure membrane filtration processes for separation of Per-and polyfluoroalkyl substances (PFAS). *Chemical Engineering Journal*, 431, 134023.

Li J, Ma J, Dai R, Wang X, Chen M, Waite TD and Wang Z, 2020. Self-enhanced decomplexation of Cu-organic complexes and Cu recovery from wastewaters using an electrochemical membrane filtration system. *Environmental Science & Technology, 55(1),* 655-664.

Li Q, Fu L, Wang Z, Li A, Shuang C and Gao C, 2017. Synthesis and characterization of a novel magnetic cation exchange resin and its application for efficient removal of Cu^{2+} and Ni^{2+} from aqueous solutions. *Journal of Cleaner Production,* 165, 801-810.

Liang W, Lu Y, Li N, Li H and Zhu F, 2020. Microwave-assisted synthesis of magnetic surface molecular imprinted polymer for adsorption and solid phase extraction of 4-nitrophenol in wastewater. *Microchemical Journal*, *159,* 105316.

Liang XM, Jiang HC, Fang JL, Hua M, Pan XH and Jiang JC, 2019. Thermal analysis of the styrene bulk polymerization and characterization of polystyrene initiated by two methods. *Chemical Engineering Communications*, *206*(4), 432-443.

Lin PH, Sermersheim M, Li H, Lee PH, Steinberg SM and Ma J, 2018. Zinc in wound healing modulation. *Nutrients*, 10(1), 16.

Ling S, Qin Z, Huang W, Cao S, Kaplan DL and Buehler MJ, 2017. Design and function of biomimetic multilayer water purification membranes. *Science advances,* 3(4), .e1601939.

Liu H, Dong J, Zhou H, Yang X, Xu C, Yao Y, Zhou G, Zhang S and Song Q, 2021. Real-Time Acid Rain Sensor Based on a Triboelectric Nanogenerator Made of a PTFE–PDMS Composite Film. *ACS Applied Electronic Materials*, *3*(9), 4162-4171.

Liu J, Yin M, Luo X, Xiao T, Wu Z, Li N, Wang J, Zhang W, Lippold H, Belshaw NS and Feng Y, 2019. The mobility of thallium in sediments and source apportionment by lead isotopes. *Chemosphere*, *219*, 864-874.

Liu K, Fu X, Lin M and Tai L, 2016. AC copper losses analysis of the ironless brushless DC motor used in a flywheel energy storage system. *IEEE Transactions on Applied Superconductivity*, 26(7), 1-5.

Liu L, Luo XB, Ding L and Luo SL, 2019. Application of nanotechnology in the removal of heavy metal from water. In Nanomaterials for the removal of pollutants and resource reutilization. *Elsevie*r 83-147

Liu S, Zhang Y, Su Z, Lu M, Gu F, Liu J and Jiang T, 2020. Recycling the domestic copper scrap to address the China's copper sustainability. *Journal of Materials Research and Technology*, 1,1-13.

Lobo C, Castellari J, Lerner JC, Bertola N and Zaritzky N, 2020. Functional iron chitosan microspheres synthesized by ionotropic gelation for the removal of arsenic (V) from water. *International Journal of Biological Macromolecules, 164*, 1575-1583.

Lofgreen JE and Ozin GA, 2014. Controlling morphology and porosity to improve performance of molecularly imprinted sol–gel silica. *Chemical Society Reviews*, *43*(3), 911-933.

Lonappan L, Rouissi T, Brar SK, Verma M and Surampalli RY, 2018. An insight into the adsorption of diclofenac on different biochars: mechanisms, surface chemistry, and thermodynamics. *Bioresource technology*, *249*, 386-394.

Lovell PA and Schork FJ, 2020. Fundamentals of emulsion polymerization. *Biomacromolecules*, *21*(11), 4396-4441.

Low W, Utomo KS, Lee HP and Rahman NA, 2023. Adsorption of zinc, copper, and iron from synthetic wastewater using watermelon (Citrullus Lanatus), mango (Mangifera Indica L.), rambutan peels (Nephelium Lappaceum L.) As bio sorbets. *Journal of Engineering Science and Technology, 18(1),* 386-405.

Ma J, Ping D and Dong X , 2017. Recent developments of graphene oxide-based membranes: A review. *Membranes,* 7(3), 52.

Ma W, Chang Q, Zhao J and Ye BC, 2020. Novel electrochemical sensing platform based on ion imprinted polymer with nanoporous gold for ultrasensitive and selective determination of As^{3+}. *Microchimica Acta*, 187(10), 1-9.

Madikizela LM, Mdluli PS and Chimuka L, 2016. Experimental and theoretical study of molecular interactions between 2-vinyl pyridine and acidic pharmaceuticals used as multi-template molecules in molecularly imprinted polymer. *Reactive and Functional Polymers*, 103, 33-43.

Mahani M, Mahmoudi F, Fassihi J, Hasani Z and Divsar F, 2021. Carbon dots-embedded N-acetylneuraminic acid and glucuronic acid-imprinted polymers for targeting and imaging of cancer cells. *Microchimica Acta*, *188*(7), 1-11.

Malhat F, Kasiotis KM, Hassanin AS and Shokr SA, 2019. An MIP-AES study of heavy metals in Egyptian honey: Toxicity assessment and potential health hazards to consumers. *Journal of Elementology*, *24*(2).

Masoumi H, Ghaemi A and Gilani HG, 2021. Evaluation of hyper-cross-linked polymers performances in the removal of hazardous heavy metal ions: A review. *Separation and Purification Technology*, *260*, 118221.

Mavroudakis E, Cuccato D and Moscatelli D, 2019. Determination of Reaction Rate Coefficients in Free-Radical Polymerization Using Density Functional Theory. In *Computational Quantum Chemistry* (47-98). Elsevier.

McKenzie TG, Karimi F, Ashokkumar M and Qiao GG, 2019. Ultrasound and sonochemistry for radical polymerization: sound synthesis. *Chemistry–A European Journal*, *25*(21), 5372-5388.

Mier A, Maffucci I, Merlier F, Prost E, Montagna V, Ruiz-Esparza GU, Bonventre JV, Dhal PK, Tse Sum Bui B, Sakhaii P and Haupt K, 2021. Molecularly Imprinted Polymer Nanogels for Protein Recognition: Direct Proof of Specific Binding Sites by Solution STD and WaterLOGSY NMR Spectroscopies. *Angewandte Chemie International Edition*, *60*(38), 20849-20857.

Mračević SĐ, Krstić M, Lolić A and Ražić S, 2020. Comparative study of the chemical composition and biological potential of honey from different regions of Serbia. *Microchemical Journal*, *152*, 104420.

Mueller JB, Fischer J, Mayer F, Kadic M and Wegener M, 2014. Polymerization Kinetics in Three-Dimensional Direct Laser Writing. *Advanced Materials*, *26*(38), 6566-6571.

Nishizawa Y, Minato H, Inui T, Uchihashi T and Suzuki D, 2020. Nanostructures, thermoresponsiveness, and assembly mechanism of hydrogel microspheres during aqueous free-radical precipitation polymerization. *Langmuir*, *37*(1), 151-159.

Ogidi OI and Otenep EJ, 2020. Determination of nutritional properties of honey from Apismellifera. *International Journal of Food Science and Nutrition*, 5(1), 23-26.

Osagie C, Othmani A, Ghosh S, Malloum A, Esfahani ZK and Ahmadi S, 2021. Dyes adsorption from aqueous media through the nanotechnology: A review. *Journal of Materials Research and Technology*, *14*, 2195-2218.

Panja S, Hanson S and Wang C, 2020. EDTA-inspired polydentate hydrogels with exceptionally high heavy metal adsorption capacity as reusable adsorbents for wastewater purification. *ACS Applied Materials & Interfaces*, *12*(22), 25276-25285.

Pavlova T, Stamatovska V, Kalevska T, Dimov I and Nakov G, 2018. Quality characteristics of honey: a review. *Proceedings of University of ruse*, *57*(10.2), 32-37.

Pirman T, Ocepek M and Likozar B, 2021. Radical Polymerization of Acrylates, Methacrylates, and Styrene: Biobased Approaches, Mechanism, Kinetics, Secondary Reactions, and Modeling. *Industrial & Engineering Chemistry Research*, *60*(26), 9347-9367.

Pohl A, 2020. Removal of heavy metal ions from water and wastewaters by sulfur-containing precipitation agents. *Water, Air, & Soil Pollution*, *231(10)*, 503.

Polyakova I, Borovikova L, Osipenko A, Vlasova E, Volchek B and Pisarev O, 2016. Surface molecularly imprinted organic-inorganic polymers having affinity sites for cholesterol. *Reactive and Functional Polymers*, *109*, 88-98.

Priya AK, Gnanasekaran L, Dutta K, Rajendran S, Balakrishnan D and Soto-Moscoso M., 2022. Biosorption of heavy metals by microorganisms: Evaluation of different underlying mechanisms. *Chemosphere*, 307, 135957.

Rahman Z and Singh VP, 2019. The relative impact of toxic heavy metals (THMs) (arsenic (As), cadmium (Cd), chromium (Cr)(VI), mercury (Hg), and lead (Pb)) on the total environment: an overview. *Environmental monitoring and assessment*, *191*(7), 1-21.

Renu A M and Singh K, 2017. Methodologies for removal of heavy metal ions from wastewater: an overview. *Interdisciplinary Environmental Review*, *18*(2), 124-142.

Ruzik L and Wojcieszek J, 2016. In vitro digestion method for estimation of copper bioaccessibility in Açaí berry. *Monatshefte Für Chemie-Chemical Monthly*, 147(8), 1429-1438.

Sajini T and Mathew B, 2021. A brief overview of molecularly imprinted polymers: Highlighting computational design, nano and photo-responsive imprinting. *Talanta Open*, *4*,100072.

Sala A, Brisset H, Margaillan A, Mullot JU and Branger C, 2022. Electrochemical sensors modified with ion-imprinted polymers for metal ion detection. *TrAC Trends in Analytical Chemistry*, 148, 116536.

Sandoval Riofrio MA, 2017. Extraction of Phorbol Esters (PEs) from Pinion cake using computationally designed polymers as adsorbents for Solid Phase Extraction (*Doctoral dissertation, University of Leicester).*

Sawan S, Maalouf R, Errachid A and Jaffrezic-Renault N, 2020. Metal and metal oxide nanoparticles in the voltammetric detection of heavy metals: A review. *TrAC Trends in Analytical Chemistry*, *131*, 116014.

Shao Z, Lu J, Ding J, Fan F, Sun X, Li P, Fang Y and Hu Q, 2021. Novel green chitosan-pectin gel beads for the removal of Cu (II), Cd (II), Hg (II) and Pb (II) from aqueous solution. *International Journal of Biological Macromolecules*, *176*, 217-225.

Shen J, Wu X, Yu J, Yin F, Hao L, Lin C, Zhu L, Luo C, Zhang C and Xu F, 2021. Hydrogen bonding interactions between arsenious acid and dithiothreitol/dithioerythritol at different pH values: A computational study with an explicit solvent model. *New Journal of Chemistry*, *45*(43), 20181-20192.

Sherlala, AIA, Raman AAA, Bello MM and Buthiyappan A, 2019. Adsorption of arsenic using chitosan magnetic graphene oxide nanocomposite. *Journal of environmental management*, *246*, 547-556.

Sis H and Uysal T, 2014. Removal of heavy metal ions from aqueous medium using Kuluncak (Malatya) vermiculites and effect of precipitation on removal. *Applied Clay Science*, *95*, 1-8.

Sixto A, Mollo A and Knochen M, 2019. Fast and simple method using DLLME and FAAS for the determination of trace cadmium in honey. *Journal of Food Composition and Analysis*, *82*, 103229.

Sun L, Guo D, Liu K, Meng H, Zheng Y, Yuan F and Zhu G, 2019. Levels, sources, and spatial distribution of heavy metals in soils from a typical coal industrial city of Tangshan, China. *Catena*, *175*, 101-109.

Sun T, Tian B, Lu J and Su C, 2017. Recent advances in Fe (or Co)/N/C electrocatalysts for the oxygen reduction reaction in polymer electrolyte membrane fuel cells. *Journal of Materials Chemistry A*, *5*(36), 18933-18950.

Suriyanarayanan S, Mandal S, Ramanujam K and Nicholls IA, 2017. Electrochemically synthesized molecularly imprinted polythiophene nanostructures as recognition elements for an aspirin-chemosensor. *Sensors and Actuators B: Chemical*, *253*, 428-436.

Suzuki K, Nishimura Y, Kanematsu Y, Masuda Y, Satoh S and Tobita H, 2012. Experimental validation of intermediate termination in RAFT polymerization with dithiobenzoate via comparison of miniemulsion and bulk polymerization rates. *Macromolecular Reaction Engineering*, *6*(1), 17-23.

Syafiuddin A, Fulazzaky MA, Salmiati S, Kueh ABH, Fulazzaky M and Salim MR, 2020. Silver nanoparticles adsorption by the synthetic and natural adsorbent materials: an exclusive review. *Nanotechnology for Environmental Engineering*, *5*(1), 1-18.

Tang T, Cao S, Xi C, Li X, Zhang L, Wang G and Chen Z, 2020. Chitosan functionalized magnetic graphene oxide nanocomposite for the sensitive and effective determination of alkaloids in hotpot. *International journal of biological macromolecules*, 146, 343-352.

Trojanowska A, Nogalska A, Valls RG, Giamberini M and Tylkowski B, 2017. Technological solutions for encapsulation. *Physical Sciences Reviews*, *2*(9).

Vetrimurugan E, Brindha K, Elango L and Ndwandwe OM, 2017. Human exposure risk to heavy metals through groundwater used for drinking in an intensively irrigated river delta. *Applied Water Science*, *7*(6), 3267-3280.

Vilela PB, Matias CA, Dalalibera A, Becegato VA and Paulino AT, 2019. Polyacrylic acid-based and chitosan-based hydrogels for adsorption of cadmium: Equilibrium isotherm, kinetic and thermodynamic studies. *Journal of Environmental Chemical Engineering, 7(5),* 103327.

Virtanen OL, Kathe M, Meyer-Kirschner J, Melle A, Radulescu A, Viell J, Mitsos A, Pich, A and Richtering W, 2019. Direct monitoring of microgel formation during precipitation polymerization of N-isopropylacrylamide using in situ SANS. *ACS omega*, *4*(2), 3690-3699.

Wang C, Fan H, Ren X, Fang J, Ma J and Zhao N, 2018. Porous graphitic carbon nitride nanosheets by pre-polymerization for enhanced photocatalysis. *Materials Characterization*, *139*, 89-99.

Wang H, Lin Y, Li Y, Dolgormaa A, Fang H, Guo L, Huang J and Yang J, 2019. A novel magnetic Cd (II) ion-imprinted polymer as a selective sorbent for the removal of cadmium ions from aqueous solution. *Journal of Inorganic and Organometallic Polymers and Materials*, 29, 1874-1885.

Wang H, Shang H, Sun X, Hou L, Wen M and Qiao Y, 2020. Preparation of thermo-sensitive surface ion-imprinted polymers based on multi-walled carbon nanotube composites for selective adsorption of lead (II) ion. Colloids and Surfaces A: *Physicochemical and Engineering Aspects*, 585, 124139.

Wang LK, Wang MHS, Shammas NK and Hahn HH, 2021. Physicochemical treatment consisting of chemical coagulation, precipitation, sedimentation, and flotation. *Integrated natural resources research*, 265-397.

Wang T, Wang Q, Soklun H, Qu G, Xia T, Guo X, Jia H and Zhu L, 2019. A green strategy for simultaneous Cu (II)-EDTA decomplexation and Cu precipitation from water by bicarbonate-activated hydrogen peroxide/chemical precipitation. *Chemical Engineering Journal, 370*, 1298-1309.

Wang W, Fang J, Pan X, Hua M, Jiang J, Ni L and Jiang, J, 2019. Thermal research on the uncontrolled behavior of styrene bulk polymerization. *Journal of Loss Prevention in the Process Industries, 57*, 239-244.

Wang X, Li X, Peng L, Han S, Hao C, Jiang C, Wang H and Fan X, 2021. Effective removal of heavy metals from water using porous lignin-based adsorbents. *Chemosphere, 279,* 130504.

Wang XX, Yu GF, Zhang J, Yu M, Ramakrishna S and Long YZ, 2021. Conductive polymer ultrafine fibres via electrospinning: Preparation, physical properties and applications. *Progress in Materials Science*, 115, 100704.

Weldeslassie T, Naz H, Singh B and Oves M, 2018. Chemical contaminants for soil, air and aquatic ecosystem. *In Modern age environmental problems and their remediation*. 1-22.

World Health Organization, 2019. Preventing disease through healthy environments: exposure to cadmium: a major public health concern (No. WHO/CED/PHE/EPE/19.4. 3). World Health Organization.

Wright AC, Fan Y and Baker GL, 2018. Nutritional value and food safety of bivalve molluscan shellfish. *Journal of Shellfish Research*, 37(4),695-708.

Xia QC, Liu ML, Cao XL, Wang Y, Xing W. and Sun SP, 2018. Structure design and applications of dual-layer polymeric membranes. *Journal of Membrane Science*, 562, .85-111.

Xie C, Huang X, Wei S, Xiao C, Cao J and Wang Z, 2020. Novel dual-template magnetic ion imprinted polymer for separation and analysis of Cd^{2+} and Pb^{2+} in soil and food. *Journal of cleaner production*, 262, 121387,

Xie L, Xiao N, Li L, Xie X and Li Y, 2020. Theoretical insight into the interaction between chloramphenicol and functional monomer (methacrylic acid) in molecularly imprinted polymers. *International Journal of Molecular Sciences*, 21(11), 4139.

Xue H, Wang X, Xu Q, Dhaouadi F, Sellaoui L, Seliem MK, Lamine AB, Belmabrouk H, Bajahzar A, Bonilla-Petriciolet A and Li Z, 2022. Adsorption of methylene blue from aqueous solution on activated carbons and composite prepared from an agricultural waste biomass: A comparative study by experimental and advanced modelling analysis. *Chemical engineering journal, 430,* 132801.

Yan H and Row KH, 2006. Characteristic and synthetic approach of molecularly imprinted polymer. *International journal of molecular Sciences*, *7*(5), 155-178.

Yang Z, Zhou Y, Feng Z, Rui X, Zhang T and Zhang Z, 2019. A review on reverse osmosis and nanofiltration membranes for water purification. *Polymers,* 11(8), 1252.

Yİldİko Ü Ata AÇ, Tanriverdİ AA and Çakmak İ, 2021. Investigation of novel diethanolamine dithiocarbamate agent for RAFT polymerization: DFT computational study of the oligomer molecules. *Bulletin of Materials Science, 44*(3),1-13.

Yousefi H, Lak E, Mohammadi MJ and Shahriyari HA, 2021. Carcinogenic risk assessment among children and adult due to exposure to toxic air pollutants. *Environmental science and pollution research*, 1-11.

Yu H, Li C, Tian Y and Jiang X., 2020. Recent developments in determination and speciation of arsenic in environmental and biological samples by atomic spectrometry. *Microchemical Journal,* 152, 104312.

Yu L, Sun L, Zhang Q, Zhou Y, Zhang J, Yang B, Xu B. and Xu Q, 2022. Nanomaterials-based ion-imprinted electrochemical sensors for heavy metal ions detection: a review. *Biosensors,* 12(12), 1096.

Zahid M, Rashid A, Akram S, Rehan ZA and Razzaq WJJMST, 2018. A comprehensive review on polymeric nano-composite membranes for water treatment. J. *Membr. Sci. Technol*, 8(1), 1-20.

Zeng J, Lv C, Liu G, Zhang Z, Dong Z, Liu J and Wang Y, 2019. A novel ion-imprinted membrane induced by amphiphilic block copolymer for selective separation of Pt (IV) from aqueous solutions. *Journal of Membrane Science*, 572, 428-441.

Zhang H, Song H, Tian X, Wang Y, Hao Y, Wang W, Gao R, Yang W, Ke Y and Tang Y, 2021. Magnetic imprinted nanoparticles with synergistic tailoring of covalent and non-covalent interactions for purification and detection of procyanidin B2. *Microchimica Acta*, *188*(1), 1-12.

Zhang L, Zhang R, Ji M, Lu Y, Zhu Y and Jin, J, 2021. Polyamide nanofiltration membrane with high mono/divalent salt selectivity via pre-diffusion interfacial polymerization. *Journal of Membrane Science, 636*, 119478.

Zhang N, Samanta SR, Rosen BM and Percec V, 2014. Single electron transfer in radical ion and radical-mediated organic, materials and polymer synthesis. *Chemical Reviews*, *114*(11), 5848-5958.

Zhang Y and Duan,X, 2020. Chemical precipitation of heavy metals from wastewater by using the synthetical magnesium hydroxy carbonate. *Water Science and Technology, 81(6),* 1130-1136.

Zhang YN, Sun Y, Cai L, Gao Y and Cai Y, 2020. Optical fiber sensors for measurement of heavy metal ion concentration: A review. *Measurement,* 158, 107742.

Zhao G, Huang X, Tang Z, Huang Q, Niu F and Wang X, 2018. Polymer-based nanocomposites for heavy metal ions removal from aqueous solution: a review. *Polymer Chemistry,* 9(26),3562-3582.

Zheng X, Zhang Y, Bian T, Zhang Y, Li, Z and Pan J, 2020. Oxidized carbon materials cooperative construct ionic imprinted cellulose nanocrystals films for efficient adsorption of Dy (III). *Chemical Engineering Journal*, 381, 122669.

Zhu F, Li L, Li N, Liu W, Liu X and He S, 2021. Selective solid phase extraction and preconcentration of Cd (II) in the solution using microwave-assisted inverse emulsion-suspension Cd (II) ion imprinted polymer. *Microchemical Journal*, *164*,106060.

Zouaoui F, Bourouina-Bacha S, Bourouina M, Jaffrezic-Renault N, Zine N and Errachid A, 2020. Electrochemical sensors based on molecularly imprinted chitosan: A review. *TrAC Trends in Analytical Chemistry*, *130,* 115982.

Chapter 3: Synthesis, characterization and use of zinc (II) IIP to remove trace elements from honey

Abstract

This chapter aims at synthesizing zinc ion imprinted polymer to remove zinc selectively from honey in the presence of competing ions. A Zn(II)-IIP and an Zn(II)-NIP were obtained by a precipitation reaction. The Zn(II)-NIP and Zn(II)-IIP were characterized by infrared spectroscopy to assess the functional groups present and absent, while surface charges were evaluated based on the pH point of zero charge. The efficiency of the synthesized polymers towards selective adsorption of Zn (II) was evaluated though batch adsorption experiments. The maximum percentage of Zn^{2+} removal using the Zn-IIP was found to be 80% when the solution pH of 7.0, adsorbent dose was 5 mg, contact time at 15 min at shaking speed of 100 rpm and initial metal ion concentration of 25 mg/L were used. The adsorption kinetic data corresponded to pseudo-second order reaction kinetics with R^2 = 0.99, indicating that the process occurred by chemisorption. The Langmuir isotherm showed an excellent fit with an adsorption capacity of up to 9.03 mg g^{-1} and R^2 = 0.99, implying that adsorption was on a monolayer surface. This study shows that zinc ion imprinted polymer has higher efficiency towards Zn^{2+} in the solution. The finding indicates that zinc ion imprinted polymer has high adsorption efficiency of 94.00 (mg/g) in removing zinc ion from the honey sample.

Keywords: Ion imprinted polymer, zinc, precipitation polymerization and atomic absorption spectroscopy

3.1. Introduction

Honey is a natural saturated sugar solution which contains nutrients and carbohydrate. Honey it is used as a food preservative (Haber et al., 2019). It contains enzyme, proteins, vitamins, lipids, flavonoids and minerals (Abdelnour et al., 2019). The honey's quality depends on the climate conditions, production methods, nectar source and processing and storage conditions (Pavlova et al., 2018). Trace metals such as cadmium, nickel, and lead, metals like zinc, copper, and chromium have been reported previously in honey samples (Squadrone et al., 2020). It is important to ensure that the levels of these metals in honey remain below the maximum allowable limit, as they play integral roles in human health and development (Adugna et al., 2020: Altundag et al., 2016). Intake of essential metals (Zn and Cu) when are above the maximum allowable limits can cause chronic disease (Varol et al., 2017). Trace metals comes

from anthropogenic sources like industrial pollution and improper procedure during maintenance stage and process of honey (Aljohar et al., 2018: Hermanns et al., 2020).

Zinc nutrient it is enforced for processes like cellular metabolism, DNA synthesis, gene expression, catalytic activity, immune function protein synthesis, cell division and wound healing (Lin et al., 2018; Maret et al., 2013; Fontana et al., 2017). Zinc is found naturally in plants and in certain foods, such as shellfish, pork, and beef. It can also be added to other foods and is available as a dietary supplement. Cold lozenges and some over-the-counter cold remedies also contain zinc. Zinc plays a role in supporting normal growth and development during pregnancy, childhood, and adolescence, as well as maintaining a proper sense of taste and smell. The body does not have a specialized storage system for zinc, so a daily intake of 40 mg is necessary to maintain a steady state. Excessive intake of zinc, above this requirement, can lead to symptoms like nausea, vomiting, and anaemia. Analytical methods, such as AAS, ICP-OES, and ICP-MS, have been developed to detect trace levels of zinc (II) in biological, pharmacological, food, and environmental samples. Stecka et al. (2014) and Aduga et al. (2020) used these methods and reported concentrations ranging from 0.13 to 15.38 µg g^{-1} and 9.96 to 16.03 µg g^{-1}, respectively.

It is important to remove zinc from honey because it can cause indigestion, vomiting and diarrhoea, and over the long term it causes low immunity and low copper levels. Different methods have been applied in extraction such as osmosis, ion exchange, filtration, electrolysis and adsorption (Charles et al., 2016; Thaçi and Gashi, 2019). Compared to other methods, the adsorption method is highly efficient and flexible (Azha et al., 2021). Carbon nanotubes, clay, and zeolite are known adsorbents for removing metals (Burakov et al., 2018; Zhou et al., 2019). However, there is still a need for low cost-effective adsorbents. This is where molecular imprinting comes in, offering a promising method with remarkable capabilities. Molecularly imprinted polymers (MIPs) have a permanent memory for the template, so that they can re-bind the target molecule selectively in a mixture of similar compounds. MIPs and ion-imprinted polymers (IIPs) differ in their recognition substance, which can be an ion or molecule. IIPs are a group of highly selective materials that can recognize specific ions even when competing ions from intricate matrices are present. (Sun et al., 2017).

In the process, the initiator undergoes splitting, resulting in the formation of initiator fragments that contain unpaired electrons known as free radicals (Nishizawa et al., 2020; Qin et al., 2018). These unpaired electrons then pair with ethylene glycol dimethacrylate (EGDMA), which is

referred to as the initiation step. During the propagation step, additional monomers are added to the growing chain. Finally, in the termination step, the two unpaired electrons join to give a polymer (Hu et al., 2020; Tian et al., 2018).

We describe the synthesis, characterisation, and use of Zn-IIP for solid phase extraction-based zinc pre-concentration in this study. Atomic absorption in flame was used to analyze the quantity of zinc. Using zinc sulphate as a template, methacrylic acid as a functional monomer, and ethylene glycol di-methacrylate as a cross-linker, the IIPs were created. FTIR was used to study the IIP's characterization. Investigations were done on the experiment's parameters, including sample pH, concentration, and flow rate. The trace amount of zinc (II) ion was enriched using this approach from an aqueous solution.

3.2. Material and methods

3.2.1. Chemicals and reagents

Methanol (99%), methacrylic acid (MAA) (99%), azobisisobutyronitrile (AIBN) (98%), ethylene glycol dimethacrylate (EGDMA) (99%), hydrochloric acid (99%) and zinc sulphate (99%) were sourced from Merck (Wadeville, South Africa). Cobalt (II) chloride (97%), copper (II) sulphate (98%), manganese (II) chloride tetrahydrate (99%), nickel (II) chloride (99%) and iron chloride (98%) were bought from Sigma-Aldrich. All the chemicals were analytical grade.

3.2.2. Synthesis of ion imprinted polymers (IIPs)

The synthesis of IIPs was carried out according to the modified procedure of Xia et al. (2017). To 70 mL ethanol (in a 250 mL one-neck round-bottomed flask), 0.116 g (0.5 mmol) $ZnSO_4$ was added as template and 422 µL (5 mmol) MAA monomer were added. To eliminate oxygen and create an inert environment, the mixture was stirred for 15 minutes. Following that, 2 mL (10 mmol) EGDMA was introduced. Before adding 50 mg (0.3 mmol) AIBN as the initiator, the solution was purged with nitrogen for 2 minutes to eliminate oxygen. After adding the initiator, the flask was greased with oil and loosely closed loosely with lead and enclosed in parafilm. The flask was heated for 7 h in an oil bath at 80^{o}C, and the product was then cooled, filtered and dried overnight. The NIPs were prepared similarly but without addition of a template.

3.2.3. Elution process

After polymerization, the IIPs and NIPs obtained were each washed 8 times with 2 M HCl to remove the ion template from the polymer. The 3 g IIP and 1 g NIP obtained, were transferred to 50 mL solid phase cartridges with a cotton wool plug in the bottom. The elution process was done in continuous mode. The eluted fractions were collected after every hour. The procedure was repeated eight times for both IIPs and NIPs. The wet IIPs and NIPs were then dried for overnight. Figure 3.1 shows synthesis of Zn (II) imprinted polymer

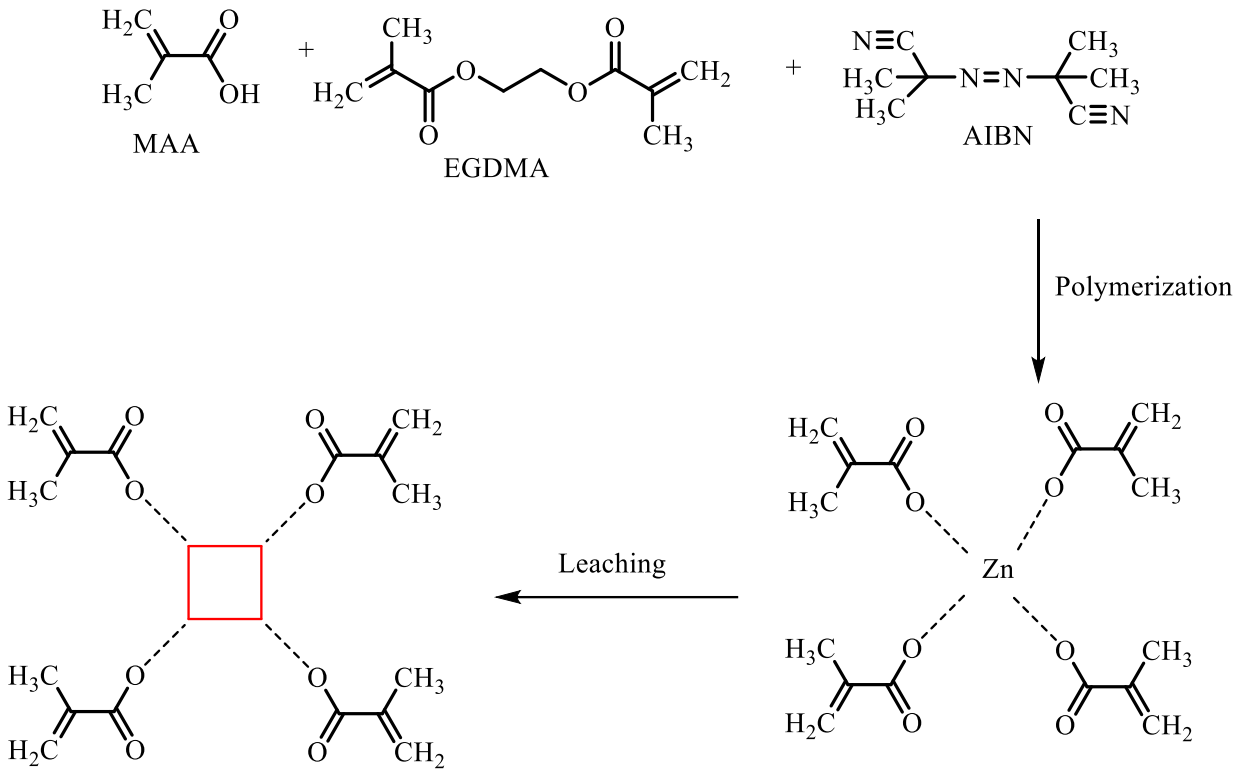

Figure 3.1: Illustration of the imprinting process to produce a Zn (II) imprinted polymer.

3.2.4. Adsorption studies

The batch adsorption experiments involved varying the parameters sample pH, temperature, contact time, mass, metal ion concentration, and shaking speed. A univariate analysis approach was employed, wherein one variable was altered while keeping the other parameters constant. To adjust the solution pH, 0.1 mol L^{-1} $NaOH/HNO_3$ was used, and for each adsorption experiment, the solutions were subsequently filtered. The resulting mixture was filtered, and the concentration of the filtrate was determined using atomic absorption spectroscopy (PinAAcle 900T from PerkinElmer). The percentage adsorption, E, and equilibrium adsorption capacity Q_e (measured in mg/g) were calculated using the following formulas:

$$E = \frac{C_i - C_f}{C_i} \quad (3.1)$$

$$Q_e = \frac{(C_i - C_f)\,V}{W} \quad (3.2)$$

where C_i and C_f = the respective initial and final concentrations of Zn (II) (mg L^{-1}),

W = sorbent weight (g), and

V = solution volume (mL).

3.2.4. Surface area measurement

A 0.01 g L^{-1} Methylene Blue standard solution was prepared and a calibration curve drawn at λ = 600 nm using UV-VIS spectroscopy. To calculate surface area, 0.1 g IIP was treated with 25 mL Methylene Blue solution until the absorbance was constant.

The surface areas of the Zn-IIP and NIP were determined using the formula

$$A_S = \frac{G.N_{av}.\Theta.10^{-20}}{M.M_W} \quad (3.3)$$

where A_s = the surface area of the imprinted polymer (m^2 g^{-1}),

G = the amount methylene blue adsorbed (g),

N_{av} = Avogadro's number (6.02×10^{23} mol^{-1}),

θ = the cross-section of the methylene blue molecule (197.2 $Á^2$),

M_W = the methylene blue molar mass (373.9 g/mol), and

M = the adsorbent mass (g).

3.2.5. Determination of pH_{pzc}

The point of zero charge (pH_{pzc}) was determined by the method proposed by Tavengwa et al. (2016) with a few modifications. Aliquots of 50 mL 0.01 M KCl solution were placed in different 50 mL centrifuge vials and adsorbent was added to each of them before the pH was adjusted with 0.1 M HCl or NaOH solution. After shaking the vials for 15 h at 100 rpm, the mixtures were filtered and the filtrate pH was measured; the pH_{pzc} value is the point where the curve pH_{final} vs $pH_{initial}$ cross, i.e. where $pH_{final} = pH_{initial}$.

3.2.6. Adsorption isotherm

A Zn^{2+} concentration range of 10 to 35 mg/L was used to evaluate the adsorption capacity. To the solution, 5 mg of Zn-IIP or NIP particles were added. The solution pH was adjusted to seven with 0.1 M NaOH or HCl, and it was then shaken at room temperature for 1 hour. After filtration, the Zn(II) concentration in the filtrate was measured using AAS. Adsorption isotherm are important for describing how the adsorbate ion interact with the surface adsorption site and represents the connection between the adsorbate on the surface of the adsorbent at equilibrium and constant temperature and the adsorbate in the surrounding phase (Chenn et al., 2022: Hu et al., 2023). Langmuir, Freundlich and Temkin isotherm models were used to explain the adsorption isotherms.

The Langmuir equation can be expressed as;

$$\frac{C_e}{q_e} = \frac{1}{q_{max} b} + \frac{C_e}{q_{e\,max}} \qquad (3.4)$$

where q_e = amount of adsorbate (mg g^{-1}) at equilibrium,

C_e = ion concentration in the solution

q_{max} = maximum sorption capacity

b = Langmuir constant

The Freundlich isotherm is suitable for surfaces that are heterogeneous, as it describes surface heterogeneity and the exponential distribution of activation energies:

$$log\, q_e = log\, K_F + \frac{1}{n} log\, C_e \qquad (3.5)$$

where K_F = Freundlich constant (mg/g)/(mg/L)^n and n is the exponent of the Freundlich model (0< n <1).

1/n = adsorption intensity. The value 1/n is also a measure of the site heterogeneity.

According to the Temkin isotherm model, the heat of adsorption of each molecule in the layer should fall linearly with coverage rather than logarithmically.

$$q_e = \frac{RT}{b} \ln(A_T C_e) \qquad (3.6)$$

$$q_e = \frac{RT}{b_T}\, In\, A_T + \frac{RT}{b_T}\, In\, C_e \qquad (3.7)$$

$$B = \frac{RT}{b_T} \quad (3.8)$$

$$q_e = B\ In\ A_T + B\ In\ C_e \quad (3.9)$$

where A_T =Temkin isotherm equilibrium binding constant (L g^{-1})

b_T = Temkin isotherm constant

R = universal gas constant (8.314 J/mol/K)

T = Temperature (298 K)

B = Constant related to heat of sorption (J/mol)

3.2.7. Adsorption kinetics

The time to completely adsorb Zn^{2+} onto the IIPs was determined. A range of Zn-IIP and NIP samples was prepared by immersing 5 mg of the polymer in 20 mL of a 25 mg/L Zn(II) solution. Over a 5-35 min time interval the samples were filtered through a membrane filter, and the metal concentration was measured using AAS. Possible adsorption mechanisms and reaction pathways that can be characterized by either a pseudo-first order or a pseudo-second order model are provided by the study of kinetics. According to this mechanism, at greater sorbate/sorbent ratios, the kinetics of the adsorption process correspond with two competing reversible second order reactions, and at lower sorbate/sorbent ratios, with reverse second order reactions. Equations (3.9) Pseudo first-order and (3.10) Pseudo second-order define the models.

$$In\ (q_e - q_t) = In\ (q_e - k_1 t) \quad (3.10)$$

$$\frac{t}{q_t} = \frac{1}{k_2\ (q_e)^2} + \frac{1}{q_e} t \quad (3.11)$$

where q_t and q_e = adsorption capacity (mg g^{-1}) of Zn (II) at time t and at equilibrium, respectively

k_1 = rate constant (min^{-1}) obtained from the pseudo-first order model,

R^2 = linear regression correlation coefficient obtained from a linear plot,

k_2 = rate constant (g $min^{-1}mg^{-1}$) for the pseudo-second order model at equilibrium, and k_2q_e and the corresponding linear regression correlation coefficient R^2 are obtained from the linear plot.

3.2.8. Selectivity studies

The selectivity study was conducted under optimized conditions for both the IIP and the NIP. The IIP or NIP (5 mg) was added to an aqueous solution of Zn^{2+}, Cd^{2+}, Pb^{2+}, and Ni^{2+} ions, each at a concentration of 2 µg/mL. These competing ions were chosen due to their identical charge, comparable ionic radii, and frequent coexistence with Zn^{2+} ions.

To achieve a sample pH of 7, 0.1 M HCl and NaOH solutions were used for adjustment. The resulting mixture was placed in a 50 mL centrifuge tube and stirred at 100 rpm for 15 minutes. After stirring, the mixture was filtered and the ion concentrations in the filtrate were measured using atomic absorption spectroscopy (AAS). The experiment was repeated three times to ensure reliability and reproducibility. The polymer was filtered using a membrane filter before further analysis. The Zn (II) distribution ratio's (K_d), selectivity factors (K), and relative selectivity factors (K′) with regard to Cd (II), Pb (II), and Ni (II), were calculated using Eqs. 3.11–3.13:

$$K_d = \frac{(C_i - C_f)V}{C_f M} \quad (3.12)$$

$$K = \frac{K_{d(Zn(II))}}{K_{d(\text{competing ions})}} \quad (3.13)$$

$$K' = \frac{K_{\text{imprinted}}}{K_{\text{non-imprinted}}} \quad (3.14)$$

where C_i = initial concentration (mg L^{-1}),

C_f = final concentration (mg L^{-1}),

V = ion solution volume (mL), and

M = sorbent mass (g).

3.3. Preparation of honey sample

Processed honey samples were purchased from a local farm in Levubu, Limpopo, South Africa. The sample was kept at 4°C until analysis. Table 3.1 shows the physico-chemical properties of the honey sample. Processed honey samples were digested following the procedure developed by Adugna et al. (2021). Briefly, in a 250-mL conical flask, 2:1 (v/v) of nitric acid and hydrogen peroxide respectively were added to 10 g of honey sample. The mixture was

subjected to evaporation until it became dry, followed by cooling to reach room temperature. Di-ionised water was added to the cooled sample and filtered. The solution was diluted with additional solvent to reach the 100-mL mark on a volumetric flask. The honey solution was analysed for selected heavy metals Cu, Fe, Ni, Zn, Pb, Mn and Co using atomic absorption spectroscopy. The honey sample pH was adjusted to 7 and the metal concentration in the solution was measured using atomic absorption spectroscopy (AAS) both before and after the addition of a spike.

Table 3.1: Physico-chemical properties of a honey sample.

Physio chemical properties	Value before digested	Value after digested
Sample pH	4.6	5.2
EC (ms cm^{-1})	2.00	2.19
TDS (mg/L^{-1})	300.67	322.97
Temperature (^oC)	28	25

3.3.1. Application of Zn-IIP in treatment of honey

A 5-mg quantity of zinc ion imprinted polymer (Zn-IIP) was introduced into a centrifuge tube containing 10 mL of honey solution. The mixture was then shaken at a speed of 100 rpm for 1 hour. Afterward, the concentration of the extracted ions was measured.

3.3.2. Sample analysis

The parameters for the instrument were set up as shown above in Table 3.2. The whole procedure was done in triplicate.

Table 3.2: Parameters of AAS determination.

Parameter	*Cu*	*Fe*	*Ni*	*Zn*	*Pb*	*Mn*	*Co*
Wavelength (nm)	324.75	248.33	232.00	307.59	283.31	279.48	240
Current (mA)	15	30	25	14	10	20	30
Slit (nm)	0.7	0.2	0.2	0.7	0.7	0.2	0.2
Lamp type	C-HCL	C-HCL	C-HCL	C-HCL	C-HCL	C-HCL	C-HCL

Energy	88	62	55	40	82	70	67

3.4. Results and discussion

3.4.1. Infrared spectra

The FTIR spectra of both Zn NIP and Zn IIP were measured and are presented in Figure 3.2 Specific absorption bands were observed in the spectra. The band at 2945 cm^{-1} is due to methyl C-H stretching. The band at 1725 cm^{-1} is due to the carbonyl vibration of EGDMA. The presence of C-O-C stretching (ester) is shown by the absorption at 1141 cm^{-1}, while the weak absorption at 1637 cm^{-1} represents C=C bonds. Additionally, a band at 945 cm^{-1} corresponds to C-H bending. The intense broad band observed at 3374 cm^{-1} indicates the presence of O-H groups. In the washed IIP spectrum, this O-H band becomes more pronounced due to the elution of the template, indicating the opening in the polymer structure. Notably, no IR bands were observed in the range of 1500-1600 cm^{-1}, which suggests that the polymerization process is complete. This finding is in line with earlier research that used a new aminothiol monomer to synthesize and characterize a highly selective polymer imprinted with mercury (II) (Firouzzare et al., 2012). and polyethylene glycol's molecular weight has an impact on the production and characteristics of aqueous polyurethane dispersions (Mumtaz et al., 2013).

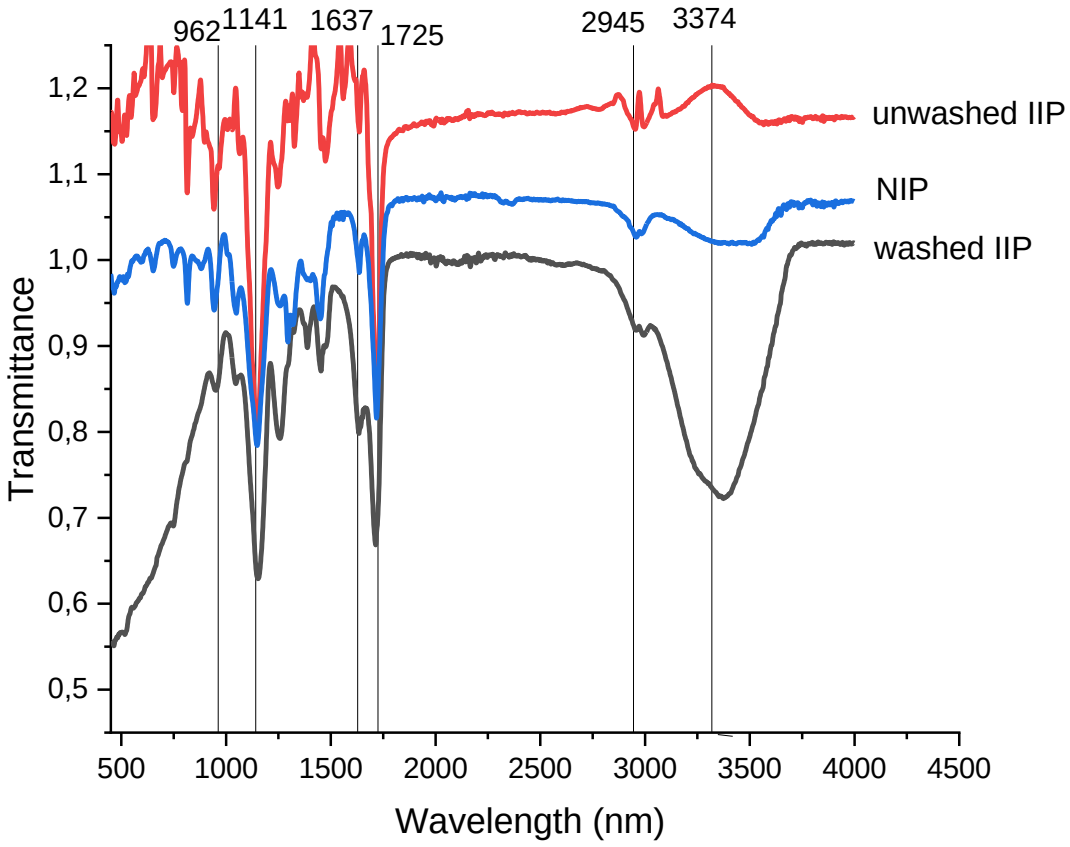

Figure 3.2: Infrared spectra of zinc (II) NIP and Zn (II) IIP washed and unwashed.

3.4.2. Measurement of surface areas

The Methylene Blue adsorption studies showed that leached Zn-IIP had a greater surface area than NIP. This difference in surface area is attributed to the leaching of Zn^{2+} ions out of the polymer, leading to the formation of specific cavities within the polymer network. The adsorption capacity of IIP and NIP is shown in Table 3.2.

Table 3.3: Specific surface areas of synthesized polymers.

Metal ion	**Surface area ($m^2 g^{-1}$)**	
	IIP	NIP
Zn^{2+}	15.02	12.34

3.4.3. Optimization of zinc uptake

3.4.3.1. Effect of solution pH and point of zero charge

Figure 3.3 shows the effect of solution pH on the Zn (II) adsorption efficiency; in acidic medium, it was low, but with increasing solution pH the adsorption of Zn (II) increased, attaining a maximum at pH 7 and then decreasing at higher pH. Figure 3.4 shows the point of zero charge, where H^+ or OH^- are absorbed and the polymer surface has zero net charge, found at pH 6.98. At low sample pH (≤ 6.98) zinc exists as Zn^{2+} coordinating with H_2O, which dissociates to form a proton and hydroxide; at this stage the Zn^{2+}species carry positive charge. At lower sample pH, the repulsive force between particles that are caused by their electric charges which influence adsorption efficiency to be low. At higher sample pH, species have negative charges during adsorption of Zn^{2+}, so that instead of adsorbing it was forming $Zn(OH)_2$ which caused the adsorption efficiency to decrease. Equation 4.15 and 4.16 shows the reaction of zinc and water at lower and high sample pH.

$$Zn^{2+} + H_2O \leftrightarrow Zn(OH)^+ + H_2 \quad (4.15)$$

$$Zn^{2+} + H_2O \leftrightarrow Zn(OH)^- + H \quad (4.16)$$

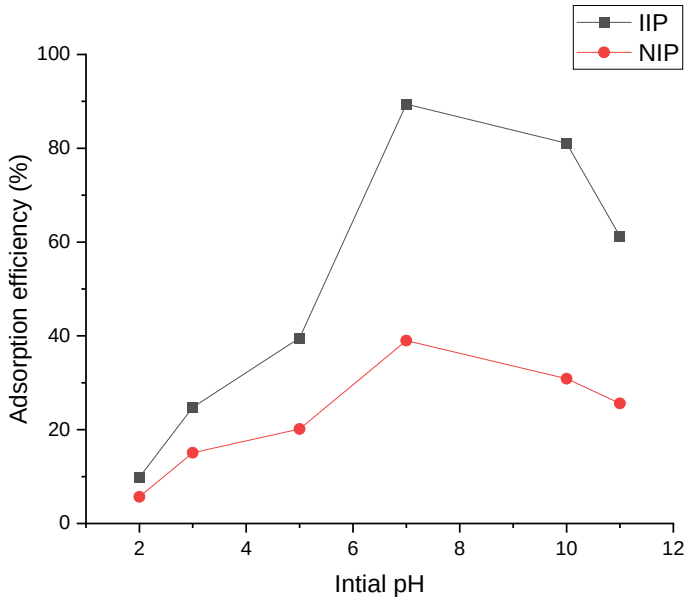

Figure 3.3: pH effect on adsorption of Zn(II) on Zn(II)-IIP and NIP. Conditions: adsorbent mass = 10 mg, initial Zn(II) concentration = 5 mg/L, contact time = 20 min, Shaking speed = 60 rpm at room temperature

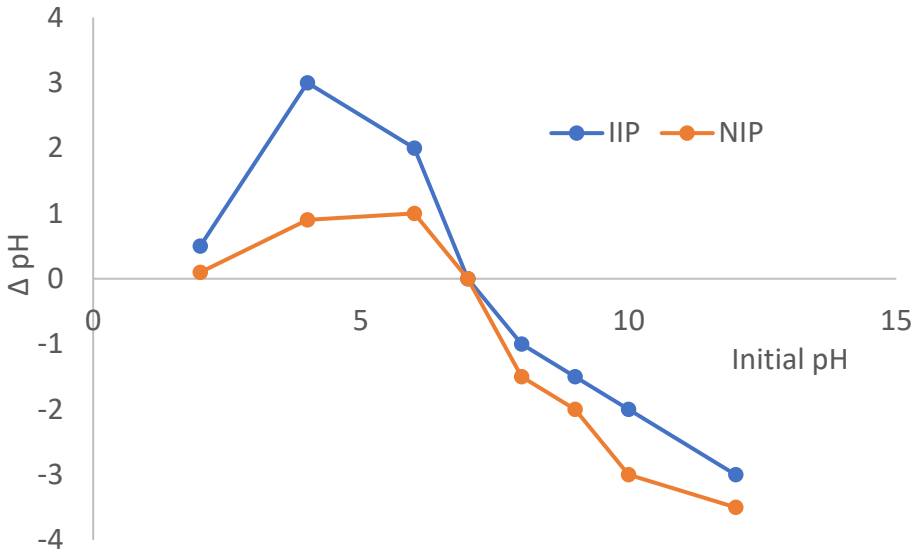

Figure 3.4: Point of zero charge of Zn (II). Conditions: 5 mg adsorbent, Shaking speed 100 rpm for 15 h.

3.4.3.2. Effect of dosage

Figure 3.5 demonstrates the impact of the adsorbent quantity on Zn (II) ion adsorption using the Zn(II) IIP and NIP. The % adsorption efficiency increased up to 5 mg adsorbent mass, after which the adsorption percentage remained constant. The increase in adsorption efficiency up to 5 mg adsorbent can be ascribed to the increase in the number of adsorption sites, increasing the availability of the template to the polymers. The following constant % adsorption efficiency was due to excess vacant sites. Non-imprinted polymer showed the same trend as ion imprinted polymer but the % adsorption efficiency was less because it had no Zn (II) specific binding sites. The optimal dosage was therefore 5 mg, in agreement with Memon et al. (2017), who also noted that increasing the mass of the ion-imprinted polymers provided more binding sites within the polymer, leading to enhanced adsorption efficiency. However, the adsorption efficiency reached its equilibrium point at a mass of 5 mg, which was identified as the optimal mass (Memon et al., 2017).

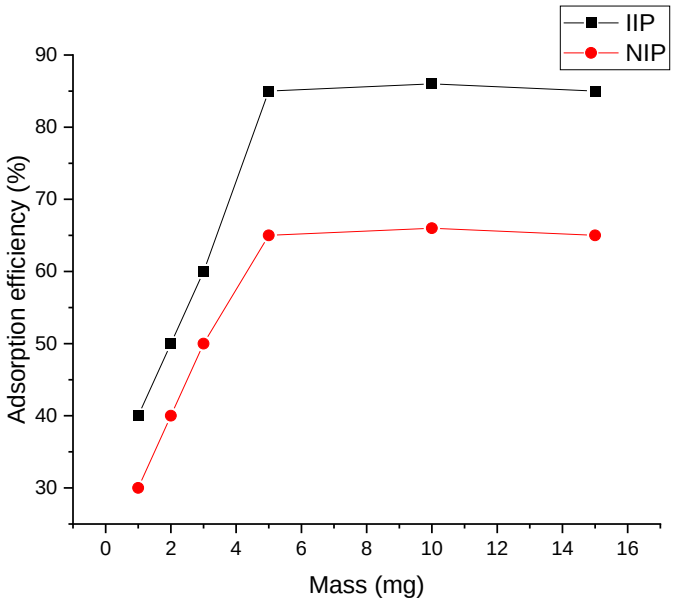

Figure 3.5: Influence of adsorbent mass on adsorption of Zn (II). Conditions: Sample pH = 7, initial concentration = 5 mg/L, contact time = 20 min, and shaking speed = 60 rpm at room temperature.

3.4.3.3. Effect of shaking speed

Figure 3.6 shows the influence of shaking speed on adsorption of zinc (II) onto Zn (II) IIP and NIP. The adsorption efficiency increased with increasing shaking speed. At low shaking speed, the Zn (II) was unable to reach the polymer binding sites. At higher shaking speed, the adsorbate was moving too fast forming the bubbles instead of adsorbing it was desorbing due to this, adsorption efficiency decreased with the increase in sharking speed. NIP adsorption efficiency was low compared to the one for IIP since there was no cavity pore created. Maximum adsorption efficiency was observed at 100 rpm. According to Memon et al. (2017), the adsorption efficiency increased with the increase in shaking speed until it reaches its maximum adsorption at 100 rpm.

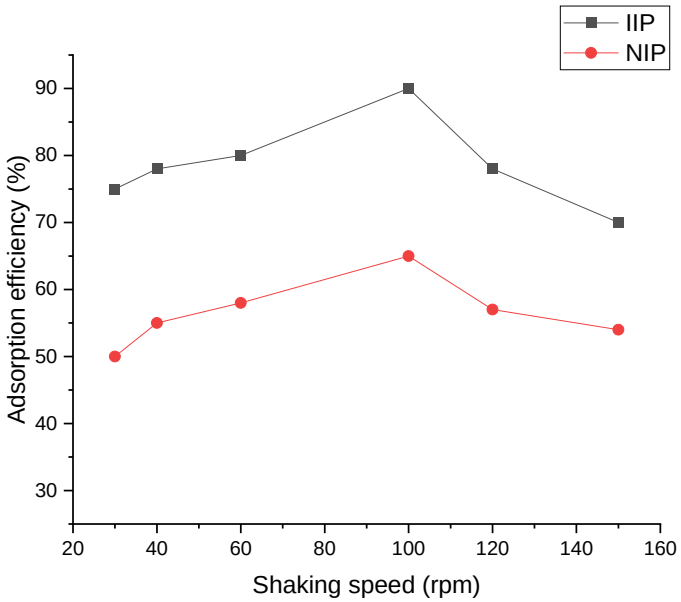

Figure 3.6: Effect of shaking speed on zinc adsorption. Conditions: Sample pH =7, contact time = 20 min, adsorbent mass = 5 mg, and initial ion concentration = 5 mg/L at room temperature.

3.4.3.4. Influence of contact time

The adsorption efficiency increases with an increase in contact time, as presented in Figure 3.7. The adsorption efficiency increased up to a maximum was reached at 15 min; this increase was due to the vacant sites available in the IIP. After 15 min, the adsorption efficiency remained constant because the vacant sites were saturated.

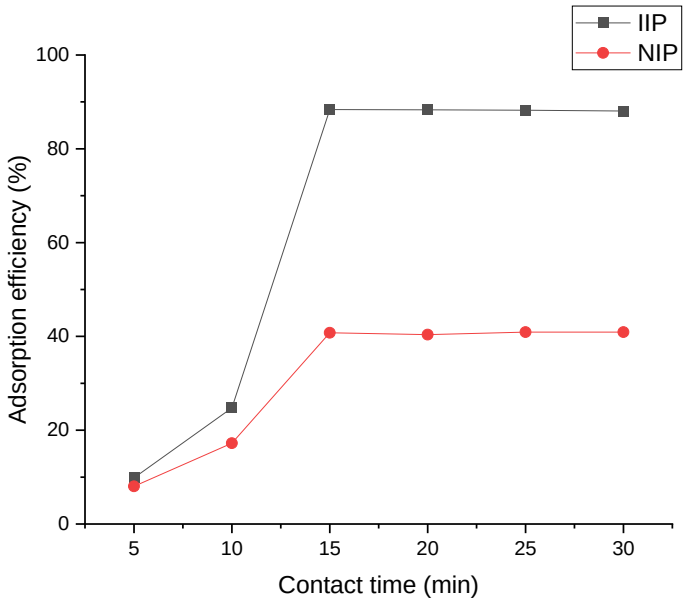

Figure 3.7: Effect of contact time on adsorption. Conditions: Sample pH = 7, initial Zn(II) concentration = 25 mg/L, adsorbent mass = 5 mg, and shaking speed = 100 rpm at room temperature.

In addition to providing data on the adsorption rate, the study of kinetic modeling sheds light on a suitable reaction mechanism. Table 3.4 displays the findings from the kinetic investigations. The pseudo-first-order kinetic model does not well fit the adsorption kinetic data, as evidenced by its lower R2 value and the notable differences between the estimated and observed adsorption capacities. Conversely, the R^2 values of the pseudo-second-order kinetic model were nearer to one, indicating a superior match to the experimental data. There was a good agreement between the estimated and experimental values of adsorption capacity (qe) for various initial concentrations of Zn (II) ions. These results suggest the pseudo-second-order kinetic model for Zn (II) ion adsorption onto the ion imprinted polymer. This suggests that the rate-limiting step is most likely chemical sorption, or chemisorption, and that the adsorption rate is more dependent on the adsorption capacity than the concentration of the adsorbate. Other ions cannot be adsorbed at the same location once one ion has been adsorbed there.

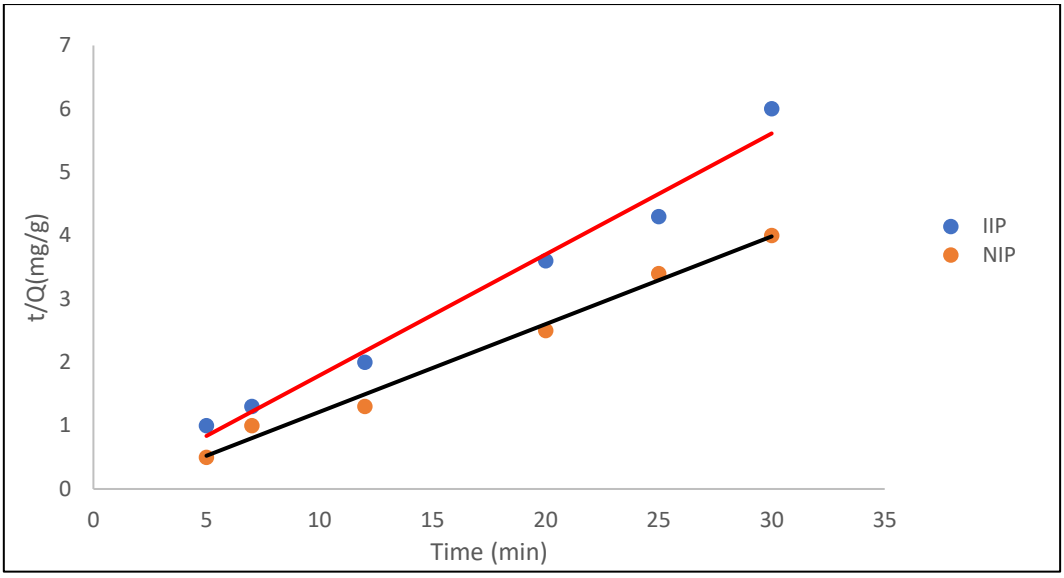

Figure 3.8: Pseudo-second-order kinetics of adsorption of Zn (II) ions by Zn(II) IIP/NIP.

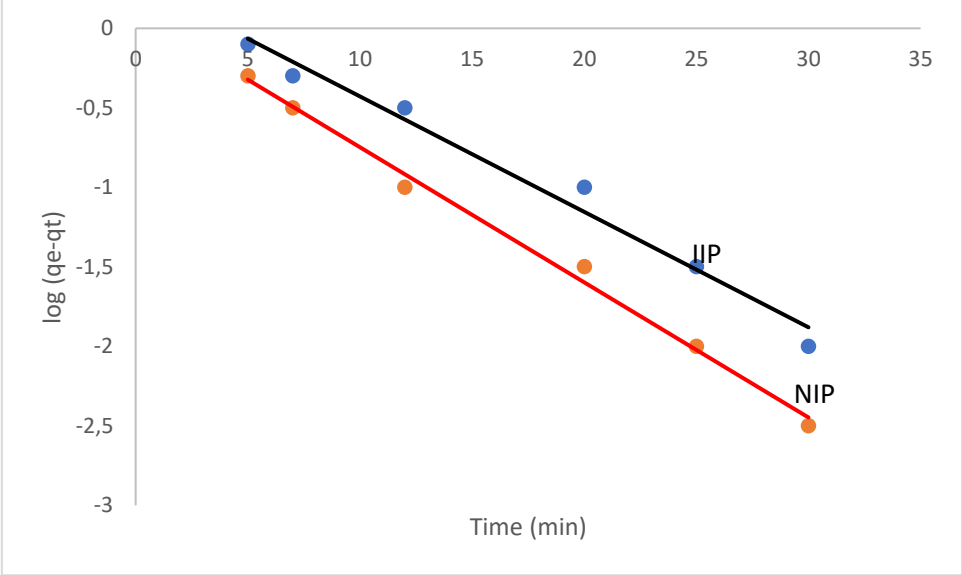

Table 3.4: Constant values for the kinetics models.

Zn (II) Concentration (mg L^{-1})	**q_e exp** (mg/g)	**K_1** (min^{-1})	**q_e** (mg/g)	**R^2**	**K_2** (g/mg.min)	**q_e** (mg/g)	**H** (mg/g.min)	**R^2**
100	4.067	0.060	1.354	0.770	0.0424	4.245	0.696	0.999
100	3.023	0.031	0.985	0.584	0.0243	2.546	0.371	0.976

3.4.3.5. Effect of zinc concentration on the adsorption isotherm

The effect of zinc concentration on adsorption is shown in Figure 3.8. A higher starting concentration resulted in higher adsorption rates, according to the sigmoidal relationship observed in the adsorption rate. Because there were more adsorption sites on the IIP, the first removal % fell as the starting concentration increased. At a Zn(II) ion concentration of 10 mg/L, the maximum adsorption efficiency of 98% was achieved, suggesting that Zn (II) had saturated the surface of the IIP. The fact that the adsorption was unaffected by additional concentration increases suggests that the polymer had achieved its saturation point, which was dependent on the starting concentration.

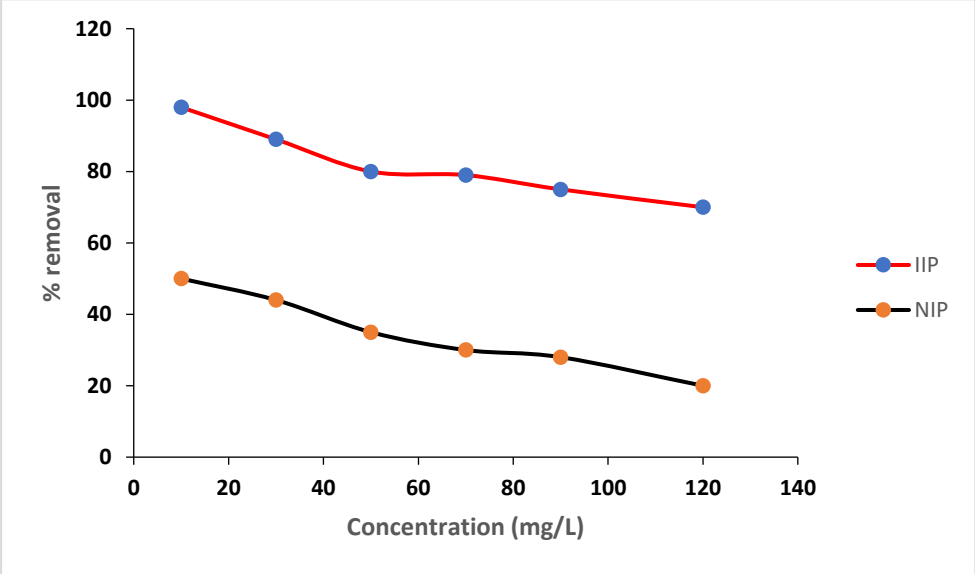

Figure 3.9: Effect of zinc concentration on adsorption. Conditions: Sample pH =7, adsorbent mass = 5 mg, contact time = 20 min, shaking speed = 100 rpm at room temperature.

Langmuir, Freundlich, and Temkin are depicted in Figures 3.10, 3.11, and 3.12, respectively. Using the Langmuir, Freundlich, and Temkin isotherms, the mechanism of zinc adsorption was investigated further (Table 3.5). Zinc adsorption onto both Zn-IIPs and the NIP matched better to the Langmuir adsorption isotherm, suggesting monolayer adsorption, according to an analysis of the Freundlich, Temkin, and Langmuir plots. The Langmuir isotherms model postulates that once the adsorption sites on the homogenous surface were occupied, no more adsorption could take place. The greater correlation coefficient (0.99), as opposed to the values of 0.90 and 0.68 obtained with the Temkin and Freundlich isotherm investigations, respectively, supports the fitting to Langmuir, which was validated by (Table 3.3).

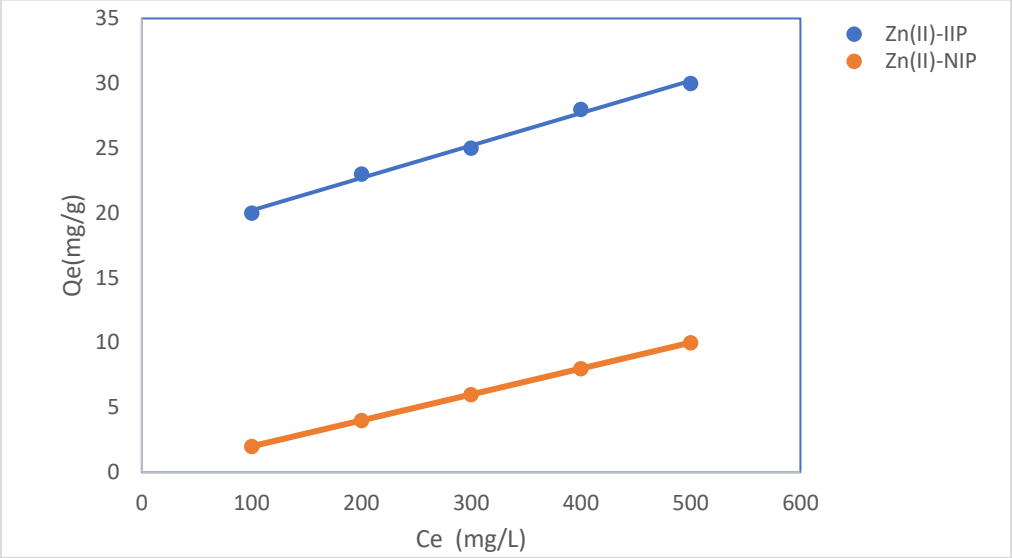

Figure 3.10: Langmuir adsorption isotherm for the adsorption of Zn (II) onto IIPs.

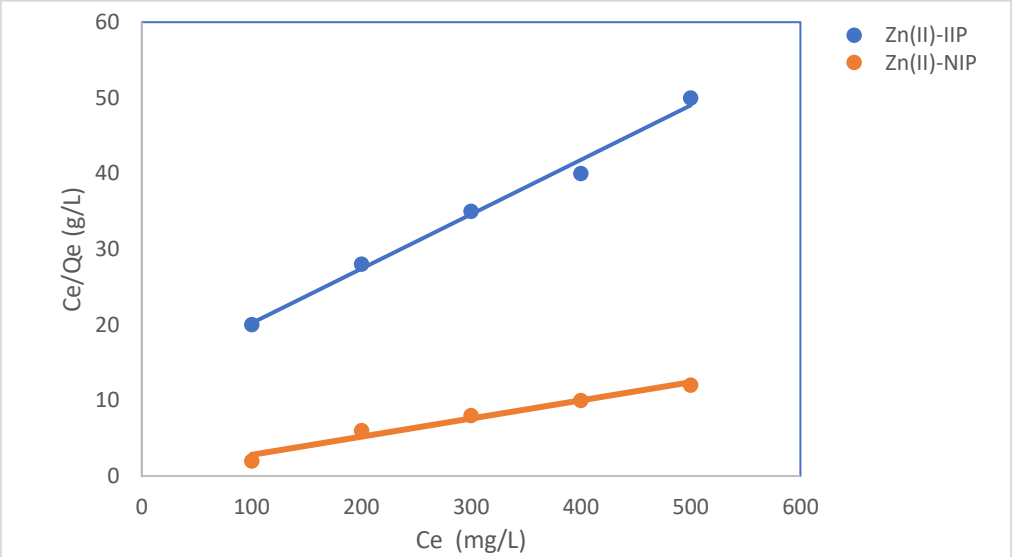

Figure 3.11: Freundlich adsorption isotherm for the adsorption of Zn (II) onto IIPs.

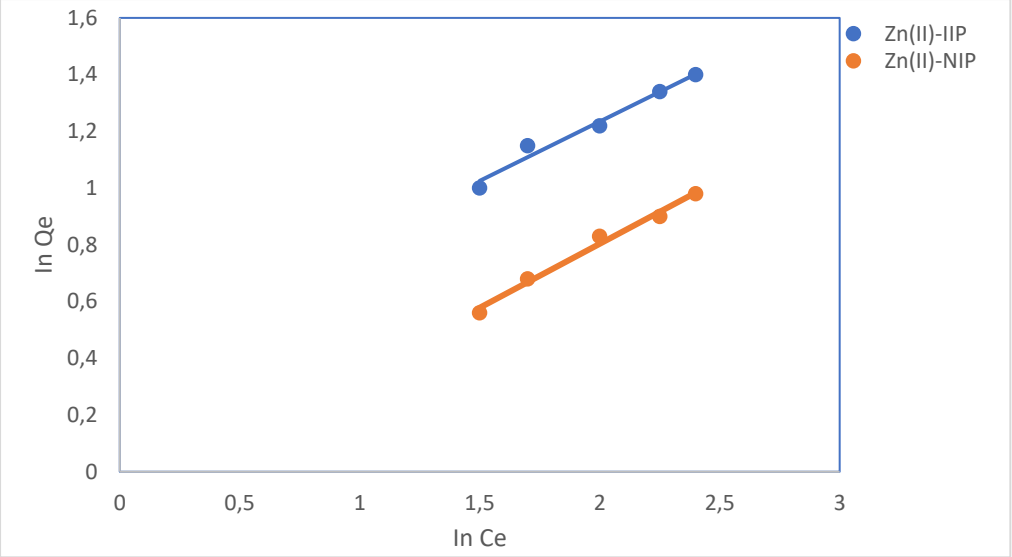

Figure 3.12: Temkin adsorption isotherm for adsorption of Zn (II) onto IIPs.

Table 3.5: Langmuir, Freundlich and Temkin values for the adsorption of Zn (II) on IIPs.

Isotherm models	**q_{max}**	**R_L**	**R^2**
Langmuir isotherm	mg/g		
	9.03	0.45	0.99
	B_T	K_T	R^2
Temkin isotherm	J mol^{-1}	L mg^{-1}	
	1.94	0.59	0.68
Freundlich adsorption	1/n	R_F	R^2
	0.74	0.61	0.90

3.4.4. Selectivity studies

The selective adsorption of zinc ions co-occurring with competing ions like (Co (II)), (Pb (IV)), and (Cu (II)) was studied. These ions have similar ionic radii (Zn (II) = 74 pm, Co (II) = 74 pm, Pb (IV)= 79 and Cu (II) = 73 pm) and have the same charge. The zinc ion imprinted polymer (Zn-IIP) exhibited a higher adsorption efficiency of 90% in the presence of these competing ions, as shown in Table 3.6.

Table 3.6: K values of the NIP and IIP

	K_d		K	K'
Adsorbent	Zn^{2+}	Cu^{2+}		4.87
IIP	395.61	37.01	10.09	
NIP	82.06	39.52	2.07	
	Zn^{2+}	Co^{2+}		8.14
IIP	1958.18	120.95	16.19	
NIP	70.07	34.98	2.00	

Figures 3.11 and 3.12 illustrate the adsorption efficiency of ions extracted by the IIP and NIP for individual ions and ion couples. The polymer demonstrated the ability to extract competing ions, as depicted in Figure 3.11. However, the highest selectivity was observed for Zn^{2+} ions, as the pores created in the polymer were specifically designed for zinc ions. Even in the presence of competing ions, the selectivity of the IIP for Zn^{2+} remained high. In contrast, the adsorption efficiency of the NIP was relatively low and comparable for all ions. This can be attributed to the absence of specific cavities in the non-imprinted polymer that would facilitate selective adsorption.

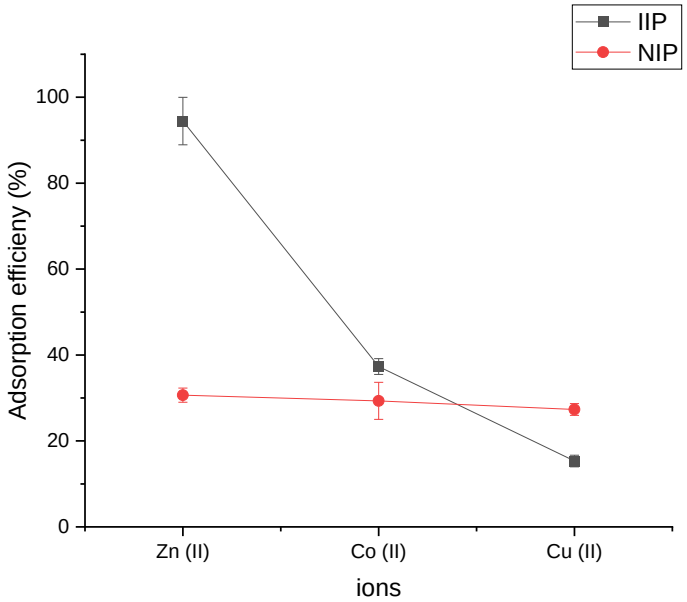

Figure 3.13: Adsorption efficiency for metal ions.

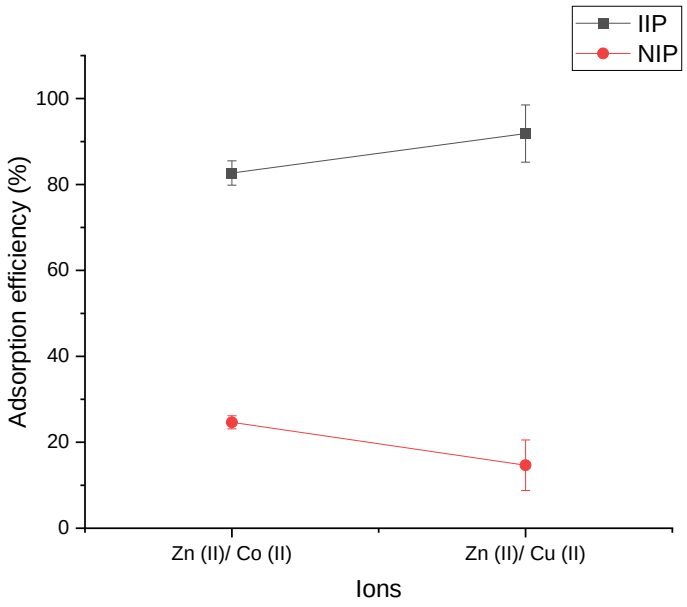

Figure 3.14: Adsorption efficiency in present of competing ions.

A competitive adsorption study was conducted in triplicate, involving species/ions with similar or comparable ionic radii that are commonly found alongside Zn (II). The distribution coefficient of the IIP was higher than that of the NIP, which is due to the selective binding sites present in the ion-imprinted polymer. Table 3.6 shows that the zinc ion-imprinted polymer exhibited greater selectivity towards Zn^{2+} compared to the other competing species. On the other hand, the non-imprinted polymer demonstrated similar affinity for all ions, as it lacked specific recognition sites for any ion.

3.5. Application of honey sample

The B vitamins: vitamin B6, folic acid, niacin, pantothenic acid, and riboflavin are all present in trace amounts in honey. Along with the minerals calcium, chromium, manganese, potassium, selenium, and others, it also contains ascorbic acid. The average concentration of zinc, potassium, magnesium, and copper in 100g of honey is 0.2–0.5 mg, 10-470 mg, 0.7–13 mg, and 0.01-0.1, respectively. According to Hungerford et al. (2020), trace element levels are generally low with the exception of zinc, iron, and manganese (Zn; 10.90 ± 24.7 mg/kg, Fe; 4.01 ± 6.98 mg/kg, and Mn; 4.48 ± 5.03 mg/kg)), which are found at higher levels in honeys from rural areas compared to those from urban areas (Zn = 4.90 ± 11.17 mg/kg, Fe = 1.576 ± 1.33 mg/kg, and Mn = 2.385 ± 2.28 mg/kg).P (1.17–100.66), Fe (1.13–10.32), Al (0.02–13.04), Mn (0.07–0.68), Zn (0.14–3.87), Cu (0.05–0.68), Ca (18.60–136.14), Mg (6.01–46.57), Na (6.10–89.98), and K (90.92–1955.75) were the main trace elements in μg g^{-1} of honey,

according to Khan et al. (2018). A honey sample was spiked with a known quantity of metal, and the recoveries were examined to evaluate the procedure. The technique detection limit and recovery outcomes for the detected elements are displayed in Table 3.7.

Table 3.7: Concentration of trace elements in honey.

Metal ion	**Concentration found in honey (mg kg^{-1})**	**Concentration after spiking (mg kg^{-1})**	**MDL(Method of detection limit)**	**Recovery %**
Cu	1.05	1.92	0.0790	87.00
Fe	6.42	7.40	0.0159	98.00
Ni	ND	5.06	0.0253	
Pb	3.04	3.99	0.2531	95.00
Mn	4.95	6.59	0.0617	110.24
Co	ND	4.12	0.2251	
Zn	11.29	13.04	0.2431	99.00

ND = not detected

3.5.1. Determination of Zn(II) ions in honey samples

When the technique was used on actual honey samples, a high adsorption effectiveness of 94% was attained (Table 3.8). This proved that the sorbent was suitable for extracting zinc (II) ions from the honey sample in a selective manner.

Table 3.8: Removal of Zinc (II) from honey sample.

Sample	**Zn^{2+} spiked mg kg^{-1}**	**RSD %**	**Zn^{2+} + IIP spiked mg kg^{-1}**	**RSD %**	**AE %**	**RSD %**
Honey sample	23.62	0.02	22.68	0.05	94.00	1.03

3.5.2. Comparative studies

A comparison of the adsorbent for removal of the zinc was done evaluating the adsorption efficiency as indicated in Table 3.9. Zinc ion imprinted polymer has higher adsorption efficiency than natural adsorbent.

Table 3.9: Comparison of adsorbent for removal of zinc (II).

Adsorbent	**Matrix**	**Adsorption capacity (%)**	**Ref**erence
Zinc ion imprinted polymer	Honey	94.00	This study
Oil palm empty fruit bunches biochar	Aqueous solution	25.49	Zamani et al. (2017)
Zinc oxide nano-material	wastewater	95.00	Primo et al., (2020)
Magnetic Chitosan	Aqueous solution	83.81	Karimi et al., (2022)
Camellia sinensis	Aqueous solution	76.00	Çelebi et al., (2020)
Natural bentonite	Aqueous solution	90.00	Esmaeil & Eslami (2019).

3.6. Conclusion

Precipitation polymerization was used to create the zinc ion imprinted polymer, and the final polymer underwent extensive characterization. The cross-linking monomer was ethylene glycol dimethacrylate, and the initiator was 2,2'-azobis (isobutyronitrile), with methanol serving as the solvent. With the zinc ion-imprinted polymer (Zn-IIP), the maximum percentage of Zn^{2+} removed was about 90% when the following ideal parameters were met: a pH of 7.0 solution, 5 mg of adsorbent, 15 minutes of contact time, 100 rpm shaking rate, and a starting Zn^{2+} concentration of 25 mg/L. High adsorption capacity and superior selectivity for Zn(II) were displayed by the Zn-IIP, allowing it to keep out competing ions such as Cd (II), Pb (II), and Cu (II). The adsorption of Zn (II) onto Zn-IIP was characterized by pseudo-second-order kinetics. Additionally, utilizing the Zn-IIP to remove zinc showed an amazing adsorption capacity 0f 98%.

References

Abdelnour SA, Abd El-Hack, ME, Alagawany M, Farag MR and Elnesr SS, 2019. Beneficial impacts of bee pollen in animal production, reproduction and health. *Journal of Animal Physiology and Animal Nutrition, 103*(2), 477-484.

Adugna E, Hymete A, Birhanu G and Ashenef, A, 2020. Determination of some heavy metals in honey from different regions of Ethiopia. *Cogent Food & Agriculture, 6*(1), 1764182.

Aljohar HI, Maher HM, Albaqami J, Al-Mehaizie M, Orfali R, Orfali R and Alrubia S, 2018. Physical and chemical screening of honey samples available in the Saudi market: An important aspect in the authentication process and quality assessment. *Saudi Pharmaceutical Journal, 26*(7), 932-942.

Altundag H, Bina E and Altıntıg E, 2016. The levels of trace elements in honey and molasses samples that were determined by ICP-OES after microwave digestion method. *Biological Ttrace Element Research, 170*(2), 508-514.

Azha SF, Shahadat M, Ismail S, Ali SW and Ahammad SZ, 2021. Prospect of clay-based flexible adsorbent coatings as cleaner production technique in wastewater treatment, challenges, and issues: A review. *Journal of the Taiwan Institute of Chemical Engineers, 120*, 178-206.

Burakov AE, Galunin EV, Burakova IV, Kucherova AE, Agarwal S, Tkachev AG and Gupta VK, 2018. Adsorption of heavy metals on conventional and nanostructured materials for wastewater treatment purposes: A review. *Ecotoxicology and Environmental Safety, 148*, 702-712.

Hu Q, Lan R, He L, Liu H and Pei X, 2023. A critical review of adsorption isotherm models for aqueous contaminants: Curve characteristics, site energy distribution and common controversies. *Journal of Environmental Management*, 329,117104.

Chen X, Hossain MF, Duan C, Lu J, Tsang YF, Islam MS and Zhou Y, 2022. Isotherm models for adsorption of heavy metals from water-A review. *Chemosphere*, 135545.

Çelebi H, Gök G and Gök O, 2020. Adsorption capability of brewed tea waste in waters containing toxic lead (II), cadmium (II), nickel (II), and zinc (II) heavy metal ions. *Scientific reports, 10(1)*,17570.

Charles J, Bradu C, Morin-Crini N, Sancey B, Winterton P, Torri G, Badot PM.and Crini G, 2016. Pollutant removal from industrial discharge water using individual and combined effects of adsorption and ion-exchange processes: Chemical abatement. *Journal of Saudi Chemical Society*, *20*(2), pp.185-194.

Esmaeili A and Eslami H, 2019. Efficient removal of Pb (II) and Zn (II) ions from aqueous solutions by adsorption onto a native natural bentonite. *MethodsX*, *6*, 1979-1985.

Fontana MF, Banga S, Barry KC, Shen X, Tan Y, Luo ZQ and Vance RE, 2011. Secreted bacterial effectors that inhibit host protein synthesis are critical for induction of the innate immune response to virulent Legionella pneumophila. *PLoS pathogens*, *7*(2), 1001289.

Fulgoni III VL, Keast DR, Bailey RL and Dwyer J, 2011. Foods, fortificants, and supplements: where do Americans get their nutrients? *The Journal of nutrition*, *141*(10), 1847-1854.

Haber M, Mishyna M, Martinez JI and Benjamin O, 2019. Edible larvae and pupae of honeybee (Apis mellifera): Odor and nutritional characterization as a function of diet. *Food Chemistry*, *292*,197-203.

Hermanns R, Mateescu C, Thrasyvoulou A, Tananaki C, Wagener FA and Cremers NA, 2020. Defining the standards for medical grade honey. *Journal of Apicultural Research*, *59*(2), 125-135.

Hu J, Yang L, Yang P, Jiang S, Liu X and Li Y, 2020. Polydopamine free radical scavengers. *Biomaterials Science*, *8*(18), 4940-4950.

Hungerford NL, Tinggi U, Tan BL, Farrell M and Fletcher MT, 2020. Mineral and trace element analysis of Australian/Queensland Apis mellifera honey. International journal of environmental research and public health, 17(17), 6304.

Karimi F, Ayati A, Tanhaei B, Sanati AL, Afshar S, Kardan A, Dabirifar Z and Karaman C, 2022. Removal of metal ions using a new magnetic chitosan nano-bio-adsorbent; A powerful approach in water treatment. *Environmental Research*, *203*, 111753.

Khan SU, Anjum SI, Rahman K, Ansari MJ, Khan WU, Kamal S, Khattak B, Muhammad A and Khan HU, 2018. Honey: Single food stuff comprises many drugs. *Saudi journal of biological sciences*, 25(2), 320-325.

Lin PH, Sermersheim M, Li H, Lee PH, Steinberg SM and Ma J, 2018. Zinc in wound healing modulation. *Nutrients*, 10(1), 16.

Maret W, 2013.Zinc biochemistry: from a single zinc enzyme to a key element of life. *Advances in nutrition*.,4(1):82-91.

Mumtaz F, Zuber M, Zia KM, Jamil T and Hussain R, 2013. Synthesis and properties of aqueous polyurethane dispersions: Influence of molecular weight of polyethylene glycol. *Korean Journal of Chemical Engineering*, *30*, 2259-2263.

Nishizawa Y, Minato H, Inui T, Uchihashi T and Suzuki D, 2020. Nanostructures, thermoresponsiveness, and assembly mechanism of hydrogel microspheres during aqueous free-radical precipitation polymerization. *Langmuir*, *37*(1), 151-159.

Pavlova T, Stamatovska V, Kalevska T, Dimov I and Nakov G, 2018. Quality characteristics of honey: a review. *Proceedings of University of Ruse*, *57*(10.2), 32-37.

Primo JDO, Bittencourt C, Acosta S, Sierra-Castillo A, Colomer JF, Jaerger S, Teixeira VC and Anaissi FJ, 2020. Synthesis of zinc oxide nanoparticles by ecofriendly routes: adsorbent for copper removal from wastewater. *Frontiers in Chemistry*, *8*, 571790.

Qin YP, Jia C, He XW, Li WY and Zhang YK, 2018. Thermosensitive metal chelation dual-template epitope imprinting polymer using distillation–precipitation polymerization for simultaneous recognition of human serum albumin and transferrin. *ACS applied materials & interfaces*, *10*(10), 9060-9068.

Squadrone S, Brizio P, Stella C, Mantia M, Pederiva S, Brusa F, Mogliotti P, Garrone A and Abete MC, 2020. Trace elements and rare earth elements in honeys from the Balkans, Kazakhstan, Italy, South America, and Tanzania. *Environmental Science and Pollution Research, 27, 12646-12657.*

Stecka H, Jedryczko D, Welna M and Pohl P, 2014. Determination of traces of copper and zinc in honeys by the solid phase extraction pre-concentration followed by the flame atomic absorption spectrometry detection. *Environmental monitoring and assessment*, *186*(10), 6145-6155.

Sun D, Zhu Y, Meng M, Qiao Y, Yan Y and Li C, 2017. Fabrication of highly selective ion imprinted macroporous membranes with crown ether for targeted separation of lithium ion. *Separation and Purification Technology*, *175*,19-26.

Thaçi BS and Gashi ST, 2019. Reverse osmosis removal of heavy metals from wastewater effluents using biowaste materials pre-treatment. *Polish Journal of Environmental Studies, 28*(1), 337-341.

Tian X, Ding J, Zhang B, Qiu F, Zhuang X and Chen Y, 2018. Recent advances in RAFT polymerization: Novel initiation mechanisms and optoelectronic applications. *Polymers*, *10*(3), 318.

Varol M, Kaya GK and Alp A, 2017. Heavy metal and arsenic concentrations in rainbow trout (Oncorhynchus mykiss) farmed in a dam reservoir on the Firat (Euphrates) River: Risk-based consumption advisories. *Science of the Total Environment*, *599*, 1288-1296.

Wright AC, Fan Y and Baker GL, 2018. Nutritional value and food safety of bivalve molluscan shellfish. *Journal of Shellfish Research*, 37(4),695-708.

Xia Y, Qiu D and Wang J, 2017. Transition-metal-catalyzed cross-couplings through carbene migratory insertion. *Chemical reviews*, *117*(23), 13810-13889.

Zamani SA, Yunus R, Samsuri AW, Salleh MA and Asady B, 2017. Removal of zinc from aqueous solution by optimized oil palm empty fruit bunches biochar as low-cost adsorbent. *Bioinorganic Chemistry and Applications*, *2017*.

Zhou Y, Lu J, Zhou Y and Liu Y, 2019. Recent advances for dyes removal using novel adsorbents: a review. *Environmental pollution*, *252*, 352-365.

Chapter 4: Synthesis of lead-ion imprinted polymers for selective extraction of Pb (II) from wastewater

Abstract

Synthesis of IIP and NIP for selective extraction of Pb (II) ions from wastewater was attempted. Precipitation copolymerization of methacrylic acid as the monomer, ethylene glycol dimethacrylate as the cross-linker, and 2,2'-azobis (isobutyronitrile) as the initiator was used to create IIPs and NIPs. After leaching the template ion out of the IIPs with 2 M hydrochloric acid, cavities in the polymer matrix formed that could selectively complex Pb (II) ions. FTIR was used to characterize the functional groups of the imprinted and non-imprinted polymers, and the ideal parameters of 50 mg of adsorbent, pH 9 of the starting solution, and 15 minutes of contact time were used to determine the point of zero charge. The IIP and NIP's adsorptive qualities were assessed using Freundlich and Langmuir isotherms. The data was better modeled by the Langmuir adsorption isotherm, as indicated by the 0.999 and 0.975 Langmuir and Freundlich correlation coefficients, respectively. The adsorption occurred on homogenous surfaces. Lead can potentially be recovered from waste water using the imprinted polymer.

Keywords: Ion imprinted polymer, thiosemicarbazide, lead (II) ion, precipitation polymerization and selective removal.

4.1. Introduction

Our society's industrial development results in significant emissions of pollutants and trace elements. In the food chain, trace elements build up. When they reach the body, they mix with inorganic substances to form complexes that are harmful to the body because they cannot break down or be expelled (Emenike et al., 2021; Sonone et al., 2020; Tang et al., 2021). One prevalent trace element that contaminates the environment is lead. Wastewater from paints, lead-acid batteries, phosphate fertilizers, and lead corrosion are its sources. Lead exposure over time can cause memory loss and low IQ.

It has been discovered that some of the trace elements in wastewater are beyond the maximum permitted limits and coexist with other competing species rather than existing alone. Owing to these reasons, a more effective technique for eliminating trace elements from native solutions had to be created (Dimpe and Nomngongo, 2017). A few of the techniques created are osmosis, liquid-liquid extraction, and membrane assisted liquid extraction (Golcs et al., 2021; Tabani et al., 2018; Ding et al., 2021). Lead may be extracted from solutions with great efficiency using adsorption techniques (Zhao et al., 2016; Zare-Dorabei et al., 2016).

Pb^{2+} removal from various solutions has been investigated for the effectiveness of a number of adsorbents, including zeolite, metal oxides (ZnO, TiO2, and iron oxide), activated carbon, and both synthetic and natural polymers (β-cyclodextrin) (Shah et al., 2017; Genç and Dogan, 2015). High activation costs and inadequate recycling restrict the use of activated carbon, despite its excellent adsorption efficiency towards Pb^{2+} (Lin et al., 2020; Lin et al., 2023; Zhanga et al., 2019; Zhao et al., 2020). Zeolites are highly susceptible to irreversible adsorption-induced deactivation (Hu et al., 2022; Luo et al., 2022; Li et al., 2023). Metal oxides are extremely sensitive to grinding conditions and can be impacted by unintentional contamination from the environment and milling media. Low cost, physical stability, porosity, homogeneous pore size distribution, and ease of regeneration characterize polymeric adsorbents. Regeneration can lessen the need for new adsorbent, which is crucial from an economic and environmental standpoint, as well as the need to dispose of spent adsorbent. According to Hassan et al. (2020) and Janoschka et al. (2015), they can operate across a wide pH range.

In the presence of closely related inorganic ions, ion-imprinted polymers are non-porous polymeric materials that, upon leaching the imprint ion, can rebind, detect, or transport the target analyte selectively (Abdallah et al., 2021; Stevens and Batlokwa, 2017; Pereao et al., 2018). Ion-imprinted polymers are distinguished by their extended shelf life, strong affinity, and target ion selectivity. When a template ion and a functional monomer are combined, the monomer self-assembles around the template. A cross-linker will be added for the polymerization process to proceed. Using an appropriate extraction porogen that leaves the memory site or binding site complimentary to a certain template, the template is eliminated following polymerization. In the solid phase, ion-imprinted polymers are used for preconcentrating, ion removal, and separation ion from coexisting ions (Xie et al., 2019: Omidi et al., 2014). According to Balouch et al. (2014) more than 96% of Pb could be recovered from real samples, and grafted-IIP retained more than 80.5% adsorption capacity (Wang et al., 2019).

Thiosemicarbazide (NH_2NH-(C=S) $=NH_2$) is a hydrazine derivative of thiocarbamic acid that is commonly used in organic synthesis of heterocyclic compounds such as pyrazoles, thiazole and triazines (Karrouchi et al., 2018). Thiosemicarbazide derivatives are used in catalysis, electrochemistry and pharmaceutical chemistry, under catalysis for redox reaction is used for antitumor, antimalarial agent, antibacterial and electrochemical sensors (Hishimone et al., 2021). Thiosemicarbazide has been used also in industry for applications like anti-corrosion

and anti-fouling effects have also been reported for these derivatives (Acharya et al., 2021 & Kanwar et al., 2015). It is a bidentate ligand which is coordinated with transition metal. It forms complexes with different cations such as zinc, iron, nickel, copper and others (Muleta et al., 2019).

In this work, a Pb (II) IIP and a NIP were produced by precipitation polymerization due to the good yield and shorter time needed compared to bulk polymerization where there is grinding and sieving. Polymers were complexed with thiosemicarbazide before applied for selective extraction of Pb ion from aqueous solution. Pb-IIPs were characterized by FTIR and point of zero charge followed by solid phase extraction of a target metal ion extracted from the wastewater onto the IIPs absorbed into the IIPs by different techniques and to determine trace elements in the wastewater.

4.2. Materials and methods

4.2.1. Chemicals and reagents

All chemicals and reagents including, methanol (CH_3OH) (99.85%) grade A, methacrylic acid ($C_5H_8O_2$) (MAA) (99.5%) grade A, azobisisobutyronitrile ($C_8H_{12}N_4$) (AIBN) (98%) A, ethylene glycol dimethacrylate ($C_{10}H_{14}O_4$) (EGDMA) (99%), lead acetate trihydrate ($C_4H_{12}O_7Pb$) (99.99%) ACS, hydrochloric acid (HCl) (37%) AR, zinc sulphate ($ZnSO_4$) (99%) AR and thiosemicarbazide (CH_5N_3S) 98% AR were sourced from Merck (Wadesville, South Africa). Cobalt (II) chloride ($CoCl_2$) (97%) LR and copper (II) sulphate ($CuSO_4$) (98%) LR were bought from Sigma-Aldrich (Johannesburg, South Africa).

4.2.2. Instrumentation

Infrared spectroscopy was implemented to differentiate the IIP functional groups before and after extraction and non-imprinted polymer (Pretoria, South Africa). The concentration of metal ions in samples was measured by Pb^{2+} ion analysis using atomic absorption spectroscopy (Pretoria, South Africa).

4.2.3. Synthesis of Pb^{2+} ion imprinted polymers (IIPs)

The modified method of Xia et al. (2017) was used to prepare Pb^{2+} IIP and NIP. The $Pb(C_2H_3O_2).2H_2O$ template (0.116 g) and 422 µL (5 mmol) $C_4H_6O_2$ were added to 70 mL methanol in a 250 mL one-neck round-bottomed flask. After stirring for 15 min to homogenize the solution it was purged to remove oxygen and provide an inert atmosphere before adding 2 mL (10 mmol) $C_{10}H_{14}O_4$. After 2 min purging of the mixture with nitrogen to displace oxygen, the $C_8H_{12}N_4$ initiator (50 mg) was added. The flask was greased, loosely closed with lead and

covered with parafilm. The flask was then heated for 7 h at 80ºC in an oil bath. After filtration, the product was collected and allowed to dry overnight. The NIPs were prepared using the same process without a template.

4.2.4. Elution of Pb^{2+} IIP

After polymerization of the IIPs and non-imprinted polymer, they were rinsed eight times with 2 M HCl to extract the template (Tavengwa et al., 2016), as shown in Figure 4.1. The obtained IIPs and NIPs (3 g and 1 g, respectively) were transferred to 50-mL solid phase cartridges with a cotton wool plug on the bottom. The elution process was done in continuous mode. The eluted was collected after every hour. The procedure was repeated eight times for both IIPs and NIPs. The wet IIPs and NIPs were dried for overnight.

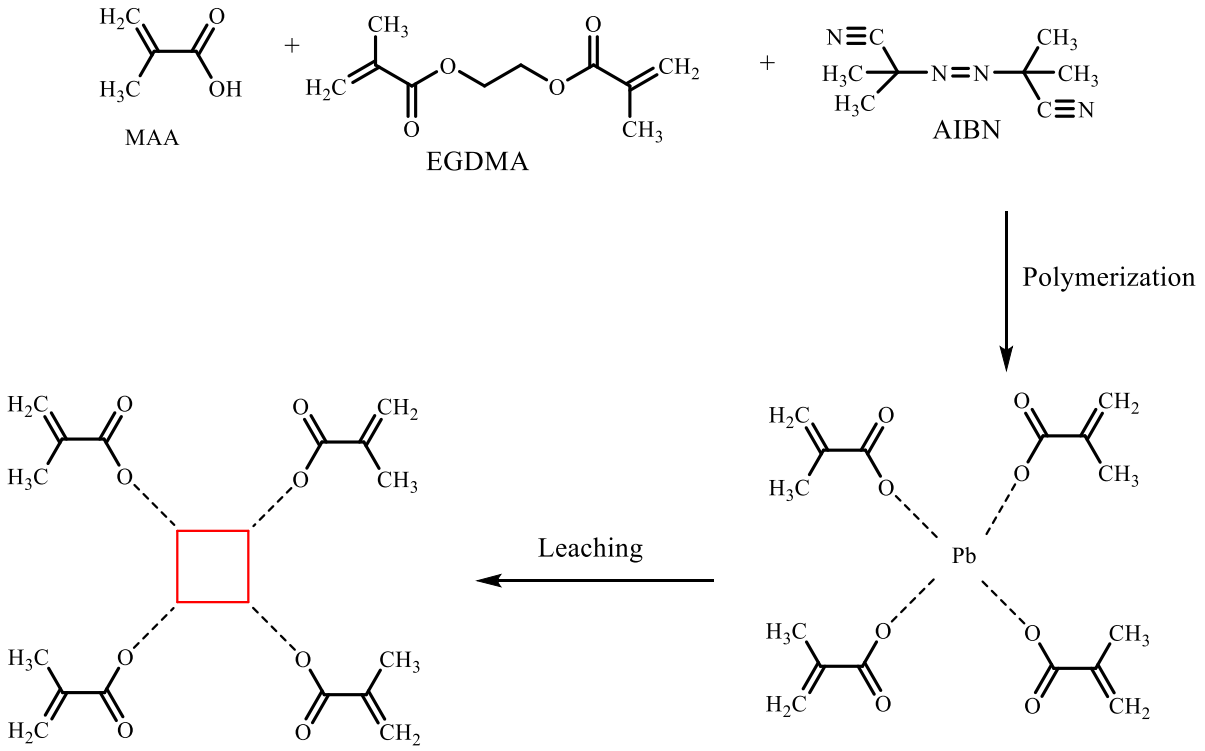

Figure 4.1: Scheme illustrating imprinting process for Pb (II) imprinted polymer.

4.2.5. Batch experiment

In a batch experiment to adsorb Pb^{2+} from aqueous solution, one parameter was investigated while keeping others constant. The parameters investigated include sample pH, dosage, contact time and concentration. Lead ion imprinted polymer of 30 mg was suspended into a Pb^{2+} solution of 5 mg/L. Sample pH was adjusted by dropwise addition of 0.1 M HCl or NaOH. Using a shaker and a centrifuge (NF 1200; PROG No. 7, RPM/RCF 4010, Time 5 min, and

ACC/BRK 5), the mixtures were agitated at 75 rpm for 20 minutes and filtered with Whatman filter papers (150 µm) for analysis with UV-VS spectrometry after being mixed with complexing agent thiosemicarbazide with a 1:3, v/v solution. The purpose of adding complexing was for Pb-IIP and Pb-NIP to be active in UV-VS. According to Bharty et al. (2019), thiosemicarbazide is commonly ligand for transitional metals. The metal complex occurs through S atom. The spectra were recorded for each sample on SP8001 spectrophotometer wavelength at the range 200-800 nm with a cuvette of 1 cm path length. The percentage adsorption E and adsorption capacity Q_e (mg g^{-1}) were computed as follows:

$$E = \frac{C_i - C_f}{C_i} \times 100 \quad (4.1)$$

$$Q_e = \frac{(C_i - C_f)\, V}{W} \quad (4.2)$$

where C_i and C_f = initial and final concentrations (mg L^{-1}) of Pb (II), respectively,

W = sorbent weight (g), and

V = solution volume (mL).

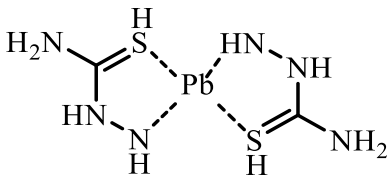

Figure 4. 2: Structure of Pb (II)- thiosemicarbazide

4.2.6. Adsorption isotherms

Over the range of 10-45 mg/L of Pb^{2+} concentration, adsorption isotherms were assessed. Pb^{2+} -IIP and Pb^{2+} -NIP (50 mg) were added to the solution after it had been brought to pH 7 with 0.1 M NaOH or HCl. After shaking the mixture for one hour at room temperature, the polymers were gathered by filtering, and UV-VIS spectroscopy was used to determine the Pb^{2+} content.

The Langmuir and Freundlich adsorption isotherms were found using the adsorption data. According to the Langmuir adsorption isotherm model, homogeneous sites are the locations of adsorption on the adsorbent's surface, and once a molecule is absorbed onto a site, it prevents other molecules from absorbing there (Buelvaj et al., 2023; Gohari et al., 2022; Kumar et al., 2019; Mohammadi et al., 2019 and Zou et al., 2023).

Langmuir equation can be expressed as

$$\frac{C_e}{q_e} = \frac{1}{q_{max}b} + \frac{C_e}{q_{e\,max}} \quad (4.3)$$

where q_e = equilibrium amount of adsorbate (mg g^{-1})

C_e = ion concentration in the solution

q_{max} = maximum sorption capacity

b = Langmuir constant

The Freundlich adsorption isotherm, on the other hand, works with heterogeneous surfaces. According to Ayawei et al. (2015), it specifies surface heterogeneity and the exponential distribution of activation energies.

$$\log q_e = \log R_F + \frac{1}{n}\log C_e \quad (4.4)$$

where R_F = adsorption capacity (L/mg), and

$1/n$ = adsorption intensity; it also indicates the relative energy distribution and the heterogeneity of the adsorbate sites.

4.2.7. Selectivity studies

The selectivity study was conducted under optimized conditions for the IIP and the NIP. The IIP or NIP (50 mg) was added to a 10 mL aqueous solution containing 0.1 µg mL^{-1} each of Co (II), Cu (II) and Ni (II). These competing ions were chosen due to their identical charge, comparable ionic radii, and frequent coexistence with Pb^{2+} ions.

The sample pH was adjusted to 9 using 0.1 M HCl or NaOH. The mixture was placed in a 15 mL centrifuge vial and stirred at 70 rpm for 15 min. The experiment was performed in triplicate. The mixture was then filtered, and thiocarbazide was complexed with the filtrate. Using AAS, the ion concentrations were determined. Eqs. 4.5–4.7 were used to calculate the distribution ratio (Kd), selectivity factor (K), and relative selectivity factor (K′) of Pb (II) in relation to Co (II), Cu (II), and Ni (II):

$$K_d = \frac{(C_i - C_f)V}{C_f M} \quad (4.5)$$

$$K = \frac{K_{d(Pb(II))}}{K_{d(\text{competing ions})}} \quad (4.6)$$

$$K' = \frac{K_{imprinted}}{K_{non-imprinted}} \quad (4.7)$$

4.2.8 Reusability studies

When used industrially, adsorbent regeneration plays a crucial role. In this study, polymers were loaded and leached several times by adding 50 mg of polymer to 20 mL of 35 mg/L Pb (II) in deionised water. The Pb(II) was leached with 20 mL 2 M HCl in continuous mode.

4.2.9. Real sample

4.2.9.1. Wastewater sampling preparation

The wastewater was collected from Limpopo Tswinga Water Waste Treatment Plant. Three samples were collected in outlet, biofilter and final and the physico-chemical properties were recorded in Table 1. All samples were acidified with nitric acid and keep it at 4 ^{o}C.

Table 4.1: Determination of metal ions in water.

Metal ion	Concentration Found ($mg.kg^{-1}$)	Concentration after spiked ($mg.kg^{-1}$)	Amount spiked ($mg.kg^{-1}$)	Recovery (%)	MDL
Pb	3.20	3.48	0.30	99.98	0.01
Cu	1.56	1.87	0.30	90.00	0.02
Fe	4.50	4.79	0.30	96.97	0.08
Zn	1.10	1.39	0.30	96.67	0.12
Cr	1.80	2.11	0.30	99.68	0.19

Table 4.2 shows the properties of wastewater from different place in in treatment plant which include the outlet, biofilter and final.

Table 4.2: Physico-chemical properties of wastewater.

Outlet	TDS (mg L^{-1})	270
	Temperature (^oC)	25.00 ^oC
	EC (µ/s)	447
	Ph	7.50
Biofilter	TDS **(**mg L^{-1}**)**	286
	Temperature (^oC)	25.8
	EC (µ/s)	445
	Ph	7.60
Final	TDS **(**mg L^{-1}**)**	286
	Temperature (^oC)	24.8
	EC (µ/s)	445
	Ph	7.60

4.2.9.2. Digestion of wastewater samples

The modified method of Ambuse et al. (2020) was applied to digest the wastewater samples. The wastewater was shaken thoroughly and filtered. It was digested in 3 mL concentrated HNO_3 and 3 mL H_2O_2 at 80^{o}C for 1 h until it was clear. The clear solution was diluted to 100 mL volumetric flask and the selected heavy metals were detected using AAS as indicated in Table 4.3. The metals that where determined were Cu, Zn, Fe and Mn as are the competitors of Pb. These metals have the same charges and are commonly found in wastewater (Qusem et al., 2021).

Table 4.3: Parameters of AA determination of heavy metals.

Parameters	**Cu**	**Fe**	**Zn**	**Pb**	**Mn**
Wavelength (nm)	324.75	248.33	307.59	283.31	279.48

Current (mA)	15	30	14	10	20
Slit (nm)	0.7	0.2	0.7	0.7	0.2
Lamp type	C-HCL	C-HCL	C-HCL	C-HCL	C-HCL
Energy	88	62	40	82	70

4.3. Results and discussion

4.3.1. Functional groups characterization of lead imprinted polymer by FTIR

The FTIR spectra depicting the functional groups of IIP leached, IIP un-leached and NIP are represented in Figure 4.3. Transmittance peak in the region 3424 cm^{-1} is present in leached IIP, unleached IIP and absent in the NIP since it shows the absorption of OH. This band frequency at 3424 cm^{-1} is broad, strong and sharp in washed IIP compared to unwashed IIP. Vibration absorption at about 1716 cm^{-1} appeared in both IIP and NIP polymer which shows the present of C=O bond, other band it is at 2951 cm^{-1} which shows the present of C-H in both polymers. There is a present of a peak in 1256 cm^{-1} and 1146 cm^{-1} in both polymer which confirm the present of C=C and C-O respectively. At a region of about 466 cm^{-1}, it shows the Pb-O present in unwashed IIP and NIP while in washed IIP its absent since it was eluted. The absence of vinyl groups in polymer materials was evident from the clear lack of an absorption band in the 1648–1638 cm-1 range, confirming the full polymerization of methacrylic acid.

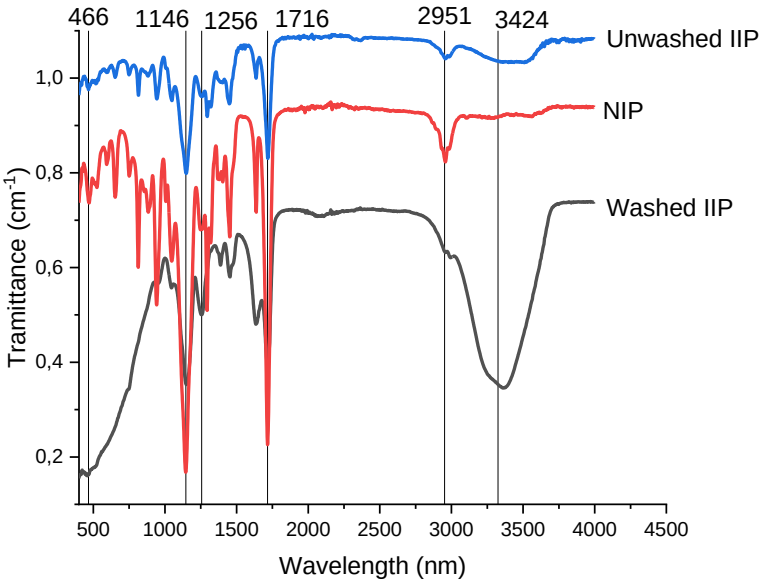

Figure 4.3: Infrared spectra of Pb (II) ion imprinted polymer/NIP.

4.3.2. Effect of sample pH

The impact of solution pH on lead adsorption efficiency is shown in Figure 4.4. The resulting data shows that below pH 2.0, the adsorption efficiency for Pb (II) ions is abnormally low. pH 9.0 was shown to be the ideal pH for optimal adsorption effectiveness. For the Pb (II) ion, an increase in adsorption effectiveness was solution pH increased from 3 to 9.0. The adsorption capabilities of Pb (II) IIP and NIP decreased at solution pH values greater than 9.0. This makes sense because as the pH of the solution drops, the polymer's surface becomes protonated, which acts as a repellent to the metal cations and prevents them from approaching. Conversely, as the pH of the solution rises, some of the functional groups begin to separate, becoming negatively charged and drawing the metal cations in. This theory is supported by the pHZPC values of Pb(II)-IIP and Pb(II)-NIP, which show that the surface became negatively charged above pH 6.0, allowing Pb^{2+} metal cations to more easily migrate to the negatively charged IIP surface. However, because $Pb(OH)_2$ is produced more frequently above pH 9 and these species have poor adsorption capabilities, the amount of adsorption reduced.

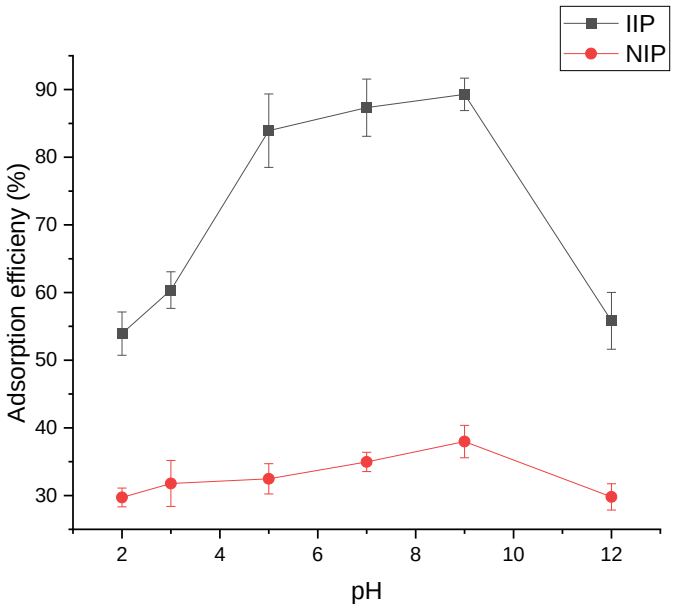

Figure 4.4: Effect of solution pH on Pb(II) adsorption. Conditions: adsorbent mass = 50 mg, initial concentration = 0.5 mg/L, contact time = 20 min, and shaking speed = 70 rpm at room temperature.

Finding the sorbent's point of zero charge (pHPZC) is necessary to understand the adsorption process. When the pH of the solution is less than pHPZC, anion adsorption efficiency is more advantageous than cation adsorption efficiency. The pHPZC is shifted to lower values by specific cation adsorption and to higher values by specific anion adsorption. Stated differently, the pH point of zero pHPZC is the pH value that, in the absence of particular sorption, results in a net zero charge on the solid polymer surface. When the charge on the polymer surface varies from zero as a function of solution pH, this happens. Plotting the Pb (II) IIP's recorded positive and negative pH changes against the pH of the starting solution, pHi, yields the pHPZC at the pH value where ΔpH equals 0. It was discovered that Pb-IIP and Pb-NIP both have a point of zero charge of 6. The cation adsorption is favoured by the implemented pH > pHPZC.

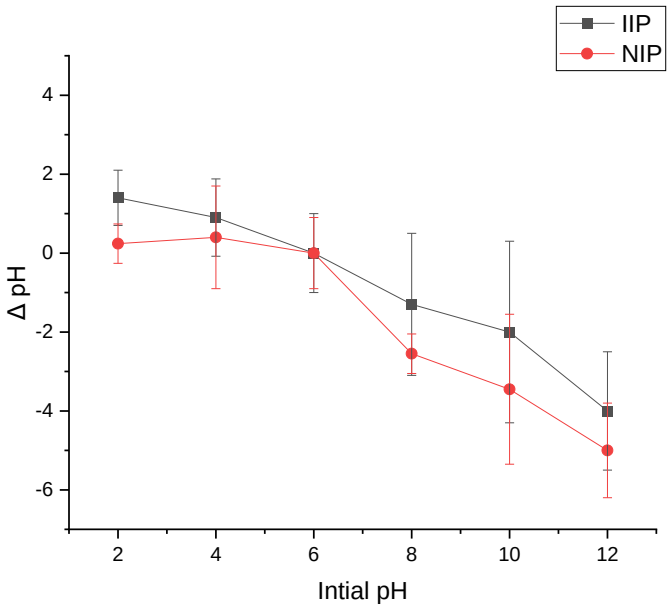

Figure 4.5: Point of zero charge Pb (II). Experimental conditions: 50 mg, shaking speed 70 rpm for 15h.

4.3.3. Adsorbent dosage

The amount of adsorbent, which was investigated in the range of 10-70 mg/100 mL, is significant. Up to 50 mg of ion-imprinted polymer, the Pb (II) removal efficiency increased with increasing adsorbent loading (Figure 4.6). The quantity of adsorption sites that are available may be the cause of this rise in adsorption effectiveness. Nevertheless, the concentration of metal ions achieved equilibrium, therefore adding more imprinted polymer did not result in any additional increase in adsorption. The imprinting effect is responsible for the Pb(II)-IIP's superior extraction efficiency (> 89.31%) by 50 mg polymer material as opposed to NIP's (> 38.13%).

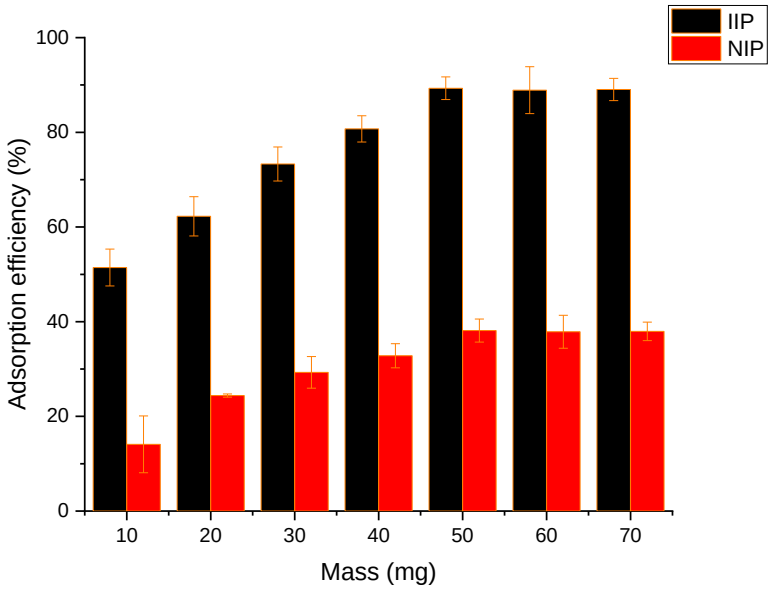

Figure 4.6: Influence of adsorbent mass on Pb (II) adsorption (n = 3, SD). Conditions: pH = 9, sample volume = 10 mL, initial concentration = 0.5 mg/L, contact time = 20 min, shaking speed = 70 rpm at room temperature.

4.3.4. Effect of time

Using both Pb(II)-IIP and NIP particles, the effect of agitation time on the adsorption of Pb^{2+} ions from aqueous solutions was investigated. As seen in Figure 4.7, the adsorption process began with rising adsorption rates and eliminated 85% of Pb (II) after 15 minutes. 15 minutes passed with no more adsorption.

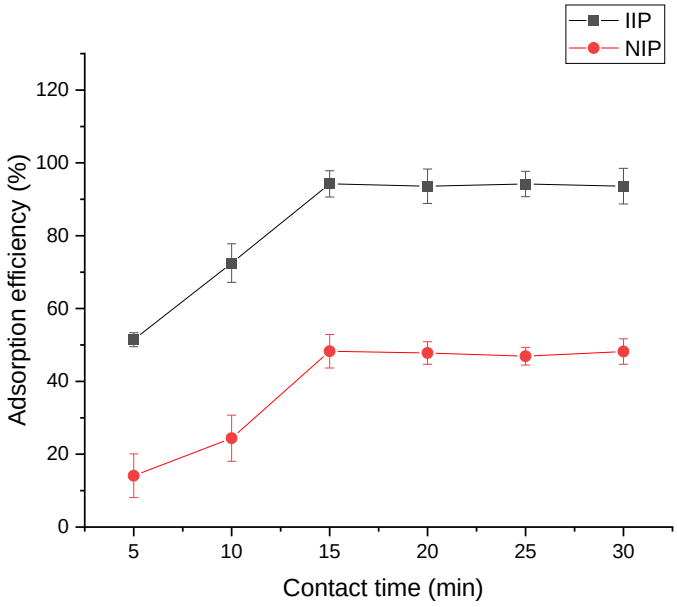

Figure 4.7: Influence of contact time on Pb(II) adsorption (n = 3, SD). Conditions: adsorbent mass = 50 mg/L, sample pH = 9, sample volume = 10 mL, and shaking speed = 70 rpm at room temperature.

4.3.5. Concentration effect

Figure 4.8 illustrates how adsorption changes with ion concentration. There was a range in Pb(II) concentration from 10 to 45 mg/L. As the Pb(II) concentration rose from 10 to 35 mg/L, the adsorption effectiveness increased while maintaining the same duration, pH, and IIP dosage. The saturation of sites caused the adsorption to become constant. Pb-IIP has more adsorption sites than Pb-NIP, as evidenced by the fact that its adsorption efficiency is higher than Pb-NIP's.

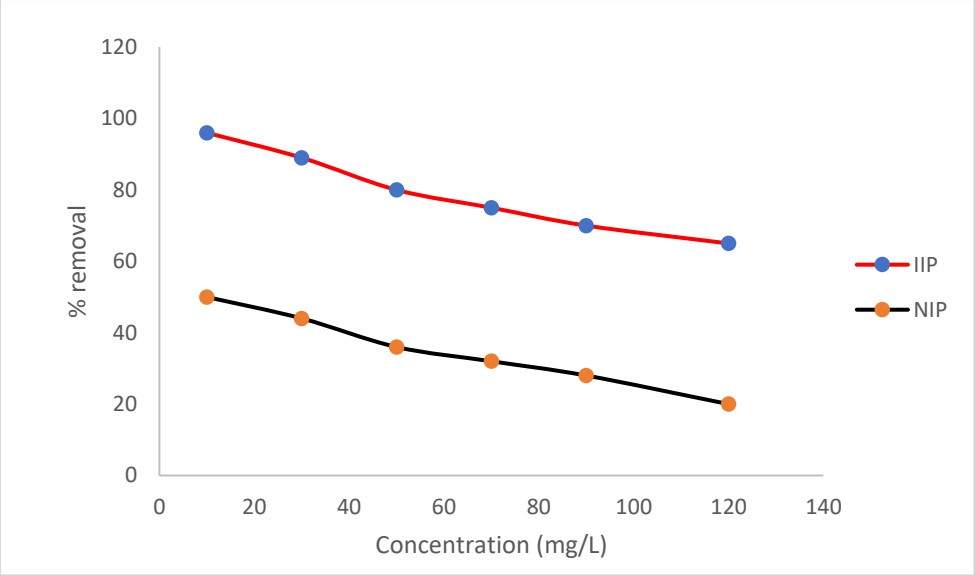

Figure 4.8: Influence of initial Pb(II) ion concentration on adsorption efficiency (n = 3, SD). Conditions: Sample pH = 9, mass = 50 mg, sample volume = 10 mL, temperature =313 K, shaking speed = 70 rpm and time = 15 min.

Figures 4.9(a) and (b) exhibit the Langmuir and Freundlich adsorption isotherms for Pb^{2+} adsorption onto NIP and IIP, and Table 4.3 displays the constants that were determined. For the Pb (II)-IIP and Pb (II)-NIP, the correlation coefficients (R_2) of the Langmuir and Freundlich adsorption isotherms were determined to be, respectively, 0.999 and 0.991 and 0.975 and 0.965. As a result, the Langmuir adsorption isotherm, which suggests monolayer adsorption, best describes the Pb (II) adsorption by the IIP and NIP. During the adsorption process, the adsorbate ion covers the adsorption site. This notion is predicated on a uniform surface of pores. Pb(II) IIP and Pb (II)-NIP were reported to have maximal adsorption capacities of 54.40 and 12.01 mg g-1, respectively. Furthermore, given that n > 1, the Freundlich model suggests that adsorption occurs more easily on Pb (II)-IIP surfaces due to the affinity between Pb (II) ions and Pb (II)-IIP.

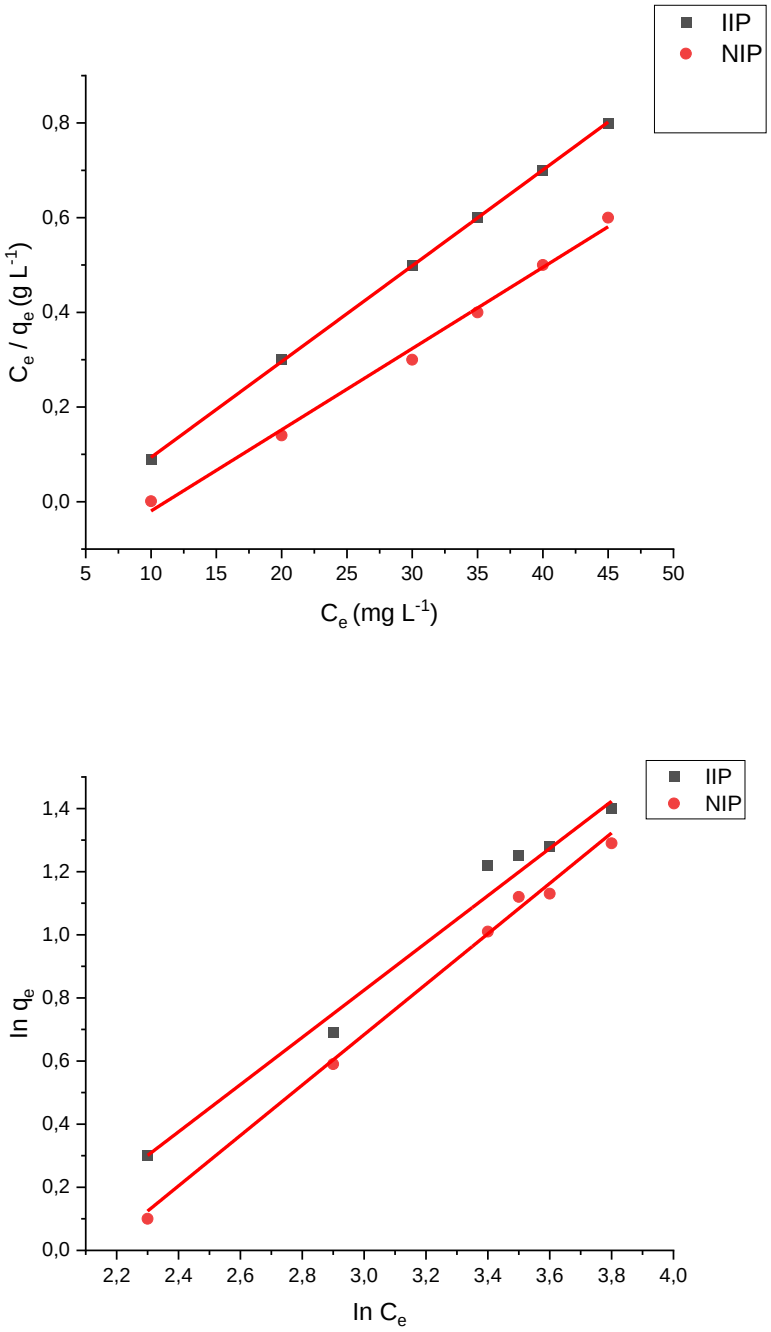

Figure 4.9: Langmuir (a) and Freundlich (b) adsorption isotherm of lead ion on the lead ion imprinted polymer. Conditions: Adsorbent dose = 50 mg, solution pH = 9 and adsorption time 3 h at room temperature.

Table 4.4: Langmuir and Freundlich isotherms

Langmuir and Freundlich adsorption isotherms						
	Langmuir			Freundlich		
Adsorbent	$q_{e\ cal}$	$q_{e\ exp}$	R^2	K_f	*n*	R^2
Pb (II)-IIP	60.54	58.4	0.999	38.40	3.28	0.975
Pb (II)-NIP	12.45	12.01	0.991	30.01	5.67	0.965

4.3.6. Selectivity studies

The above mentioned work shows that the Pb (II) imprinted polymer has suitable sites for the target ion, with the right cavity size, thus increasing the selectivity. It shows that the Pb (II)-IIP can recognize specifically Pb (II) ions, due to the size and morphology of the cavities imprinted in the polymer. The Pb^{2+} IIP selectivity coefficients (K) versus Co^{2+}, Cu^{2+} and Ni^{2+} were found to be 94.67, 43.55, and 177.75, respectively, as shown in Table 4.5. The selectivity of IIP was always higher than the selectivity of NIP, as presented in Figures 4.10 and 4.11. The IIP has a high selectivity due to the monomer that provides specific binding sites for the target ion.

Table 4.5: Selectivity study of Pb (II) ion imprinted polymer.

	Non-imprinted polymer		Ion imprinted polymer		
Metal ion	K_d	K	K_d	K	K'
Pb^{2+}	1.19		8.71		
Co^{2+}	0.09	13.37	0.09	94.67	7.08
Cu^{2+}	0.14	8.32	0.20	43.55	5.23
Ni^{2+}	0.06	20.16	0.05	177.75	8.82

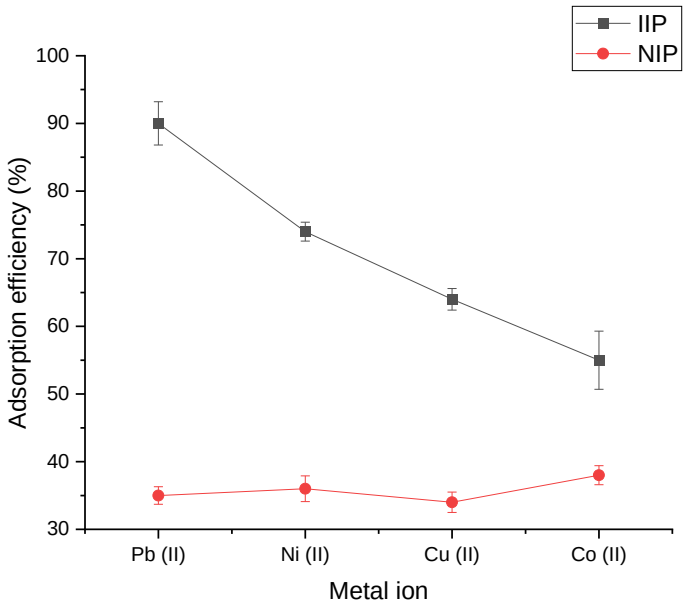

Figure 4.10: Adsorption efficiency for metal ions.

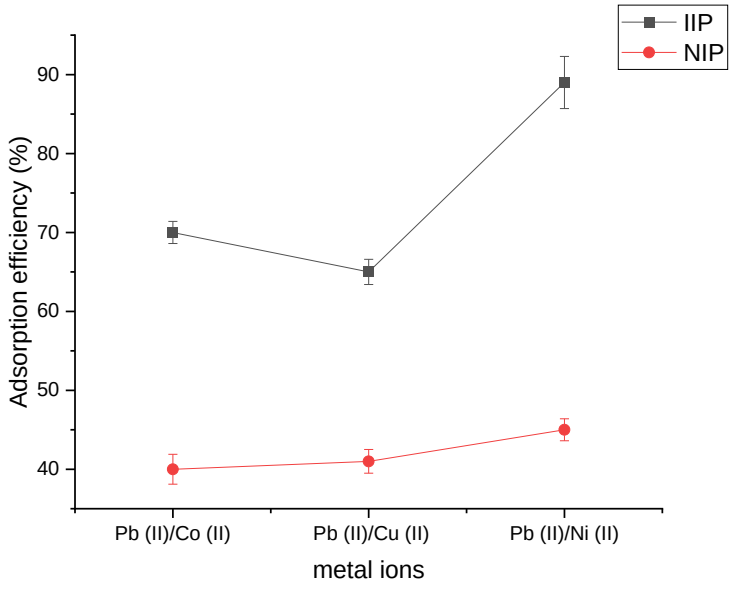

Figure 4.11: Adsorption efficiency in the presence of competing ions.

4.3.7 Removal of Pb (II) from wastewater.

Three samples were collected at Tswinga, where the outlets have higher concentrations followed by biofilter and final samples. Lead ion imprinted polymer show a high adsorption efficiency above 90% for all samples, as indicated in Table 4.6.

Table 4.6: Removal of Pb (II) from wastewater samples, n = 3.

Sample	Pb^{2+} spiked	RSD %	Pb^{2+} + IIP spiked	RSD %	AE %	RSD %
Outlets	3.48	0.02	2.55	0.05	93.00	1.03
Biofilter	3.00	0.01	2.03	0.03	97.00	0.05
Final	2.60	0.09	1.66	1.02	94.00	0.09

Percentage removal of Pb (II) from wastewater with Pb (II) IIP as adsorbent was higher than when using a lead ion imprinted interaction polymer network, as shown in Table 4.7.

4.3.8. Comparison studies

The removal efficiency of the Pb (II) ion imprinted interpenetrating polymer network was lower, which may have been caused by the complexing monomer chitosan, the porogen used which was toluene, and the crosslinking agent which was tetraethyl-orthosilicate (TEOS).

Table 4.7: Comparative study for removal of Pb (II).

Sorbent	Extraction of Pb (%)	Sample	Reference
Lead ion imprinted interpenetrating polymer network	91.5	Wastewater	Hande et al., (2016)

Activated carbon	98.0	Water	Lakshmikandhan and Ramadevi (2019)
Ion imprinted polymer	95 %	Wastewater	This study

4.3.9. Reusability studies

The ability to reuse an adsorbent is crucial in evaluating the IIP efficiency and to develop applications that are reliable, economic and sustainable. Ion imprinted polymers are stable and reusability they can perform over 100 adsorption regeneration cycles (Kupai et al., 2017). Chain length affects both flexibility and strength (longer chains equal greater strength), side groups polar side groups increase the attraction between polymer chains, strengthening the polymer and cross-liking polymer chains are joined by covalent bonds, which harden and complicate the melting of the polymer. These properties allow these polymers to be generated and reused. Because hydrochloric acid increases pore diameter, it facilitates easier absorption and desorption. Figure 4.12 shows that there is very little decline in adsorption after the same polymer is used seven times.

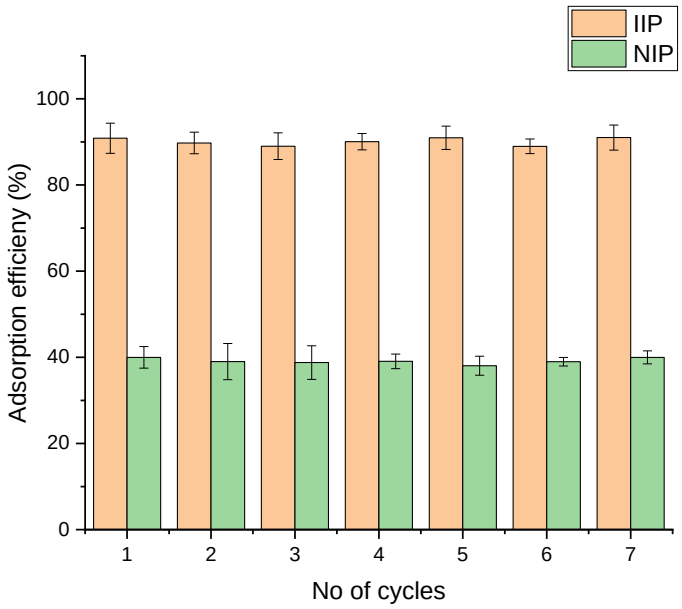

Figure 4.12: Reusability study of Pb (II) ion imprinted polymer.

4.4. Conclusion

Precipitation polymerization was used to create a lead (II) IIP. Using infrared spectroscopy, the functional groups of the lead IIP and NIP were identified. The maximum adsorption efficiency was achieved under the following conditions: sample pH = 9, adsorbent mass = 50 mg, Pb(II) concentration = 35 mg/L, and contact time = 15 min. The adsorption efficiency was examined in batches for various parameters. The Langmuir isotherm promoted Pb(II) adsorption on Pb (II) ion imprinted polymers. The Pb (II) IIP's selectivity was demonstrated by the increased Pb (II) removal in the selectivity research, with a selectivity coefficient above 40. Three authentic samples were gathered, and the concentrations of heavy metals found were Fe > Pb > Cr > Cu > Zn. It was shown that Pb (II) IIP removed more than 90% of Pb (II) from wastewater. Additionally, the reusability study was assessed seven times, and the high adsorption effectiveness of 90% indicated that the waste material would be useful for future use in this investigation.

References

Abdallah AB, El-Kholany MR, Molouk AFS, Ali TA, El-Shafei AA and Khalifa ME, 2021. Selective and sensitive electrochemical sensors based on an ion imprinting polymer and graphene oxide for the detection of ultra-trace Cd (ii) in biological samples. *RSC advances, 11(49),* 30771-30780.

Acharya PT, Bhavsar ZA, Jethava DJ, Patel DB and Patel HD, 2021. A review on development of bio-active thiosemicarbazide derivatives: Recent advances. *Journal of Molecular Structure*, *1226,*129268.

Ambushe AA, Letsoalo MR, Lovia D, Matabane CPM, Molele LS, Godeto TW and Magadzu T, 2020. Assessment of potentially toxic elements and their species in selected water systems in Limpopo province.

Ayawei N, Ekubo AT, Wankasi D, Diko ED, 2015. Adsorption of Congo red by Ni/Al-$CO_{3:}$ equilibrium, thermodynamics and kinetics studies. *Oriented Journal of Chemistry.* 31(3),1307.

Balouch A, Talpur FN, Kumar A, Shah MT and Mahar AM, 2019. Synthesis of ultrasonic-assisted lead ion imprinted polymer as a selective sorbent for the removal of Pb^{2+} in a real water sample. *Microchemical Journal,* 146,.1160-1168.

Baranowska B I, Gutowska I, Rybicka M, Nowacki P and Chlubek D, 2012. Neurotoxicity of lead. Hypothetical molecular mechanisms of synaptic function disorders. *Neurologia i neurochirurgia polska*, *46*(6),569-578.

Bharty MK, Bhariti A, Chaurasia R, Chaudhari UK, Kushawaha SK, Sonkar PK, Ganesan V and Butcher RJ, 2019. Synthesis and characterization of Mn (II) complexes of 4-phenly (phenyl-acetyl)-3- thiosemicarbazide, 4-amino-50phenyl-1,2,4-triazole-3-thiolate and their applications towards electrochemical oxygen reduction reaction. *Polyhedron,*173,114125.

Buelvas DDA, Camargo LP, Salgado IKI, Vicentin BLS, Valezi DF, Dall'Antonia LH, Tarley CRT and Di Mauro E, 2023. Study and optimization of the adsorption process of methylene blue dye in reusable polyaniline-magnetite composites. *Synthetic Metals, 292,* 117232.

Dimpe KM and Nomngongo P, 2017. A review on the efficacy of the application of myriad carbonaceous materials for the removal of toxic trace elements in the environment. *Trends in Environmental Analytical Chemistry*, *16*, 24-31.

Ding C, Yi M, Liu B, Han C, Yu X and Wang Y, 2020. Forward osmosis-extraction hybrid process for resource recovery from dye wastewater. *Journal of Membrane Sci ence*, *612*,118376.

Emenike EC, Iwuozor KO and Anidiobi SU, 2021. Heavy metal pollution in aquaculture: sources, impacts and mitigation techniques. *Biological Trace Element Research*, 1-17.

Genç N and Dogan EC, 2015. Adsorption kinetics of the antibiotic ciprofloxacin on bentonite, activated carbon, zeolite, and pumice. *Desalination and Water Treatment*, *53*(3),785-793.

Gohari RM, Safarnia M, Koohi AD and Salehi MB, 2022. Adsorptive removal of cationic dye by synthesized sustainable xanthan gum-g p (AMPS-co-AAm) hydrogel from aqueous media: Optimization by RSM-CCD model. *Chemical Engineering Research and Design, 188,* 714-728.

Golcs Á, Bezúr L, Huszthy P and Tóth T, 2021. Liquid-liquid extraction and facilitated membrane transport of Pb 2+ using a lipophilic acridono-crown ether as carrier. *Journal of Inclusion Phenomena and Macrocyclic Chemistry*, *99*(1),117-129.

Googerdchian F, Moheb A, Emadi R and Asgari M, 2018. Optimization of Pb (II) ions adsorption on nanohydroxyapatite adsorbents by applying Taguchi method. *Journal of hazardous materials*, *349*,186-194.

Hande PE, Kamble S, Samui AB and Kulkarni PS, 2016. Chitosan-based lead ion-imprinted interpenetrating polymer network by simultaneous polymerization for selective extraction of lead (II). *Industrial & Engineering Chemistry Research*, *55*(12), 3668-3678.

Hassan MF, Sabri MA, Fazal H, Hafeez A, Shezad N and Hussain M, 2020. Recent trends in activated carbon fibers production from various precursors and applications—A comparative review. *Journal of Analytical and Applied Pyrolysis*, *145*,104715.

Hishimone PN, Hamukwaya E and Uahengo V, 2021. The C2-symmetry colorimetric dye based on a thiosemicarbazone derivative and its cadmium complex for detecting heavy metal cations (Ni2+, Co2+, Cd2+, and Cu2+) collectively, in DMF. *Journal of Fluorescence*, *31*(4),999-1008.

Hu ZP, Han J, Wei Y and Liu Z, 2022. Dynamic evolution of zeolite framework and metal-zeolite interface. *ACS Catalysis, 12(9),* 5060-5076.

Janoschka T, Martin N, Martin U, Friebe C, Morgenstern S, Hiller H, Hager MD and Schubert U.S., 2015. An aqueous, polymer-based redox-flow battery using non-corrosive, safe, and low-cost materials. *Nature*, *527*(7576),78-81.

Jia M, Zhang Z, Li J, Ma X, Chen L and Yang X, 2018. Molecular imprinting technology for microorganism analysis. *TrAC Trends in Analytical Chemistry*, *106*,190-201.

Kanwar S, Mehta DK and Das R, 2015. Greener Approach as a Recent Advancement in the Synthesis of Thiadiazole. *International Journal of Pharmaceutical Sciences Review and Research*, *33*,140-147.

Karrouchi K, Radi S, Ramli Y, Taoufik J, Mabkhot YN and Al-Aizari FA, 2018. Synthesis and pharmacological activities of pyrazole derivatives: A review. *Molecules*, *23*(1), 134.

Kori RK, Singh MK, Jain AK and Yadav RS, 2018. Neurochemical and behavioral dysfunctions in pesticide exposed farm workers: A clinical outcome. *Indian Journal of Clinical Biochemistry*, *33*(4),372-381.

Kumar KV, Gadipelli S, Wood B, Ramisetty KA, Stewart AA, Howard CA, Brett DJ and Rodriguez-Reinoso F, 2019. Characterization of the adsorption site energies and heterogeneous surfaces of porous materials. *Journal of materials chemistry A*, *7(17)*, 10104-10137.

Kupai J, Razali M, Buyuktiryaki S, Kecili R and Szekely G, 2017. Long-term stability and reusability of molecularly imprinted polymers. *Polymer chemistry*, *8*(4), pp.666-673.

Lakshmikandhan K and Ramadevi A, 2019. Removal of lead in water using activated carbon prepared from Acacia catechu. *Water SA*, *45*(3), 374-382.

Lee D, Lee JC, Nam JY and Kim HW, 2018. Degradation of sulfonamide antibiotics and their intermediates toxicity in an aeration-assisted non-thermal plasma while treating strong wastewater. *Chemosphere*, *209*, 901-907.

Li Y, Chen D, Xu X, Wang X, Kang R, Fu M, Guo Y, Chen P, Li Y and Ye D, 2023. Cold-Start NO x Mitigation by Passive Adsorption Using Pd-Exchanged Zeolites: From material design to mechanism understanding and system integration. *Environmental Science & Technology*.

Li Y, Zhang X, Zhang P, Liu X and Han L, 2020. Facile fabrication of magnetic bio-derived chars by co-mixing with Fe3O4 nanoparticles for effective Pb2+ adsorption: properties and mechanism. *Journal of Cleaner Production*, *262*, 121350.

Lin Y, Zhang X, Wang Y, Shi E, Lin H and Chen G, 2023. Removal of Pb2+ and Cd2+ from irrigation water and replenishment of mineral nutrients using a low-cost mineral

adsorbent derived from potassium-rich aluminum silicates. *Journal of Environmental Chemical Engineering*, 109282.

Luo J, Xu H, Liang X, Wu S, Liu Z, Tie Y, Li M and Yang, D, 2022. Research progress on selective catalytic reduction of NO x by NH3 over copper zeolite catalysts at low temperature: reaction mechanism and catalyst deactivation. *Research on Chemical Intermediates*, .1-37.

Madikizela LM, Tavengwa NT, Tutu H and Chimuka L, 2018. Green aspects in molecular imprinting technology: From design to environmental applications. *Trends in Environmental Analytical Chemistry*, *17*,14-22.

Mohammadi E, Daraei H, Ghanbari R, Athar SD, Zandsalimi Y, Ziaee A, Maleki A and Yetilmezsoy K, 2019. Synthesis of carboxylated chitosan modified with ferromagnetic nanoparticles for adsorptive removal of fluoride, nitrate, and phosphate anions from aqueous solutions. *Journal of Molecular Liquids*, *273*, 116-124.

Moyo B, Matodzi V, Legodi MA, Pakade VE and Tavengwa NT, 2020. Determination of Cd, Mn and Ni accumulated in fruits, vegetables and soil in Thohoyandou town area, South Africa. *Water SA*, 46 (2), 285-290.

Muleta F, Alansi T and Eswaramoorthy R, 2019. A Review on Synthesis, Characterization Methods and Biological Activities of Semicarbazone, Thiosemicarbazone and Their Transition Metal Complexes J. *Nat. Sci. Res*, *9*,33.

Nuithitikul K, Phromrak R and Saengngoen W, 2020. Utilization of chemically treated cashew-nutshell as potential adsorbent for removal of Pb (II) ions from aqueous solution. *Scientific reports*, *10*(1), 1-14.

Omidi F, Behbahani M, Abandansari HS, Sedighi A and Shahtaheri SJ, 2014. Application of molecular imprinted polymer nanoparticles as a selective solid phase extraction for preconcentration and trace determination of 2, 4-dichlorophenoxyacetic acid in the human urine and different water samples. *Journal of Environmental Health Science and Engineering*, *12*(1),1-10.

Pereao O, Bode-Aluko C, Fatoba O, Laatikainen K and Petrik L, 2018. Rare earth elements removal techniques from water/wastewater: A review. *Desalin. Water Treat*, *130*, 71-86.

Putra WP, Kamari A, Yusoff SNM, Ishak CF, Mohamed A, Hashim N and Isa IM, 2014. Biosorption of Cu (II), Pb (II) and Zn (II) ions from aqueous solutions using selected waste materials: Adsorption and characterisation studies. *Journal of Encapsulation and Adsorption Sciences*, *2014*.

Qusem NA, Mohammed RH and Lawai DU, 2021. Removal of heavy metals from wastewater:A comprehensive and critical review. *Npj Clean Water*, 4(1),1-15.

Sajini T, Gigimol MG and Mathew B, 2019. A brief overview of molecularly imprinted polymers supported on titanium dioxide matrices. *Materials today chemistry*, *11*,283-295.

Shah MS, Tsapatsis M and Siepmann JI, 2017. Hydrogen sulfide capture: from absorption in polar liquids to oxide, zeolite, and metal–organic framework adsorbents and membranes. *Chemical reviews*, *117*(14),9755-9803.

Singh N, Kumar A, Gupta VK and Sharma B, 2018. Biochemical and molecular bases of lead-induced toxicity in mammalian systems and possible mitigations. *Chemical research in toxicology*, *31*(10),1009-1021.

Sonone SS, Jadhav S, Sankhla MS and Kumar R, 2020. Water contamination by heavy metals and their toxic effect on aquaculture and human health through food Chain. Lett. *Appl. NanoBioScience, 10(2),* 2148-2166.

Stevens MG and Batlokwa B, 2017. Multi-templated Pb-Zn-Hg ion imprinted polymer for the selective and simultaneous removal of toxic metallic ions from wastewater. *International Journal of Chemistry, 9(5),* 58114.

Tabani H, Nojavan S, Alexovič M and Sabo J, 2018. Recent developments in green membrane-based extraction techniques for pharmaceutical and biomedical analysis. *Journal of pharmaceutical and biomedical analysis*, 160,244-267.

Tang Y, Liu Y, Chen Y, Zhang W, Zhao J, He S, Yang C, Zhang T, Tang C, Zhang C. and Yang Z, 2021. A review: Research progress on microplastic pollutants in aquatic environments. *Science of the Total Environment, 766,* 142572.

Tavengwa NT, Hintsho N, Durbach S, Weiersbye I, Cukrowska E and Chimuka L,2016. Extraction of explosive compounds from aqueous solutions by solid phase extraction using β-cyclodextrin functionalized carbon nanofibers. *Journal of environmental chemical engineering,* 4(2),2450-2457.

Vengosh A, Jackson RB, Warner N, Darrah TH and Kondash A, 2014. A critical review of the risks to water resources from unconventional shale gas development and hydraulic fracturing in the United States. *Environmental science & technology*, *48*(15),8334-8348.

Wang L, Li J, Wang J, Guo X, Wang X, Choo J and Chen L, 2019. Green multi-functional monomer based ion imprinted polymers for selective removal of copper ions from aqueous solution. *Journal of colloid and interface science*, 541, 376-386.

Xie X, Ma X, Guo L, Fan Y, Zeng G, Zhang M and Li J, 2019. Novel magnetic multi-templates molecularly imprinted polymer for selective and rapid removal and detection of alkylphenols in water. *Chemical Engineering Journal*, *357*,56-65.

Zare-Dorabei R, Ferdowsi SM, Barzin A and Tadjarodi A, 2016. Highly efficient simultaneous ultrasonic-assisted adsorption of Pb (II), Cd (II), Ni (II) and Cu (II) ions from aqueous solutions by graphene oxide modified with 2, 2′-dipyridylamine: central composite design optimization. *Ultrasonics sonochemistry*, *32*, 265-276.

Zhang X, Wang W, Luo S and Lin Q, 2019. Preparation of discrete cage-like oxidized hollow carbon spheres with vertically aligned graphene-like nanosheet surface for high performance Pb2+ absorption. *Journal of colloid and interface science, 553*, 484-493.

Zhao C, Wang X, Zhang S, Sun N, Zhou H, Wang G, Zhang Y, Zhang H and Zhao H, 2020. Porous carbon nanosheets functionalized with Fe_3O_4 nanoparticles for capacitive removal of heavy metal ions from water. Environmental Science: *Water Research & Technology, 6(2),*331-340.

Zhao J, Liu J, Li N, Wang W, Nan J, Zhao Z and Cui F, 2016. Highly efficient removal of bivalent heavy metals from aqueous systems by magnetic porous Fe3O4-MnO2: Adsorption behavior and process study. *Chemical Engineering Journal*, *304*, 737-746.

Zhu F, Zhu C, Wang C and Gu C, 2019. Occurrence and ecological impacts of microplastics in soil systems: a review. *Bulletin of Environmental Contamination and Toxicology*, *102*(6),741-749.

Zou C, Xu Z, Nie F, Guan K and Li J, 2023. Application of hydroxyapatite-modified carbonized rice husk for the adsorption of Cr (VI) from aqueous solution. *Journal of Molecular Liquids, 371*,121137.

Chapter 5: Conclusions and recommendations

5.1 Conclusions

Ion imprinted polymers were successful synthesized using precipitation polymerization. IIPs were synthesized using zinc sulphate and lead acetate as template, EGDMA as crosslinking agent, and methanol as porogen, MAA as functional monomer and AIBN as initiator. Polymers were characterized by FTIR for functional groups and to distinguish NIPs, IIPs washed/unwashed. IIPs were used as absorbent to extract Zinc and lead from wastewater and honey.

The parameters that affect adsorption of ion imprinted polymer were optimized at batch mode and calculated in terms of enrichment factors. The optimum enrichment factors for Zinc ion imprinted polymer: sample pH= 7, adsorbent dose was 5 mg, contact time at 15 min and shaking speed at 100 rpm. The optimum enrichment factor for lead ion imprinted polymer: sample pH= 9, mass =50 mg, concentration =35 mg/L at 15 min.

The adsorption isotherm Langmuir and Freundlich were investigated for both zinc and lead ion imprinted polymer. The adsorption for both polymers favours Langmuir isotherms.

The selectivity study was also done, Pb (II)- ion imprinted polymers and Zn (II)- ion imprinted polymers were selective in present of competing ions

Ion imprinted polymers are re-usable, they were evaluated 7 times and the adsorption efficiency was at 90 %. The adsorption efficiency of ion imprinted polymers were above 90%.

5.3 Recommendation

This study recommend that the material be characterized using the following techniques:

- Energy dispersive spectroscopy (EDS) for analysis of composition and constituent of IIPs/NIPs polymer that has been synthesized.
- Thermogravimetric analysis (TGA) to analyse purity, decomposition and stability of the temperature between IIPs/NIPs, stability affect the surface charge.
- Scanning electron microscopy (SEM) is used to recognized porosity and pores (cracks) form. SEM will show morphology (roughness and smoothness) of the surface differences between IIPs/NIPs.
- Brunauer-Emmett-Teller (BET) measurement will provide the pore volume and average pore diameter, where the porous and rough will indicate cavities which will distinguish between IIPs and NIPs.

Appendix

Figure A 1: Atomic absorption spectrometer

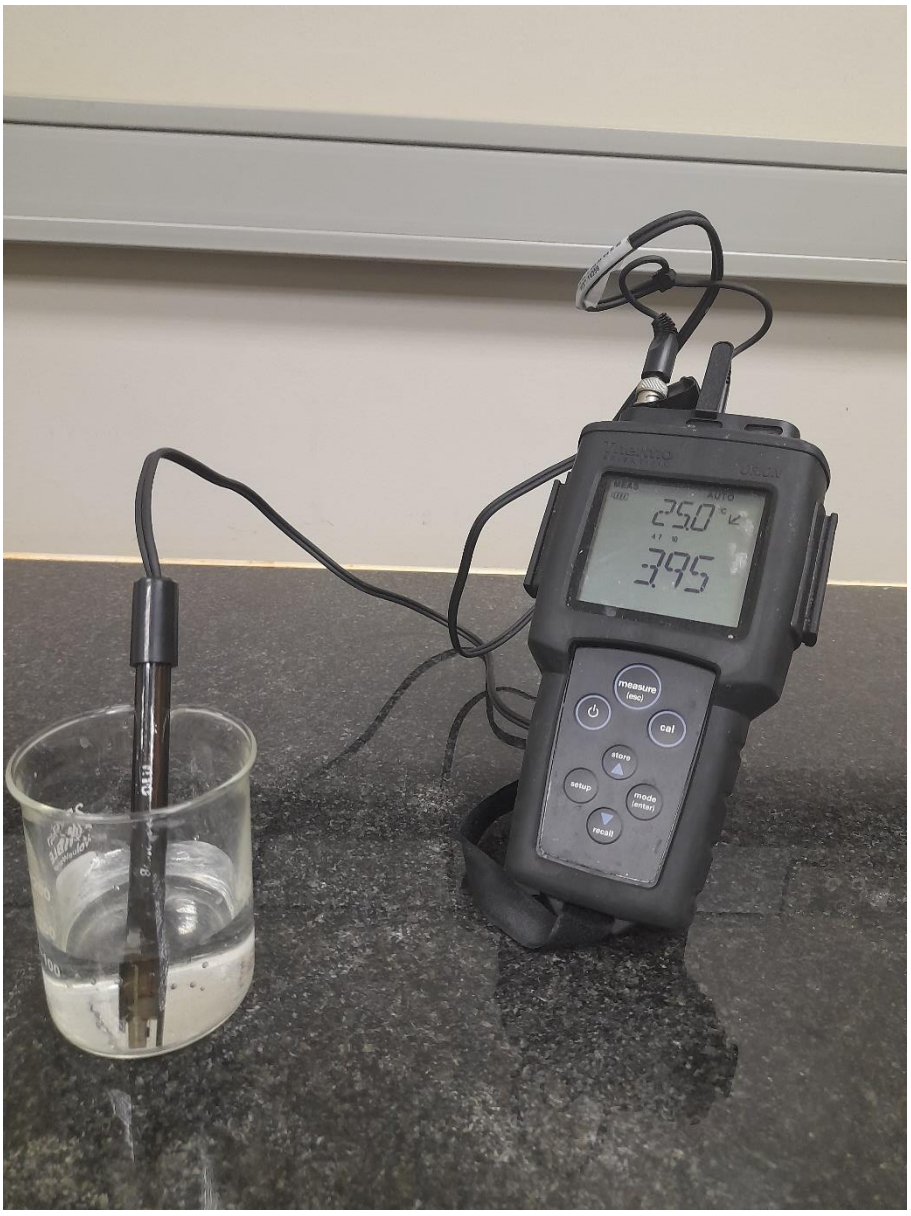

Figure A 2: pH meter

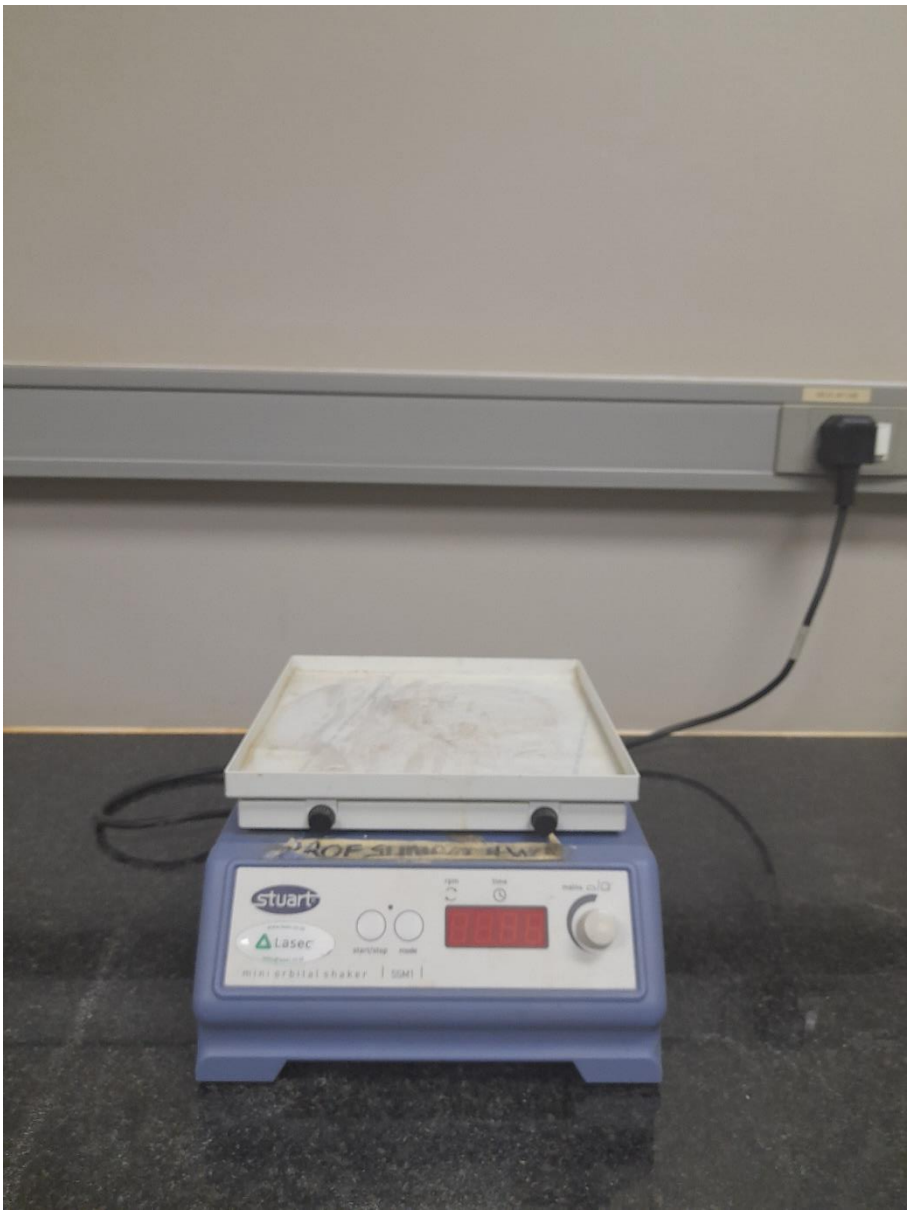

Figure A 3: Shaker

Figure A 4: Outlet

Figure A 5: Inlet

Figure A 6: Biofilter